SEMICONDUCTOR GRADE, SOLAR SILICON PURIFICATION PROJECT

Motorola Report No. 2257/12

JPL CONTRACT NO. 954442

FINAL TECHNICAL REPORT

by

W. M. Ingle, R. S. Rosler, S. W. Thompson, R. E. Chaney

February 1976 - January 1979

PREPARED BY

MOTOROLA, INC. SEMICONDUCTOR GROUP
5005 E. McDowell Road
Phoenix, Arizona 85008

AUG 1979
RECEIVED
NASA STI FACILITY
ACCESS DEPT.

TABLE OF CONTENTS

LIST OF FIGURES

LIST OF TABLES

ABSTRACT

In February, 1976 D.O.E./J.P.L. funding was initiated for Motorola's low cost poly silicon program. In the process, SiF_4, a low cost by-product is reacted with mg silicon to form SiF_2 gas which is polymerized. The $(SiF_2)_x$ polymer is heated forming volatile Si_xF_y homologues which disproportionate (C.V.D.) on a silicon particle bed forming silicon and SiF_4.

During the initial phases of the investigation the silicon analysis procedure relied heavily on S.S.M.S. and E.S. analysis. These analysis demonstrated that major purification had occurred and some samples were indistinguishable from semiconductor grade silicon (except possibly for phosphorus). However, more recent electrical analysis via crystal growth reveal that the product contains compensated phosphorus and boron. Work on the control or removal of the electrically active donors and acceptors could yield a product suitable for solar application.

The low projected product cost and short energy payback time suggest that the economics of this process will result in a cost less than the J.P.L./D.O.E. goal of $10/Kg.

Finally, following a successful demonstration of the pilot facility, the process appears to be readily scalable to a major silicon purification as was proposed by Motorola and R. Katzen.

1.0   INTRODUCTION

1.1   Background

In 1975 E.R.D.A. initiated the Low Cost Solar Silicon Array Project to demonstrate a technology capable of producing economically feasible photovoltaic solar energy conversion. The basic goal was development of alternate advanced technologies capable of producing electrical power at 50¢/peak watt. For this goal to be attained, a research-intensive, multi-disciplined investigation was required.

The investigation was divided into 5 major tasks, the first of which was the silicon materials task. The major goals of this task were:

i) Low Cost Silicon Production (< $10/Kg, 1975 $)

ii) High Volume Production (>1000 metric ton/yr)

iii) High Purity (at least, "solar grade")

iv) Short energy payback period (<1 year)

1.2 $(SiF_2)_x$ Polymer Process

In February 1976, JPL/DOE funding was initiated for Motorola's low cost silicon purification project. The purpose of this investigation has been to convert metallurgical grade silicon (mg Si) into semiconductor grade silicon (sg Si) via a 3 step $(SiF_2)_x$ polymer transport purification process. The first step[1] involves the reaction of SiF_4 with mg Si to yield gaseous SiF_2:

$$SiF_4 + Si \xrightarrow{\sim 1300^{\circ}C} 2SiF_2 \qquad \text{Step 1}$$
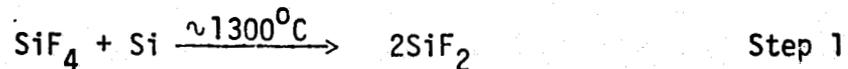
This is followed by a polymer formation step.[2]

$$xSiF_2 \xrightarrow{-45^{\circ} \text{ to } -100^{\circ}C} (SiF_2)_x \qquad \text{Step 2}$$
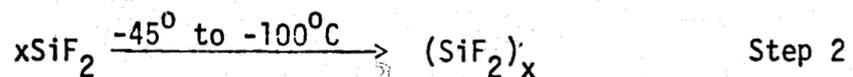
The polymer is then converted into high purity silicon, SiF_4 and higher homologues.[3]

$$(SiF_2)_x \xrightarrow{360-850^{\circ}C} Si + SiF_4 + Si_yF_z \qquad \text{Step 3}$$

1
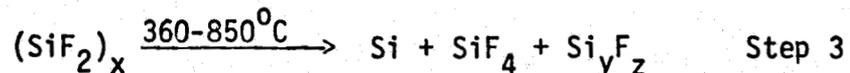
The various purification steps which are inherent to this process are:

i) At $\sim$1300^{o}C where the mg silicon is converted into SiF$_2$ very little fluorination of the impurities occurs because the Si-F bond energy of 142 kcal/mole is extremely strong. It would have to be broken to form another bond, to a different element, which would in most cases be energetically unfavorable.

ii) Nearly all the known metal fluorides that are stable and volatile at 1300°C are either unstable or non-volatile at room temperature.

iii) Finally in the condensation/polymerization step at temperatures lower than -45°C only those impurities which are liquids or solids at that temperature will be incorporated. For example, Margrave et.al.[3] found that possible dopants such as BF$_3$, PF$_3$, PF$_5$, AsF$_3$, etc. would only incorporate into the polymeric $(SiF_2)_x$, if the condensation temperature was below the boiling points of the impurities.

1.3   Silicon Purity

Chemical methods of silicon analysis were used extensively to evaluate the product of the SiF$_4$ transport process. Emission spectroscopy (ES) and spark source mass spectroscopy (SSMS) were used for semi-quantitative and quantitative analyses respectively. The limitations of these methods were established through a sample exchange with other contractors.

Other potentially sensitive techniques, such as neutron activation analysis, were investigated by JPL, but did not offer sufficient reliability or economy to be used during this project.

SSMS analysis of samples produced during this project were comparable with semiconductor grade (sg) silicon; however, in the latter stages of this project in-house crystal growth studies were undertaken to more clearly define the electrical character and purity of the project. Samples of these crystals were supplied to JPL. The resistivities of these samples were near the low end of the useful solar cell resistivity range and indicated compensation.

1.4   Cost and Energy Requirements for Solar Silicon Production

For any process to produce lost cost silicon it must use a low cost starting material. To reduce the cost even further one develops a system where the indirect materials are recycled and the form of the indirect materials at the end of the cycle is directly usable for the next cycle (i.e., no high cost processing or indirect materials purification steps). The $(SiF_2)_x$ polymer purification processes meet all three of these criteria.

In this process, the starting material is mg silicon selling presently at $1.50/Kg, which is well within the cost goals. The indirect material is SiF_4. Every year, the fertilizer companies of America produce millions of pounds of H_2SiF_6 by the fluorination of silicate rocks in the production of fertilizers. H_2SiF_6 is readily converted into low cost high purity SiF_4 as recently demonstrated by S.R.I. International.[4] Consequently, with low cost mg Si and SiF_4 as starting material (with SiF_4 being recycled, 95-97%), the projected cost of silicon production by the $(SiF_2)_x$ polymer process is much less than $10/Kg Si.

In 1978[5] Solarex Corporation published a report comparing energy payback periods for a number of current technologies being funded by JPL/DOE. Figure 1.4.1 is a reprint from that report. The authors of that report recognize the fact that it is difficult to assess with high reliability an absolute energy payback time on processes which are still at the lab scale. Concerning the $(SiF_2)_x$ polymer process they state "The total expenditure of about 30 kWh per Kg refined silicon may prove to be an understatement in the future. Yet the indication that this refinement process is very energy inexpensive must be acknowledged."

1.5   Format of the Final Report

The secion following the Introduction has been titled Technical Presentations. It is a composite of five sections depicting the research and development on the $(SiF_2)_x$ polymer transport purification process over the last three years. In the five sections will be found descriptions of experimental apparatus and procedures or engineering, followed by results from these experiments and discussions of the relevance of these results. Following the Technical Presentation section are sections on Conclusions and Recommendations and on New Technology.

3
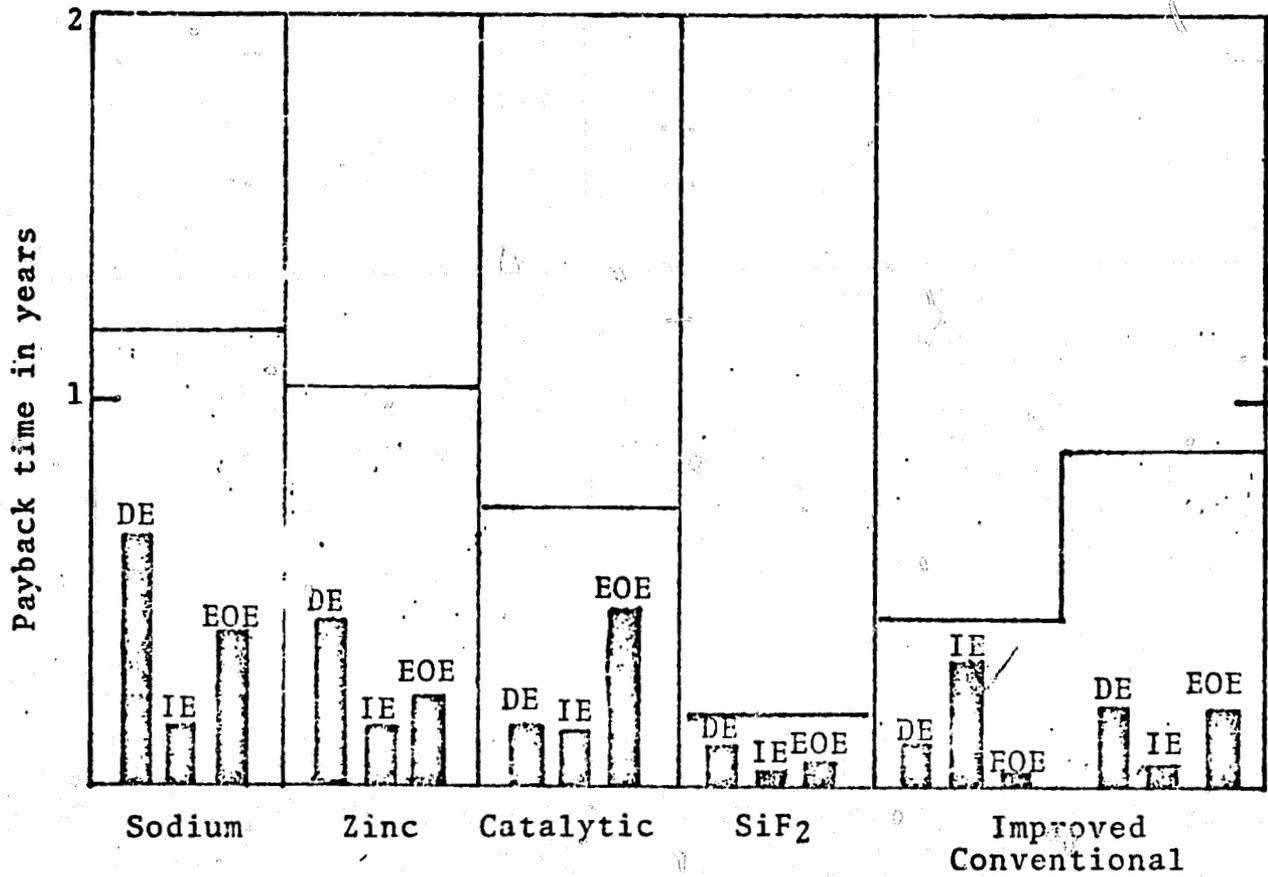
Figure 1.4.1 Payback times of alternative refinement processes.

4

2.0   TECHNICAL PRESENTATIONS

2.1   Mass Spectral Study of the Reaction of SiF_4 with Silicon

2.1.1   Introduction

The reaction parameters and stoichiometry affecting the formation of silicon difluoride in the heterogeneous reaction

$$Si + SiF_4 \xrightarrow{1300^{\circ}C} 2 SiF_2 \qquad (1)$$
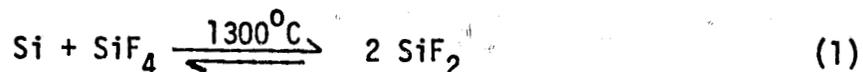
have been studied in a flow system. The flow system data have been analyzed in terms of quantitatively measurable system parameters and via GC/MS for species identification. The product ratios have been examined to maximize formation of SiF_2 from reactions. A thermodynamic analysis of reaction step 1 has been conducted. The results of this analysis are included in Appendix I.

It was shown by Pease[2] that silicon difluoride gas ($SiF_2(g)$) can be conveniently prepared from silicon and silicon tetrafluoride at low pressures (<50 torr) and at temperatures above $1050^{\circ}C$. In these studies Pease showed that SiF_2 could be formed with a 50% yield from reactants. However, in spite of considerable effort directed toward SiF_2 reactions[1-3] comparatively little work has focused on initial SiF_2 formation conditions.

The effects of SiF_4 flow rate, SiF_4 purity, Si particle size, impurities in the Si charge, reaction temperature and reaction pressure on the silicon difluoride formation reaction have been examined. Our work has shown that considerable enhancement in the yield of SiF_2 can be obtained under optimized reaction conditions.

2.1.2   Experimental

2.1.2.1 Reaction System

Figure 2.1.1 is a schematic diagram of the reaction system consisting basically of a furnace, the Si charge tube and two condensation traps. A horizontally mounted 24 inch Marshall high temperature resistance heated furnace
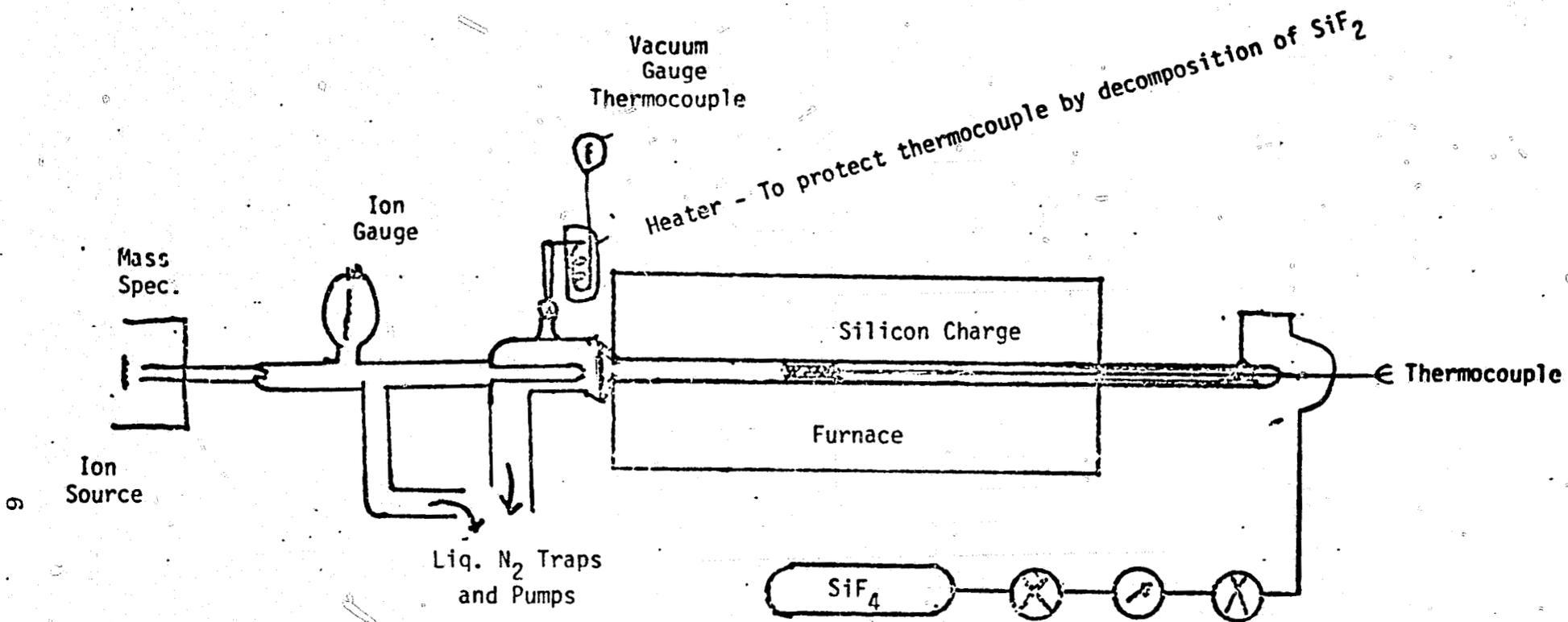
Figure 2.1.1 Diagram of step 1 reactor adapted via line of sight to mass spectrometer.

was used to heat the silicon to temperatures up to 1350°C. The reaction tube consisted of a 1.5 inch quartz liner into which silicon chunks were packed. A Mullite outer-tube was employed as a sleeve around the quartz reaction tube thereby reducing major deformation of the quartz tube at elevated temperatures. Temperature measurements were made with a Pt/Rh thermocouple located axially within the silicon charge material.

In order to remove possible surface contaminants, the silicon charge was subjected to a 1 minute etch with a 5:1:1 mixture of 40% HF, conc. HNO_3 and acetic acid, thoroughly rinsed in deionized water, dried under nitrogen and sized. Commercial silicon tetrafluoride (nominally 99.6% pure supplied by Synthatron Co.) was used as obtained or was purified to eliminate possible sulphur dioxide and oxygen contamination by passage over an iron wire at 800°C.[3]

SiF_4 was monitored and introduced into the vacuum system by a Matheson flow controller at flows between 12.5 sccm and 400 sccm. The gases emerging from the quartz reaction tube were sampled by an in-line mass spectrometer utilizing the solid inlet of the source detector. All mass spectral data were obtained with a model 3300 Finnigan Quadrupole integrated GC/MS/Data System mass spectrometer. The mass spectrometer was modified by the addition of a digital four place voltmeter for accurate determination of voltages across the E.I. source.

Rapid quenching of the remainder of the product gases was accomplished by trapping the gases in two traps arranged in series with trap temperatures of -78°C and -196°C. The former was obtained with an isopropyl alcohol/carbon dioxide slush bath and the latter with liquid nitrogen.

A conventional quartz and Pyrex vacuum system employing greaseless high vacuum Kontes Teflon spopcocks and greaseless o-ring joints was used to handle the volatile products.

Residual background pressures of $<10^{-2}$ torr were typical.

2.1.2.2 Silicon Packing

In order to obtain a high transport efficiency, the packing geometry and particle size of the silicon charge within the reactor was varied. Particle sizes ranging from 22 mesh to 5 mesh were found to be suitable under our reaction conditions.

The packing procedure found to be most suitable was to place large diameter chunks (1-2 cm) at the ends of the furnace hot zone followed by intermediate (0.2 - 1 cm) chunks. In the center of the charge were placed chunks of 0.2 cm or less. It should be noted that several packing geometries were found to work satisfactorily, and that the geometry chosen allowed a high SiF_4 flow rate without the evolution of small silicon particles from the silicon charge.

2.1.2.3 Flow Characteristics

Flow characteristics within the silicon charge calculated via a modified Reynolds number showed that transitional flow occurs over the flow ranges of 4 sccm to 400 sccm.

2.1.2.4 Residence Times of Reactants and Products

Residence times were determined by measuring flow rates and pressure drops across the reactor tube. Table 2.1-1 lists typical data collected at $1350^{\circ}C$ for the reaction $SiF_4 + Si \longrightarrow 2SiF_2$.

Table 2.1-1 Residence times of reactants and products

SiF_4 Flow Rate sccm	Pressure (torr)		Residence Time (sec)
	Upstream	Downstream	
394	18.2	0.20	0.220
591	22.2	0.34	0.179
729	27.1	0.41	0.177

2.1.2.5 SiF_2 Detection

Analysis of reactants and products emerging from the reaction tube was accomplished by line of sight mass spectroscopy in the E.I. source mode. It was observed that when electron voltages were ≥ 21.0 the SiF_3^+ ion (m/e = 85) is the most intense ion peak in the mass spectra of both SiF_2 and SiF_4. Evidently, considerable fragmentation and recombination occurs resulting in the formation of the SiF_3^+ ion from SiF_2. One possible route is

$$2SiF_2 \xrightarrow{\geq 21 \text{ eV}} SiF_4 + Si \qquad (4)$$

$$SiF_4 \xrightarrow{\geq 18 \text{ eV}} SiF_3^+ + F^- \qquad (5)$$
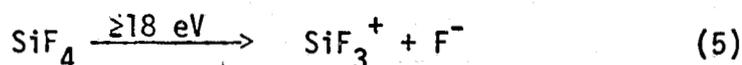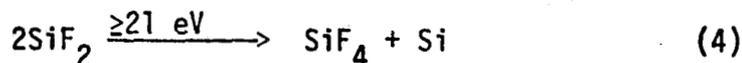
It is interesting to note that the magnitude of the SiF_4^+/SiF_3^+ ratio in the mass spectrum of SiF_2 at 70 eV is much less than the corresponding ratio from the SiF_4 spectra also obtained at 70 eV. This suggests that the above reaction sequence is not the only route to the formation of SiF_3^+ from SiF_2. Varying the E.I. source electron voltage from 70 to 15 eV while recording spectra of SiF_2 revealed that the maximum SiF_2^+/SiF_3^+ ratio (about 20:1) could be obtained at E.I. voltages between 18 and 21 eV. The standard voltage for this investigation was chosen to be 19.5 eV although other electron ionization voltages in the range are equally suitable.

Margrave[3] et.al. state that SiF_2 and SiF_4 account for at least 99.5% of the gaseous species present in equation (1). Further, they report no gaseous polymers formed and that the gas phase reaction

$$SiF_2 + SiF_4 \longrightarrow Si_2F_6 \qquad (6)$$
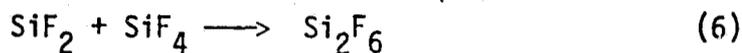
was not observed. Consequently, it was concluded that at 19.5 eV the peak observed at m/e = 85 was due to the SiF_3^+ derived from unreacted SiF_4 and not SiF_2 or Si_2F_6. Thus it is possible to optimize the parameters affecting the SiF_2 generation by monitoring the ratio of the SiF_2^+/SiF_3^+ ions at 19.5 eV.

2.1.2.6 Data Analysis

In order to facilitate data acquisition and interpretation, a data handling computer program, AVO M/E was developed to use with the Finnigan GC/MS data system. The program is capable of processing to a user specified degree of sophistication the numerous data values generated in a typical SiF_2 generation experiment.

2.1.2.7 Impurity Effects on Reaction Step 1

To investigate the effect of impurities in the starting materials on the reaction rate, experiments were conducted in which the rate of SiF_2 production is directly followed using the GC/MS data system. In order to establish a standard reaction rate in which the effects of impurities are minimal, semiconductor grade (sg) polysilicon was used as a standard for the SiF_2 transport reaction. The reaction was then repeated under identical conditions of temperature, pressure, and SiF_4 flow rate with Fe-doped sg poly-silicon, Al-doped sg polysilicon and metallurgical grade (mg) silicon. Table 2.1-2 lists the impurity concentrations for various silicon input materials. The sg polysilicon had been mechanically crushed and therefore the data listed in Table 2.1-2 does not reflect the purity of typical sg polysilicon. It can be seen from Table 2.1-2 that the etched sg polysilicon has impurity concentrations considerably lower than unetched sg poly, indicating that the impurities in unetched sg poly were acquired from the crushing process used to obtain particle sizes that optimize the gaseous flow rate.

2.1.2.8 Mass Balance Experiments

Mass balance experiments were undertaken directed at correlating SiF_2 and SiF_4 counts with measured weights and partial pressures of reactant and products of reaction 1. The accurate determination of the stoichiometry was studied in conjunction with the mass balance experiments. The stoichiometry of reaction step 1 has been found to be 1:1:2 and the mass balance indicates that substantial losses of material due to unpredicted side reactions does not occur.

Table 2.1-2 Impurity concentrations in sg polysilicon
after mechanical crushing compared with mg
silicon as measured by emission spectroscopy.

Element	Detection Limit ppm/wgt	mg Si[a]	sg Poly Si	Etched sg Poly Si[b]
Cu	0.5	20	<1	0.5
Fe	2	1500	>100	n.d.
Al	5	1000	n.d.	n.d.
Cr	5	640	n.d.	n.d.
Mn	1	330	>0.5	n.d.
V	5	230	n.d.	n.d.
Ti	1	110	n.d.	n.d.
Ni	5	40	>0.5	n.d.
Mg	0.5	2.6	5±3	n.d.

(a) Typical values observed for mg Si.

(b) 5:1:1 $HF/HNO_3/CH_3CO_2H$, diluted 2:1, etch 1 min; 30 min. D.I. water rinse.

2.1.3 Results and Discussion

2.1.3.1 Effect of Temperature and Impurities on SiF_2 Generation

The first step of the SiF_2 transport process involves the reaction of $SiF_{4(g)}$ with silicon to yield gaseous SiF_2.

$$Si + SiF_4 \underset{\sim 1300^{o}C}{\rightleftharpoons} 2SiF_2 \qquad (1)$$
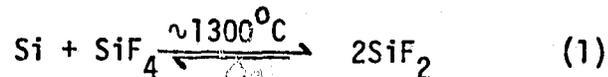
In order to optimize the rate of production of high purity silicon from mg silicon via the SiF_2 transport process, it was desirable to define at least the basic parameters involved in the rate of this reaction in terms of the three main variables: temperature, SiF_4 flow rate and impurity concentrations.

In a preliminary investigation[6] possible catalysis of reaction 1 was observed arising from impurities found in mg silicon. If these impurities in mg Si did affect the rate, then it was desirable to identify them in order to optimize the production of silicon via the transport process.

Consequently, a series of experiments was undertaken in order to define the basic reaction variables. Experiments were conducted at temperatures of 850, 950, 1050, 1150, 1250 and $1350^{o}C$. However, since the SiF_2 counts at temperatures below $1150^{o}C$ are insignificant, these lower temperatures will not be included in the data presented. To establish a standard reaction rate in which the effect of impurities on reaction step 1 was minimal, SiF_2 transport reactions were performed between semiconductor grade polycrystalline (sg poly) Si and purified SiF_4.

Figure 2.1.2 is a graph of the ratio of SiF_2 (m/e = 66) counts/SiF_4 (m/e = 85) counts emerging from the reaction chamber versus SiF_4 flow into the reaction chamber for a sg poly Si charge. It can be seen that the ratio at $1350^{o}C$ is greater than $1250^{o}C$, indicating that a greater concentration of SiF_2 is produced at $1350^{o}C$ than $1250^{o}C$ for equivalent flows.

Having established a base of correlation using sg poly Si, experiments were undertaken to establish the cause of possible catalysis. Two samples of sg poly Si were doped with the two major impurities in mg Si, namely Al and Fe (0.5% and 1% by weight respectively).
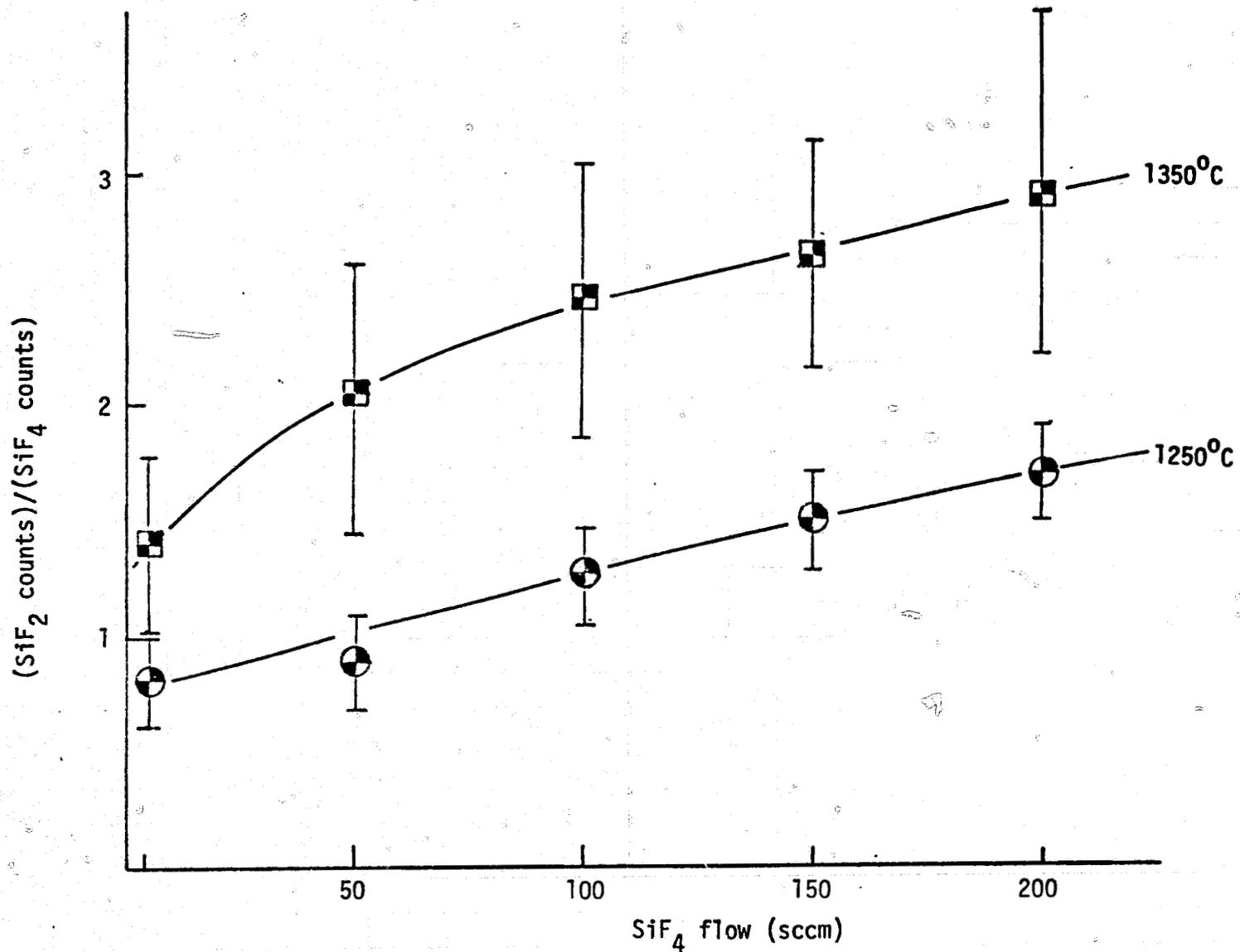
Figure 2.1.2 Ratio SiF_2/SiF_4 counts versus SiF_4 flow for sg poly Si and purified SiF_4.

13

Figure 2.1.3 shows results of experiments conducted at $1150^{\circ}C$, $1250^{\circ}C$ and $1350^{\circ}C$ for sg poly Si doped to 0.5% Al. Figure 2.1.3(a) shows that SiF_4 counts decrease with temperature, $1350^{\circ}C$ being the lowest for equivalent flow rates, while Figure 2.1.3(b) shows that SiF_2 counts increase with temperature. Figure 2.1.3(c) shows that again, as with the poly Si + SiF_4 reaction, the SiF_2/SiF_4 ratio is greater at $1350^{\circ}C$ than at lower temperatures. However, a maximum ratio was reached at a flow of about 100 sccm and then a decrease in the SiF_2/SiF_4 ratio was noted. This is reminiscent of some oxidation reactions in which the rate limiting step involves surface diffusion. Cooling of the charge by impinging SiF_4 and apparent flow characteristics represent other possibilities.

Figures 2.1.4(a) and 2.1.4(b) are graphical presentations of the SiF_2 transport reaction involving Fe doped (1%) poly and purified SiF_4. Again we see an increase of SiF_2 counts and a decrease of SiF_4 counts as the temperature is increased. The ratio of SiF_2/SiF_4 at $1350^{\circ}C$ is greater than that at $1250^{\circ}C$ (Figure 2.1 4(c) and the magnitude is similar to that observed in the previous two examples, namely a maximum ratio of 3.

To further investigate the shapes of the previously described ratios versus SiF_4 flow graphs, an extensive series of experiments was conducted on the mg Si + SiF_4 reaction. These experiments were designed to obtain the maximum amount of data concerning the reaction between mg Si and purified and unpurified SiF_4 to allow analysis on a statistically significant basis. Here, over 1200 individual spectra were collected and subjected to an analysis based on a two sided 90% confidence interval. Flows were increased by a factor of 2 over the previously studied flow range, i.e., flows between 4 sccm and 400 sccm were obtained as opposed to the 4 to 200 sccm flow range studied in the impurity doped runs.

Several facts are apparent from the graphs representing this data which are presented in Figure 2.1.5.

(1) The SiF_2/SiF_4 ratio is greater at $1350^{\circ}C$, whereas the ratio at $1300^{\circ}C$ lies between the 1250° and $1350^{\circ}C$ ratios.

(2) The SiF_2/SiF_4 ratio is approximately 3, indicating the rate of the SiF_2 production is not significantly affected by impurities in mg Si.

14
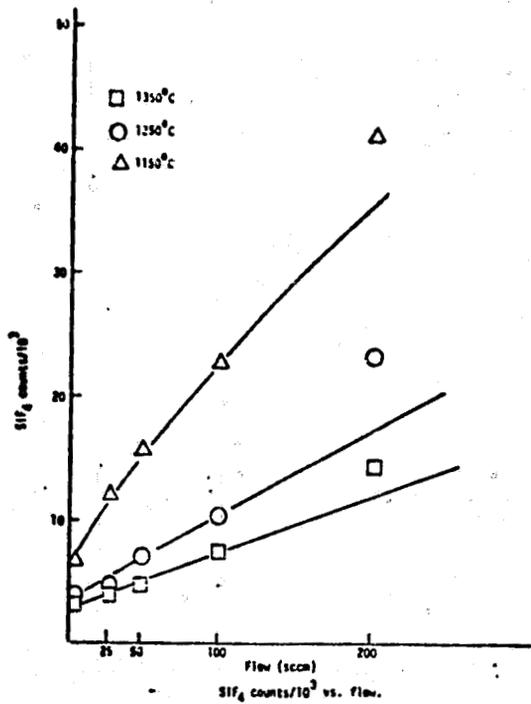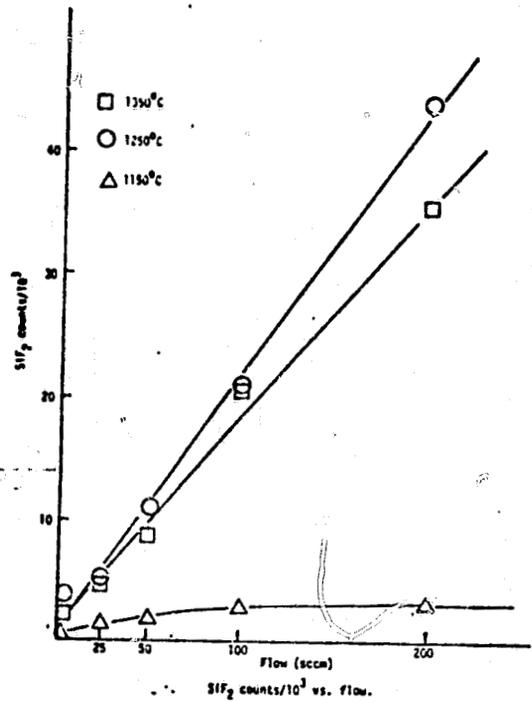
Figure 2.1.3 (a)

Figure 2.1.3 (b)
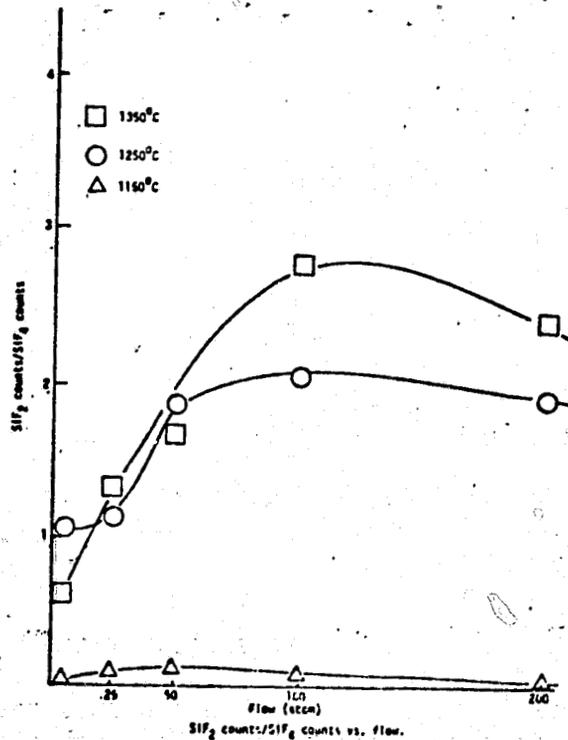
Figure 2.1.3 (c)

Figure 2.1.3 Counts and ratios of reactants and
products versus SiF_4 flow for Al doped
sg poly Si and purified SiF_4.

15
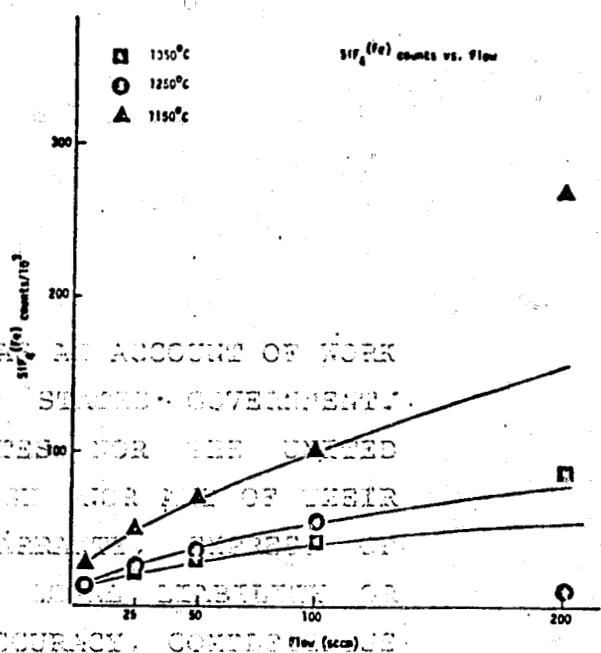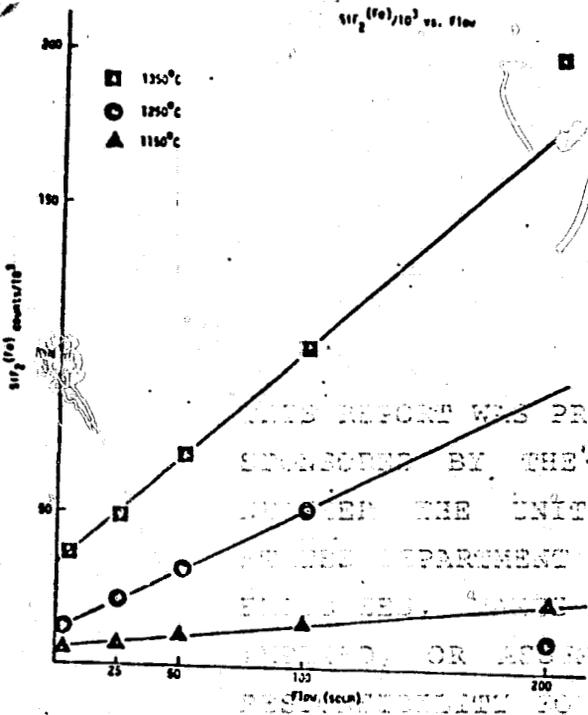
Figure 2.1.4 (a)
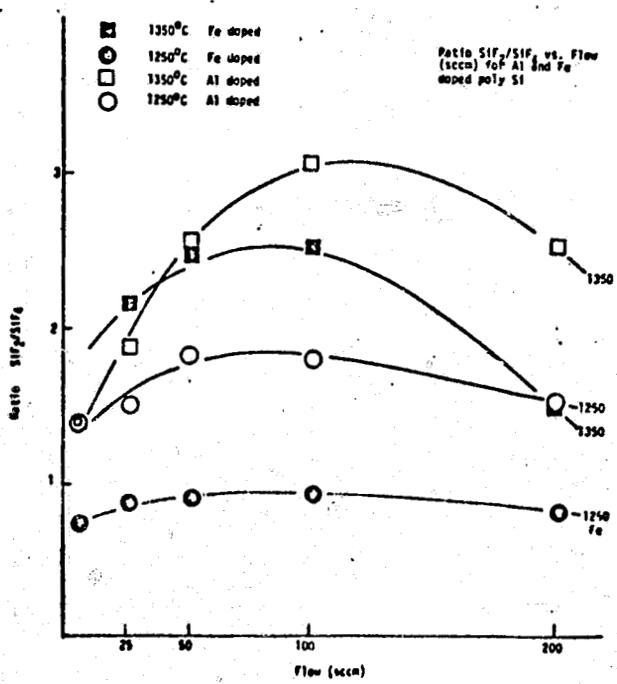
Figure 2.1.4 (b)

Figure 2.1.4 (c)

Figure 2.1.4 Counts and ratios of reactants
and products versus SiF_4 flow for
Fe doped sg poly Si and purified SiF_4.

(SiF$_2$ counts)/(SiF$_4$ counts) vs. SiF$_4$ flow
for the reaction mg Si + SiF$_4$ $\longrightarrow$ 2SiF$_2$

1350°C

1250°C
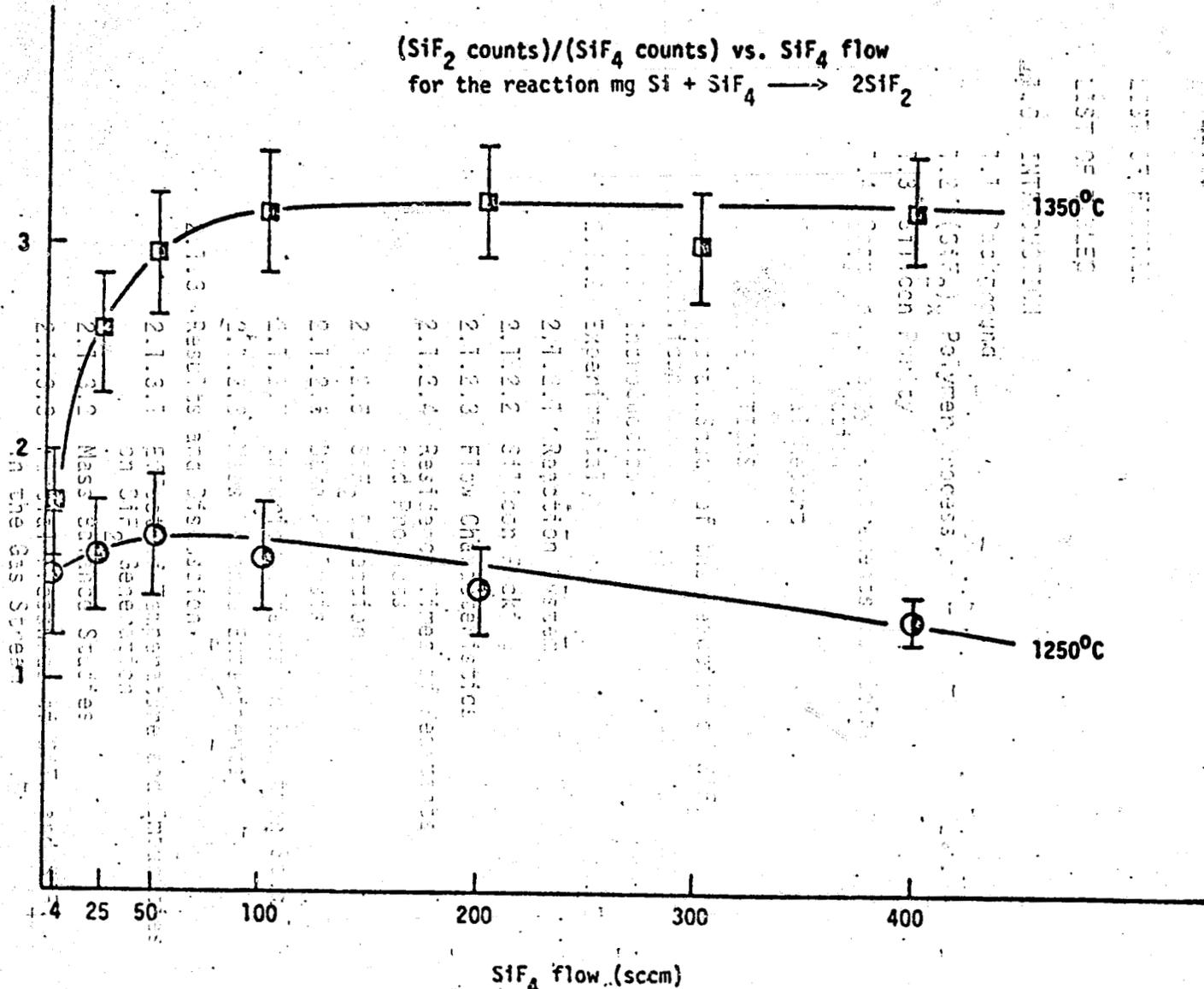
SiF$_4$ flow (sccm)

Figure 2.1.5   Ratio SiF$_2$/SiF$_4$ counts versus SiF$_4$ flow for mg Si and SiF$_4$.

(3) At flows greater than approximately 100 sccm at 1350°C, the SiF_2/SiF_4 ratio becomes approximately constant up to the highest measured flow. Therefore, the optimum flow rate with regard to polymer formation is determined by the efficiency of the SiF_4 recovery, and economic factors governing reaction run time.

(4) No major difference in the ratio of SiF_2/SiF_4 was observed within the imposed 90% probability constraint, for reactions involving purified and unpurified SiF_4.

2.1.3.2 Mass Balance Studies

In order to derive information regarding the SiF_2 concentration under specified reaction conditions and to examine the reliability of the ratio of SiF_2 to SiF_4, a series of mass balance experiments was undertaken. In conjunction with these studies, data regarding the stoichiometry was collected.

A prerequisite to accurate mass balance determination is precise knowledge of the weight of SiF_4 delivered by the mass flow controller with time. Due to the corrosive nature of SiF_4, no previous direct calibration had been made. Thus, an accurate calibration of the Matheson flow controller was performed for flows between 12.5 and 200 sccm. Matheson reports a gas conversion factor for their flow controller of 0.394 for SiF_4.[7] A value of 0.51 $\pm$ 0.01 was obtained in our calibration experiments using a SiF_4 flow of 100 sccm, under our laboratory conditions.

Use of this conversion factor allows accurate calculation of the number of moles SiF_4 delivered. Procedures were developed to recover unreacted SiF_4 which were accurate to within $\pm$ 0.01 gms at 25°C. Hence a knowledge of the weight of polymer recovered coupled with the weight of silicon consumed during the reaction provided information for (i) accurate mass balance calculations, (ii) correlation of counts to actual weight of reactants and products, and (iii) stoichiometric determination of reaction 1.

Experiments conducted at 1350°C showed that ∿75% of the reactant SiF_4 was consumed in the reaction. Furthermore, a stoichiometry for reaction 1,

$$x \; SiF_4 + y \; Si \longrightarrow z \; SiF_2, \text{ was determined by}$$

$$1 \; SiF_4 + 1 \; Si \longrightarrow 2 \; SiF_2 \qquad \qquad \text{Step 1}$$

at $1350^{\circ}C$.

Table 2.1-3. Stoichiometry of reaction Step 1

$$x = 6.82 \cdot 10^{-2} \text{ moles } SiF_4 \text{ reacted}$$
$$y = 6.6 \cdot 10^{-2} \text{ moles } Si \text{ reacted}$$
$$z = 1.35 \cdot 10^{-1} \text{ moles } SiF_2 \text{ produced}$$

These stoichiometric experiments involved weighing the unconverted polymer produced and the assumption that formation of the polymer followed reaction step 2.[2]

$$z \; SiF_2 \xrightarrow{\; <45^{\circ}C \;} (SiF_2)_z \qquad \qquad \text{Step 2}$$
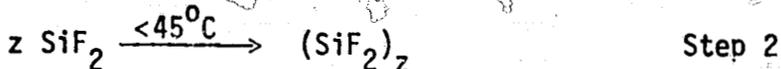
Mass balance results for reaction step 1 were such that total weight products/ total weight reactants differed by less than 1%.

$$\frac{\Sigma \text{ products}}{\Sigma \text{ reactants}} \geq 0.99$$

It is concluded from the stoichiometry, percent SiF_4 conversion and mass balance experiments that reaction step 1 is correct as written using our experimental apparatus and procedure. Further, a 75% conversion of SiF_4 was obtained, a considerable increase over previous workers (Table 2.1-4) due mainly to our higher operating temperature.

Table 2.1-4.

	Percent SiF_4 Conversion	Ref.
Pease	40%	1
Margrave	48%(a)	3,7
This work	75%	

(a) Calculation based on reference 3

19

2.1.3.3 Partial Pressures of SiF$_2$ and SiF$_4$ in the Gas Stream

While the ratio of SiF$_2$/SiF$_4$ counts in the gas stream provides insight into the conditions leading to maximum formation of SiF$_2$ from reactants, the partial pressures of the reactants and products in the gas stream are also of interest. Consequently effort was focused at correlating the counts of SiF$_2$ and SiF$_4$ under given reaction conditions with the partial pressure of SiF$_2$ and SiF$_4$ in the gas stream. This calculation was based on the following data: (i) the total downstream pressure measured, (ii) the mole fraction of SiF$_2$ and SiF$_4$ derived from an accurate mass balance, (iii) the observed stoichiometry, and (iv) the counts of SiF$_2$ and SiF$_4$ measured by the GC/MS for the 1200 spectra comprising the mg Si + SiF$_4$ reaction at 1350°C and 1250°C. Two assumptions were made to allow the conversion from counts to partial pressures: (i) that 99% of the downstream gas mixture was SiF$_2$ and SiF$_4$[3], (ii) that the polymer formation followed reaction step 2.

Figure 2.1.6 is a graph of the calculated downstream partial pressure of SiF$_2$ and SiF$_4$ versus SiF$_4$ flow into the reaction chamber for mg Si at 1350°C for flows up to the maximum measured 1.2 gms SiF$_4$/minute. It is of interest to note that while the partial pressures of SiF$_2$ and SiF$_4$ are observed to increase with SiF$_4$ flow into the reaction chamber up to the highest SiF$_4$ flow measured, Margrave[8] states that polymerization occurs if the pressure of SiF$_2$ exceeds 1 to 2 torr. The total downstream pressure at the highest flow measured is less than 0.50 torr and hence no polymerization is expected. However, 1 to 2 torr may represent the upper limit of total pressure of products and may have contributed to lower SiF$_4$ conversions due to less efficient pumping.

Partial Pressure vs. SiF$_4$ Flow
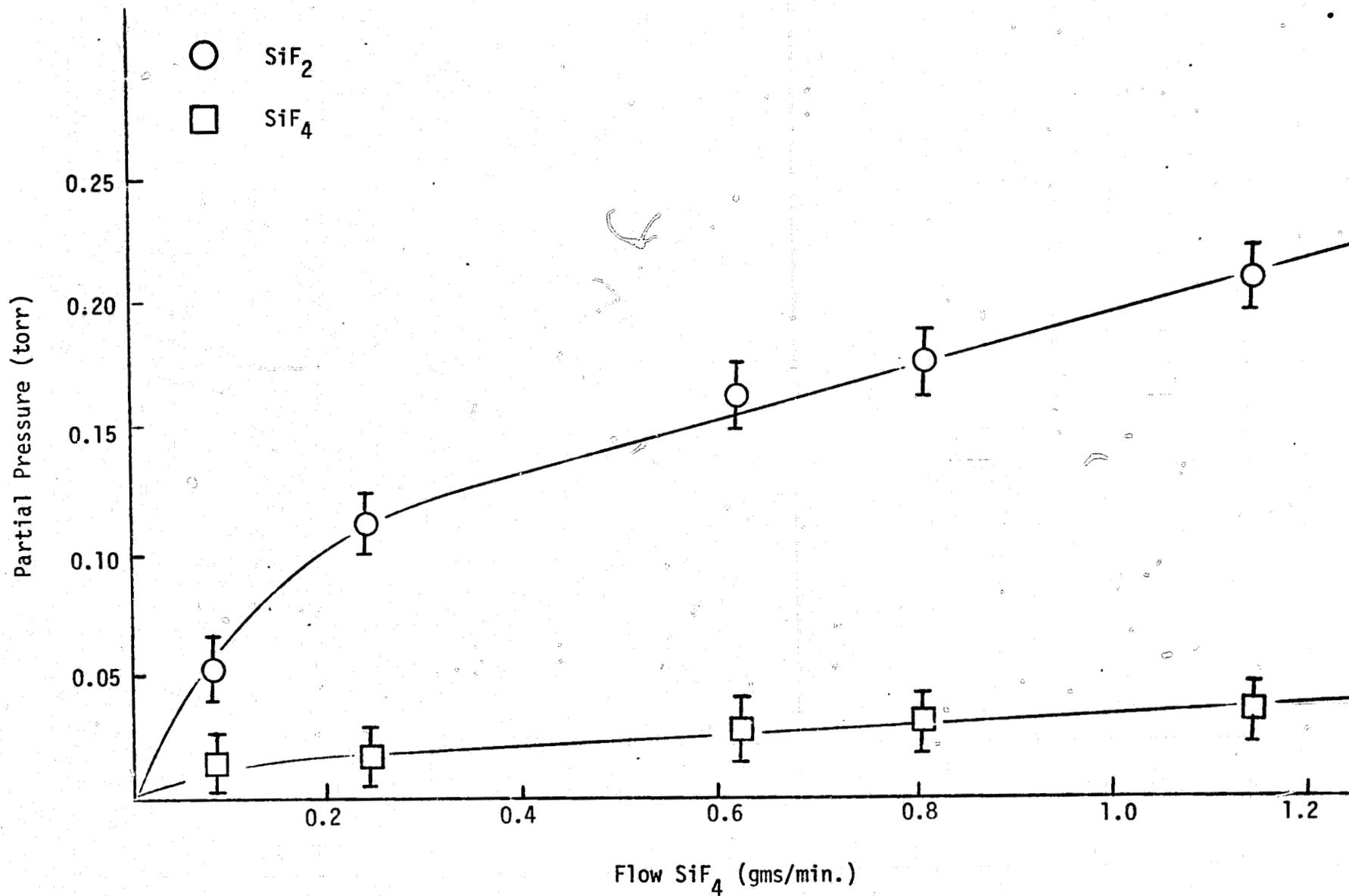
Figure 2.1.6 Partial pressures of SiF$_4$ versus SiF$_4$ flow for mg Si at 1350°C.

2.2   Thermal Disproportionation of $(SiF_2)_x$ Polymer

2.2.1   Introduction

Subsequent to the analysis of stoichiometry, mass balance and chemical feasibility of reaction step 1, a series of experiments was undertaken to study the conversion of polymer into product via reaction steps 3a and 3b

$$(SiF_2)_x \xrightarrow{\ \ >360^{\circ}C\ \ } Si + SiF_4 + SiF_y F_z \qquad \text{Step 3a}$$

$$Si_x F_y \xrightarrow{\ \ \geq 730^{\circ}C\ \ } Si(crystalline) + SiF_4 \qquad \text{Step 3b}$$
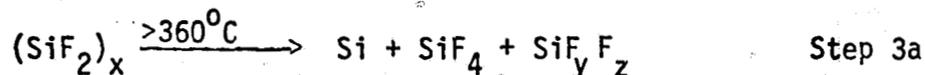
The major products of step 3a being Si and SiF_4. In our initial experiments directed at optimization of steps 3a and 3b, conversion of the polymer appeared to follow a sequence of reactions different from the previously reported steps 3a and 3b. Specifically, at temperatures of $170^{\circ}C$ to $200^{\circ}C$ a phase change occurred and oils appeared at the interface of the polymer film and the heated polymer condensation surface. Further heating of the polymer resulted in a rapid formation of gaseous products.. It was concluded that conversion of $(SiF_2)_x$ polymer into silicon was not a direct process as described in steps 3a and 3b but involved the intermediate formation of $Si_n F_{2n+2}$ homologues as the major product[*].

These conclusions were verified by mass spectrometry which provided data consistent with the published literature on $(SiF_2)_x$ polymer conversion. Therefore reaction step 3a required to be rewritten as:

$$(SiF_2)_x \xrightarrow{\ \ \Delta\ \ } Si_x F_y \uparrow \qquad \text{Step 3a}$$

Elucidation of a new reaction sequence required examination of the feasibility of thermal disproportionation of the $Si_x F_y$ homologues into silicon. The initial effort was directed at definition of the homologue disproportionation chemistry on heated quartz surfaces. The homologue conversion step was de-termined to be:

$$Si_x F_y \xrightarrow{\ \ \Delta\ \ } Si + SiF_4 \qquad \text{Step 3b}$$

---

[*]$Si_n F_{2n+2}$ refers to species following the $Si_2 F_6$, $Si_3 F_8$ etc. series, a subset of the more general abbreviation $Si_x F_y$, which also includes the $Si_N F_{2N}$ species.

The conversion efficiencies and reaction parameters derived from these early studies were subsequently tested on a conversion apparatus with greater surface area and consequently greater throughput potential; i.e., a heated, silicon particle fixed bed.

A kinetic analysis regarding the homologue conversion on fixed beds was performed. The desirability of higher homologue throughput and higher conversion efficiencies led to the development of a low pressure fluidized bed for thermal disproportionation. Data regarding homologue conversion efficiencies was generated. A final extension of the low pressure fluidized bed concept for homologue conversion was the development of a low pressure pneumatic particle lifter, the latter being designed for maximum homologue throughput. Data relating homologue residence time and conversion efficiencies was generated.

2.2.2 Preliminary Experiments Involving Polymer Conversion: The Condensation-Disproportionation Coil

2.2.2.1 Experimental

In our initial experiments directed at optimization of the reaction steps involving conversion of $(SiF_2)_x$ polymer according to reaction step 3a an apparatus was designed for low temperature capture of $SiF_2(g)$ to form $(SiF_2)_x$ polymer and subsequent high temperature conversion of the polymer into silicon.

The apparatus used consisted of a small 2 inch coil reactor fitted with a condensation disproportionation coil (hereafter termed C-D coil) shown in Figure 2.2.1a.

The C-D coil consisted of a helical spiral of 0.5 inch quartz tubing with gaseous inlet and outlet facilities fixed inside a 2 inch diameter quartz column.

A high temperature, high resistance Alumel wire was fixed inside the quartz spiral with electrical connections made to two 140 V/12 A Variac transformers connected in series. Apertures at inlet and outlet ports allow insertion of thermocouples for temperature monitoring.

23

Figure 1(a)

36 inch quartz C-D coil

(1) inlet/out/electrical connection apperture

(2) quartz spiral

(3) trap
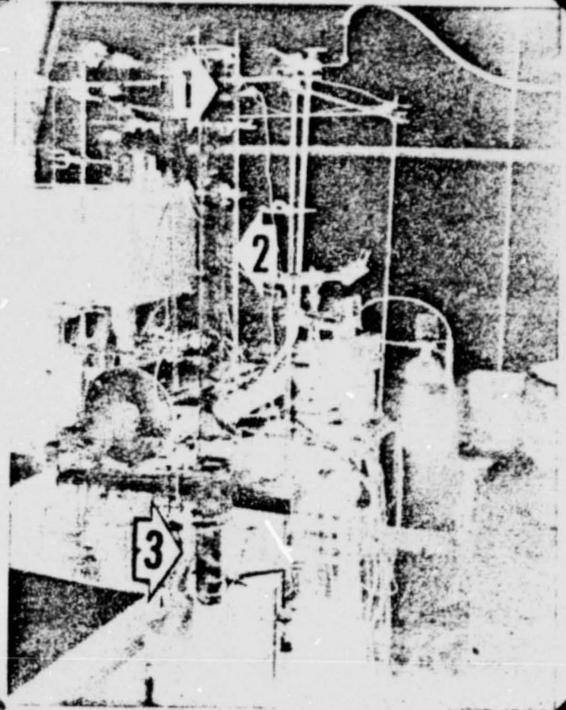
Figure 1(b)

Close up of 36 inch quartz C-D coil

(1) N_2/He inlet/outlet

(2) Thermocouple apperture

(3) Electrical connection

(4) Alumel heating with inside quartz spiral
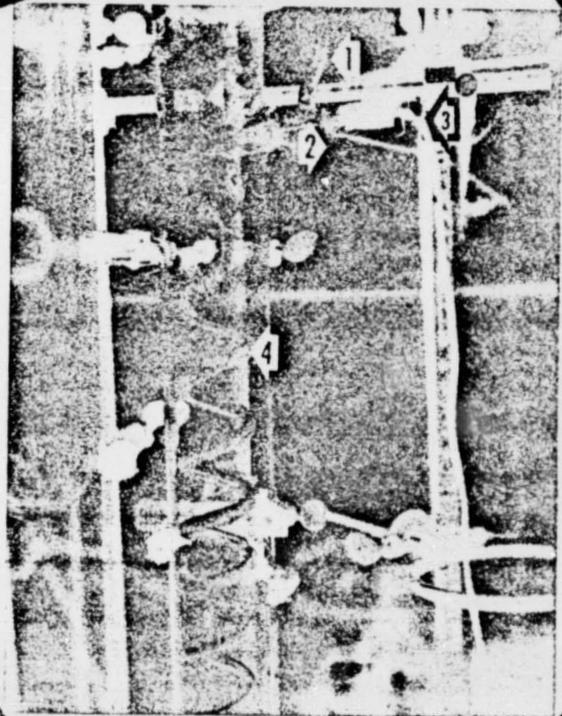
Operation of the coil involved passage of liquid nitrogen through the inner quartz helix facilitating condensation of gaseous SiF_2 into polymer $(SiF_2)_x$. Temperatures on the helix as low as $-196^{\circ}C$ were achieved by this technique. Subsequent to condensation of $(SiF_2)_x$ upon the coil, conversion of the polymer (reaction step 4) was brought about by passing an electrical current through the wire running down the center of the helix. This caused the wire to heat, resulting in conversion of the polymer adhering to the coil.

The most effective procedure for achieving temperatures between $0^{\circ}C$ and $-100^{\circ}C$ involved heating the wire concurrent with passage of liquid N_2 down the spiral. Temperatures constant to $\pm 1^{\circ}C$ were obtained with this method.

2.2.2.2 Results

Three sets of experiments involving polymer conversion were performed using the C-D coil. The first involved low temperature ($-175^{\circ}C$) condensation of $(SiF_2)_x$ on the C-D coil utilizing reaction conditions found in previous experiments to optimize SiF_2 production. The second set involved $-100^{\circ}C$ condensation of $(SiF_2)_x$ on the coil, and the third set was run at temperatures between $-70^{\circ}C$ and $-35^{\circ}C$. The polymer formed in these experiments was converted under the same conditions at temperatures between 0 and $550^{\circ}C$.

Regarding condensation temperature, a temperature of $-69^{\circ}C$ was found to effectively condense the polymer on the first three coils of the quartz helix.

It was concluded that $-69^{\circ}C$ is sufficient to trap gaseous SiF_2 on the 36 inch C-D coil yet allow only a minimum amount of SiF_4 to co-condense with the polymer.

In our initial experiments, conversion of the polymer via reaction step 3 appeared to follow the same sequence of steps for all three sets of experiments described above. Specifically, at temperatures of +170 to $200^{\circ}C$ oils appeared at the interface of the polymer and the heated quartz spiral. The

unconverted polymer was thus separated from the coil by these oils and fell under gravity to the bottom trap. (Figure 2.2.1(a)).

The polymer in the trap was heated to between 0 and $510^{\circ}C$ at a rate of $\sim10^{\circ}C/$minute. It was observed that at $250\text{-}300^{\circ}C$ the polymer melted liberating oils and leaving a residue. Further heating resulted in a rapid formation of oils at approximately $390^{\circ}C$, followed by formation of silicon from the latter at $410\text{-}510^{\circ}C$.

Margrave reported that at $200\text{-}350^{\circ}C$ $(SiF_2)_x$ decomposes to give per-fluorosilanes, Si_nF_{2n+2} and leaves a silicon rich polymer.[7]

$$[(n + 2)/x] \; (SiF_2)_x \longrightarrow Si_nF_{2n+2} + 2(SiF) \quad polymer$$

Further, he states that at $400^{\circ}C$ the decomposition becomes very rapid yielding mainly SiF_4 and Si. These observations are consistent with ours. In addition, we observed that the reaction at $400^{\circ}C$ coincides with the formation of oils from the "silicon rich polymer."

We observed that the polymer conversion appears to involve initial formation of oils, followed by thermal disproportionation to Si. Mass spectral analysis of the Si_xF_y fragments liberated upon heating of the polymer are listed in Table 2.2-1 together with the temperature at which they were observed.

Table 2.2-1 Mass spectrum of volatile components of
polymer thermal decomposition.

$Si_nF_{(2n+1)}$	m/e	$T^{\circ}C$
$Si_2F_5^+$	151	180
$Si_3F_7^+$	217	285
$Si_4F_9^+$	283	Liberated from cold trap after passing $500^{\circ}C$ quartz coil

Table 2.2-1 is not inclusive but does indicate that the lower molecular weight fragments were liberated in the initial heating stages.

2.2.3 Thermal Disproportionation of Homologues on a Heated Quartz Surface

2.2.3.1 Experimental

In these experiments thermal disproportionation of the homologues liberated from the polymer as discussed in the previous section was demonstrated on a modified 2 inch quartz reactor at temperatures up to $850^{\circ}C$ using the batch method for polymer formation. Quartz was chosen as the preferred substrate for initial thermal disproportionation studies due to the ease of construction, modification, and cleaning of a quartz reactor as opposed to more conventional substrates such as silicon, tungsten or molybdenum. A batch method of polymer formation and conversion was chosen due to the greater capability of obtaining quantitative results as opposed to a semi-continuous method of deposition and conversion. It will be noted however, that data obtained using the batch method of polymer conversion is directly applicable to a semi-continuous mode of polymer formation and conversion.

A system was designed utilizing the basic concepts of the condensation-disproportionation coil, while incorporating a high temperature zone for the disproportionation reaction. In this apparatus the volatile products of the oils generated at low temperatures $\leq 400^{\circ}C$ were passed across a high temperature $(750^{\circ}C - 950^{\circ}C)$ quartz hot zone (hot collar) where disproportionation into silicon occurred. Volatiles, not disproportionated, condensed in a cool zone $(>170^{\circ}C)$ above the hot collar, then passed back through the hot zone and disproportionated. They then liberated volatiles and/or condensed into the bottom trap where they were again heated above their boiling point liberating the more volatile constituents. This reflux-disproportionation technique allowed separation of volatile homologues as in a more conventional fractional distillation but offered the advantage that collection and subsequent disproportionation of the individual homologues was not required, because the separation was affected by their disproportionation into silicon upon exposure to the high temperature zone.

Further, it was found that with each pass of the hot zone, the number of components remaining in the homologue mixture was reduced as would occur in a conventional fractional distillation. Figures 2.2.2(a) and 2.2.2(b) show this reflux-disproportionation apparatus after a typical high temperature polymer conversion.

Figure 2.2.2(a) - Reflux-disproportionation apparatus.

(1) Polymer condensation trap -78°C

(2) Hot collar 850°C

(3) Vertical reflux column

(4) SiF_4 trap
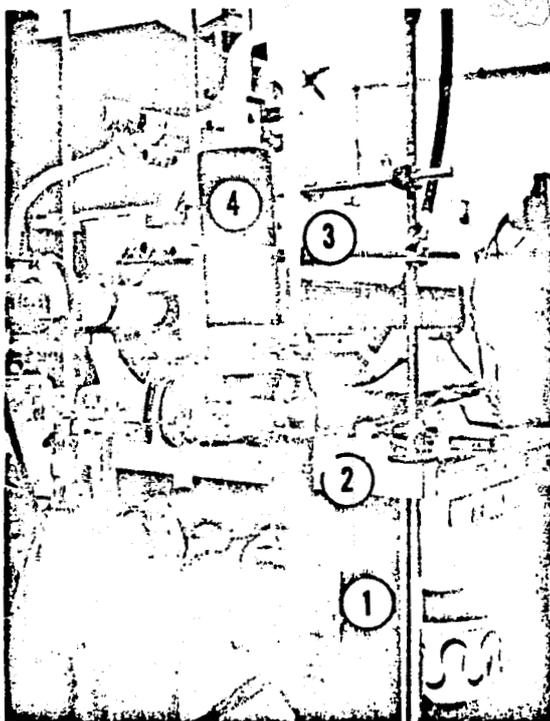
Figure 2.2.2(b) — Close up view of trap and hot collar regions of reflux-disproportionation apparatus after a successful conversion experiment.

(1) Polymer condensation trap - note absence of oils

(2) Hot collar zone, quantitative conversion to silicon apparent

(3), (4), (5) Regions adjacent to hot zone, note lack of oils formed in these areas indicating complete conversion in hot collar zone (2).
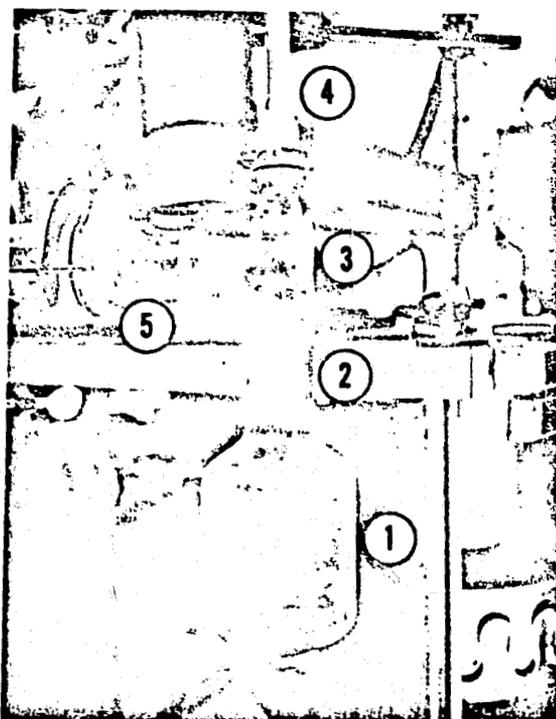
In these experiments SiF_4 was passed across a 15 inch zone of mg silicon heated at 1350°C at a flow of 0.24 gms SiF_4 per minute (unless otherwise indicated) for polymer formation reaction times varying from 30 to 90 minutes.

Formation of polymer from SiF_2 took place in trap 1 (Figure 2.2.2 (a)) at -78°C in a isopropyl·dry ice slush bath; unreacted SiF_4 was collected in trap 4 (Figure 2.2.1(a)). Subsequent to polymer formation, the slush bath was replaced with a heating mantle (region (1), Figures 2.2.2(a) and 2.2.2(b)). Then a high resistance furnace heating element was wrapped around the 4" long constriction adjacent to the polymerization trap (region 2, Figures 2.2.2(a) and 2.2.2(b)) and connected to a 140 V/10A Variac transformer. This hot collar was heated to 850°C before power was applied to the heating mantle surrounding the condensation trap. The temperature of the condensation trap was raised to 400°C at a heating rate of 10°C/minute with disproportionation of the oils into silicon in the hot zone occurring over a temperature range 200°C to 400°C.

Under these reaction conditions no evidence was observed of oil formation from condensed volatiles in regions 3, 4, and 5 of Figure 2.2.2(b). This apparatus and operation technique was used to obtain mass spectral data correlating species liberated during thermal conversion with pressure and temperature. Further, data from this apparatus was collected to calculate the % SiF_4 conversion for the reaction between SiF_4 and mg Si, % homologue conversion, overall silicon to silicon yield, mass balance for the reaction step and stoichiometry for the homologue to silicon conversion.

2.2.3.2 Results and Discussion

2.2.3.2.1 Mass Spectral Analysis of Homologues

Analysis of data correlating pressure changes occurring during polymer conversion with polymer conversion temperature and homologue composition is summarized in Figures 2.2.3 and 2.2.4. It will be noted that both figures show the same trend, a shoulder at approximately 260°C to 280°C, a peak maximum
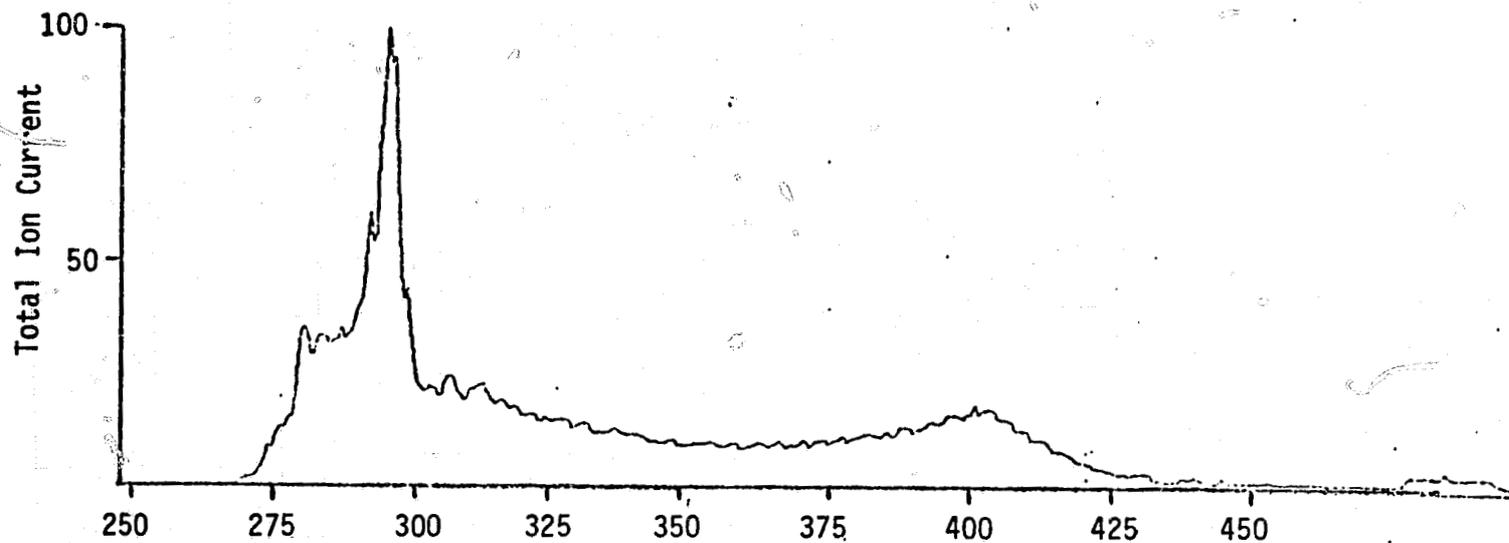
Figure 2.2.3   Sum of total ions counted during polymer conversion versus temperature.
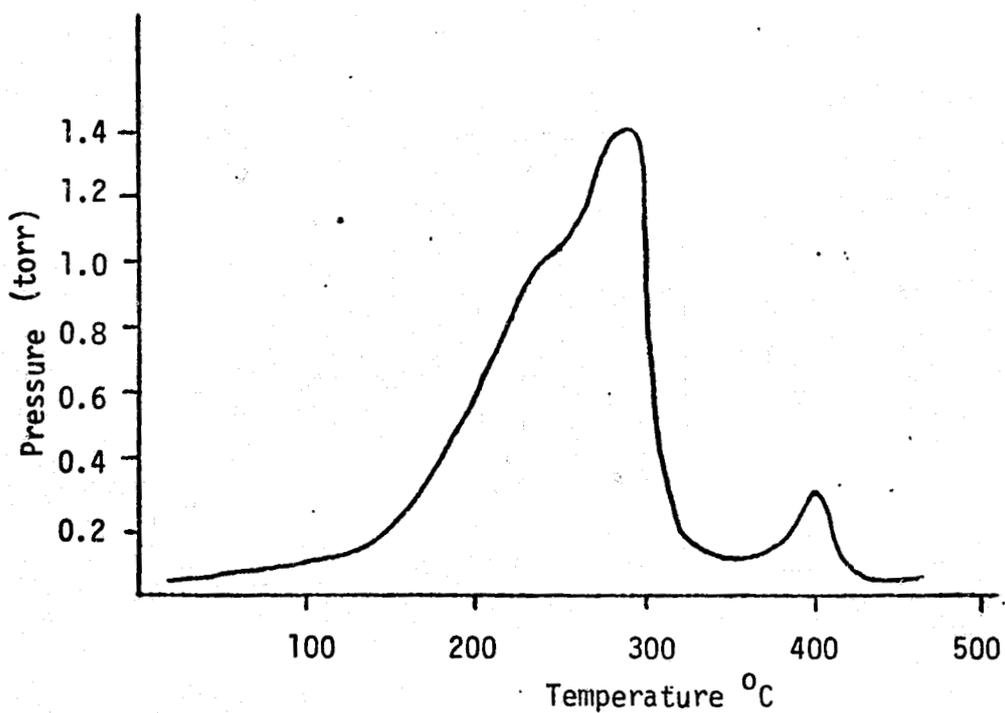
Figure 2.2.4   Pressure variation with temperature for products liberated during homologue conversion.

31

at $290^{\circ}C$ to $300^{\circ}C$ and a second smaller peak at $400^{\circ}C$. Figures 2.2.5(a) to 2.2.5(e) are mass spectra taken at the temperatures of approximately 250°, 280°, 295°, 350°, and $400^{\circ}C$. Temperatures indicated in Figure 2.2.3 are extrapolated from Figure 2.2.4 as the latter represents a more accurate temperature measurement involving the mean of three temperature measurements made with a thermocouple located adjacent to the reactor vessel wall. Possible assignments of the mass spectra of volatile components of the polymer decomposition shown in Figures 2.2.5(a) to 2.2.5(e) are listed in Table 2.2-2. Comparison of Figures 2.2.5(a) to 2.2.5(e) with Figures 2.2.3 and 2.2.4 show that as temperature is increased from $250^{\circ}C$ (Figures 2.2.5(a) to $350^{\circ}C$ (Figure 2.2.5(d) a variation in the concentration of $Si_2F_5^+$ is observed. Further, the $F_3Si-O^+=SiF_2$ peak at m/e 167 becomes insignificant at temperatures above $350^{\circ}C$. Comparison of Figure 2.2.4 with Figures 2.2.5(a) through 2.2.5(d) shows that this is the region of maximum pressure. Consequently, Si_2F_6 may well contribute significantly to the pressure change over this range. It is of interest to note that although not apparent in Figure 2.2.5(c), an enlarged spectrum of the latter reveals evidence of $Si_3F_7^+$ at m/e 217, which likely also contributes to the pressure variation between $250^{\circ}C$ and $350^{\circ}C$. Finally, the spectrum at $400^{\circ}C$ reveals evidence of mainly SiF_4, which is consistent with the observation that the product in the reaction vessel converts into silicon at this temperature, the proposed reaction step being:

$$Si_xF_y \xrightarrow{\;T > 400^{\circ}C\;} Si + SiF_4 \qquad\qquad \text{Step 3b}$$
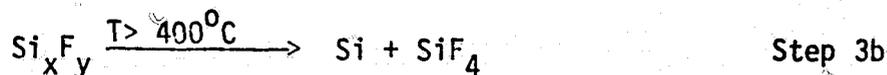
2.2.3.2.2 Experiments Involving Homologue Conversion

Effort was directed toward obtaining data on polymer conversion efficiency, mass balance of homologue conversion and stoichiometry for the reaction step involving conversion of homologues into silicon and SiF_4. In order to generate data for calculations of the above quantities, an accurate knowledge of the (a) stoichiometry, (b) mass balance and (c) SiF_4 conversion efficiency was determined. Our previous work had shown that the stoichiometry
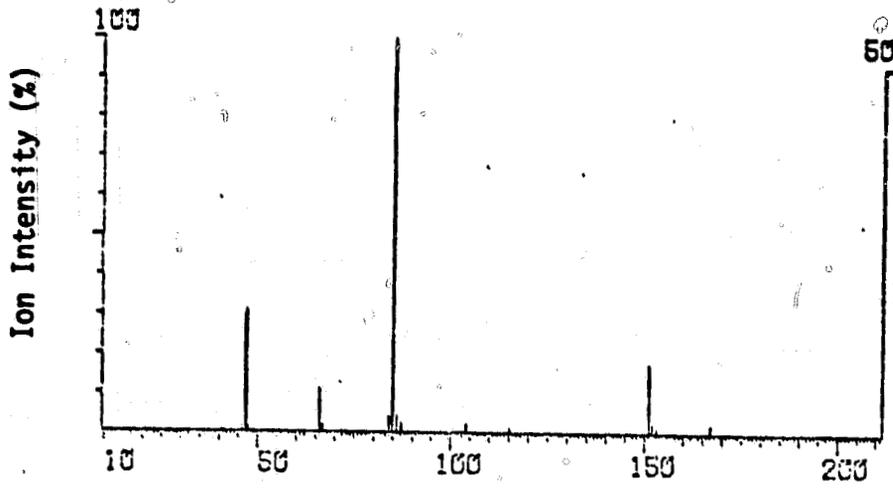
Figure 2.2.5(a) Mass spectrum of volatile components from hmologue conversion at 250°C ± 5°C.
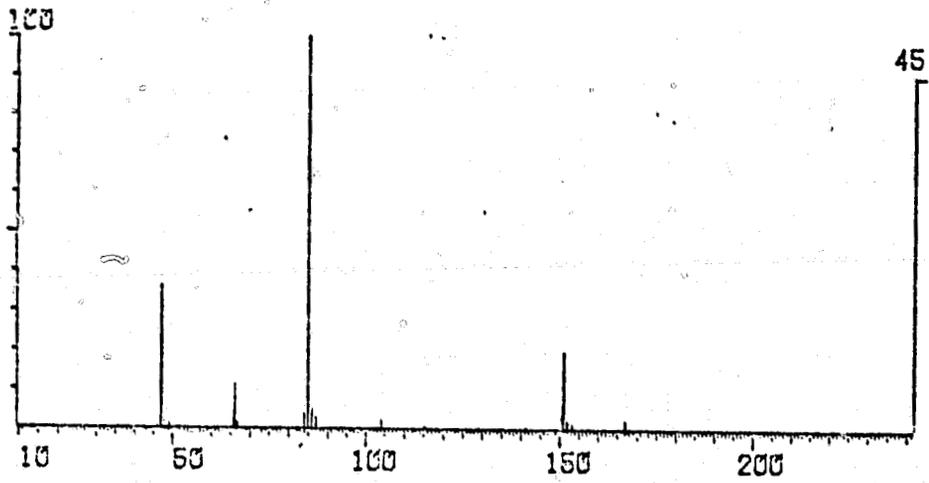
Figure 2.2.5(b) Mass spectrum at 280°C ± 5°C.
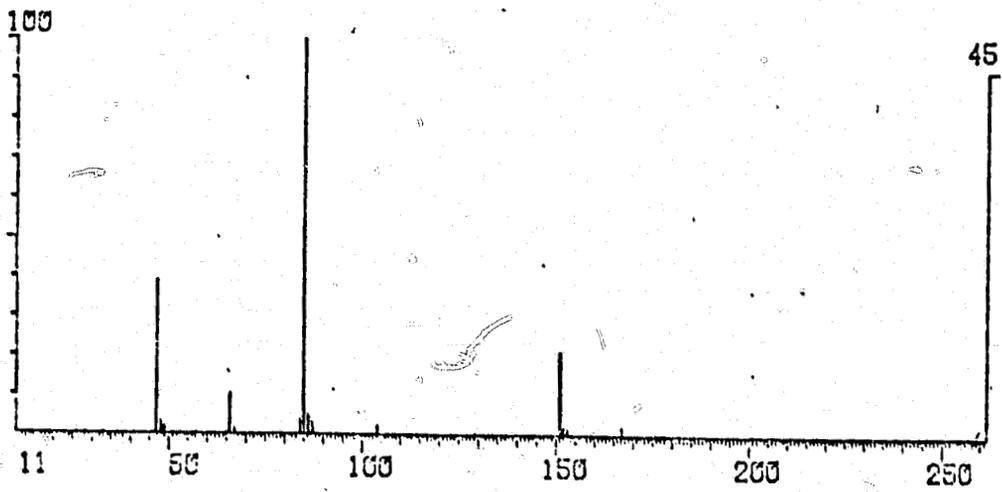
Figure 2.2.5(c) Mass spectrum at 295°C ± 5°C.

33
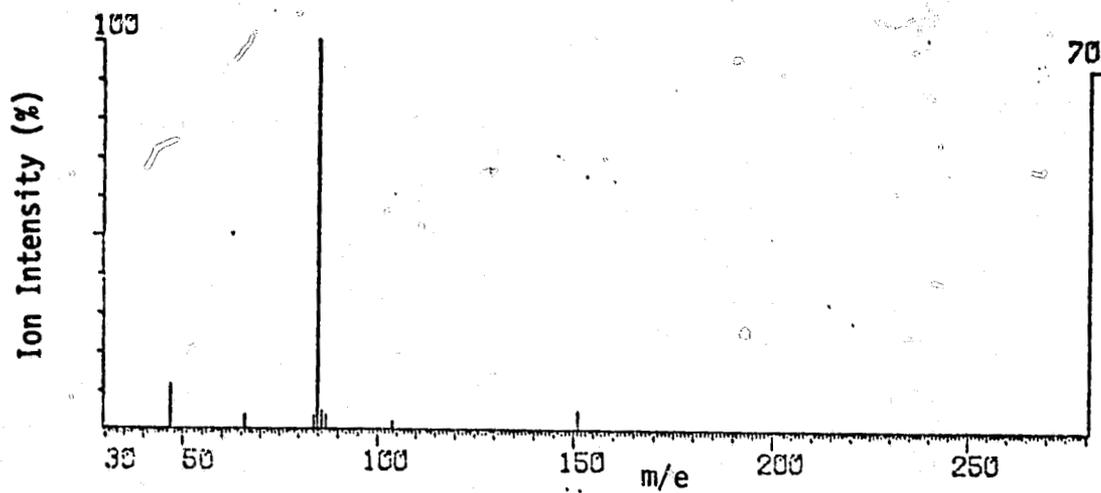
Figure 2.2.5(d) Mass spectrum at 350°C ± 5°C.
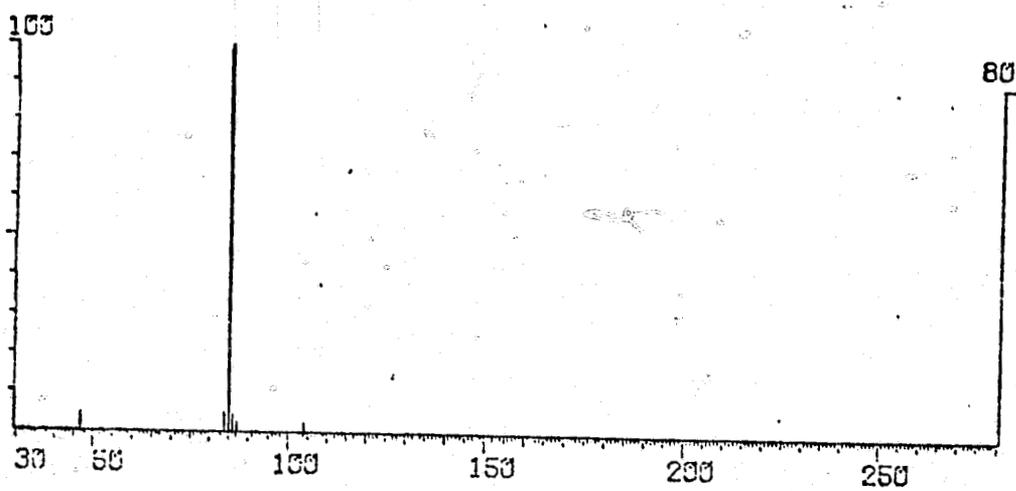
Figure 2.2.5(e) Mass spectrum at 400°C ± 5°C.

34

TABLE 2.2-2

Table 2.2-2   Mass spectrum of volatile components
of SiF_2 polymer decomposition

m/e	Possible Assignment
167	$F_3Si-O^+=SiF_2$
153	Isotope of m/e 151
152	" " " "
151	$Si_2F_5^+$
104	SiF_4^+
87	Isotope of m/e 85
86	" " " "
85	SiF_3^+
84	Unassigned
67	Isotope of m/e 66
66	SiF_2^+
49	Isotope of m/e 47
48	" " " "
47	SiF^+

of reaction step 1 is accurately 1:1:2 (Section 2.1.3.2).

$$Si + SiF_4 \longrightarrow 2SiF_2 \qquad \text{reaction step 1}$$

Further, it had been shown that the mass balance for step 1 is such that

$$\frac{\Sigma \text{ Products}}{\Sigma \text{ Reactants}} = \geq 0.99$$

Table 2.2-3 lists data for the efficiency for SiF_4 conversion. It will be noted that the mean SiF_4 conversion efficiency derived from a larger data base is 78% conversion versus the previously reported 75% conversion efficiency.

Knowledge of a, b, and c described in the previous paragraph allows calculation of weight of silicon reacted (in these particular experiments weighing the charge after reaction was impractical), weight of polymer formed, and leads to the calculation of mass balance and stoichiometry for the homologue conversion.

Table 2.2-4 presents data comparing weight of silicon consumed during reaction step 1 and actual weight of silicon produced following homologue conversion. Here it will be noted that homologue conversion efficiency is between 52% and 76%, depending on hot zone residence time which is directly related in this standard reaction system to weight of polymer formed.

Table 2.2-5 presents the polymer conversion efficiency derived from the calculated yield of polymer and the weight of unconverted polymer. Comparison of the average conversion efficiencies using these two methods of calculation shows good correlation.

Table 2.2-6 shows data for the mass balance, listing the amounts of material consumed and material formed. The quotient obtained indicates that within the experimental limits for obtaining the weight of unconverted polymer the sum of the reactants consumed equals that of products formed.

36

TABLE 2.2-3

Table 2.2-3 SiF_4 CONVERSION EFFICIENCY

Run	Run Time	Flow	gms. SiF_4 Delivered	gms. SiF_4 Unreacted	% SiF_4 Conversion
1	90(min)	0.24(g/min)	21.60(g)	6.07(g)	72%
2	20	0.24	4.8	0.9	81
3	40	0.24	9.6	2.3	76
4	60	0.28	16.8	4.6	73
11	60	0.24	14.4	3.10	79
12	60	0.24	14.4	3.60	75
13	60	0.24	14.4	3.10	79
14	45	0.24	10.8	2.5	77
15	45	0.24	10.8	2.4	78
16	45	0.24	10.8	1.7	84
18	60	0.24	14.4	2.95	80
					$\overline{78}$

Mean SiF_4 Conversion   78%
efficiency

TABLE 2.2-4

Table 2.2-4 % POLYMER CONVERSION BASED ON SILICON INPUT, OUTPUT

FLOW = 0.24 g/min.

Run	Run Time	gms. SiF_4 Reacted	Moles SiF_4 Reacted	gms. Si Reacted	gms. Formed After Conversion	% Polymer Conversion
6	30 min.	5.62(g)	0.054 moles	1.51(g)	1.10(g)	72%
7	30	5.62	0.054	1.51	1.35	89
8	30	5.62	0.054	1.51	1.0	66
						76%
14	45	8.3	0.080	2.24	1.1	49
15	45	8.4	0.081	2.26	1.2	53
16	45	9.1	0.088	2.45	1.3	53
17	45	8.6	0.083	2.3	1.2	52
						52%
11	60	11.3	0.109	3.04	1.2	39
12	60	10.8	0.104	2.90	2.2	76
13	60	11.3	0.109	3.04	1.7	56
18	60	11.45	0.11	3.08	1.6	52
						56%
10	90	16.85	0.162	4.54	2.4	52%

38

Table 2.2-5   % POLYMER CONVERSION BASED ON POLYMER
FORMED AND POLYMER UNCONVERTED

FLOW = 0.24 g/min.

Run	Run Time	gms. SiF_4 Reacted	gms. Si Reacted	gms. Polymer Formed	gms. Polymer Unconverted	% Polymer Conversion
11	60 min.	11.3(g)	3.04(g)	14.34(g)	6.05(g)	58%
12	60	10.8	2.90	13.7	4.7	66
13	60	11.3	3.04	14.34	5.5	62
						$\overline{62\%}$
16	45	9.1	2.45	11.55	5.1	56
17	45	8.6	2.3	10.9	4.1	62
						59%

39

Table 2.2-6   MASS BALANCE

FLOW = 0.24 g/min.

Run	Run Time	gms. Material In	gms. Material Out	gms. Out / gms. In
11	60 min.	14.34(g)	10.95(g)	0.76
13	60	14.34	13.3	0.93
16	45	11.55	9.1	0.79
			Mean =	0.83

Table 2.2-7 lists data for calculation of the stoichiometry of the homologue conversion to Si and SiF_4 based on actual weights of silicon produced and SiF_4 liberated. We note that for each mole of silicon formed one mole of SiF_4 is generated.

Thus, the thermal disproportionation of homologues into silicon on a heated surface was demonstrated. An overall silicon to silicon yield of 59% for this experimental system was achieved.

2.2.4   Residual Homologue Conversion

2.2.4.1 Experimental

In the previous section data on homologue conversion efficiency on a heated quartz surface was presented. It was shown that under non-optimized reaction conditions, polymer conversion efficiencies of from 60% to 80% could be reproducibly achieved. Further, it was observed that following thermal conversion, the unconverted volatile fraction (20% to 40%) reformed a polymer-like material at liquid N_2 temperatures.

$$(SiF_2)_x \xrightarrow{\Delta} Si_xF_y \xrightarrow{>>400^oC} Si + SiF_4 + (SiF_2)'_x$$

$$(SiF_2)'_x \xrightarrow{\Delta} Si + SiF_4$$
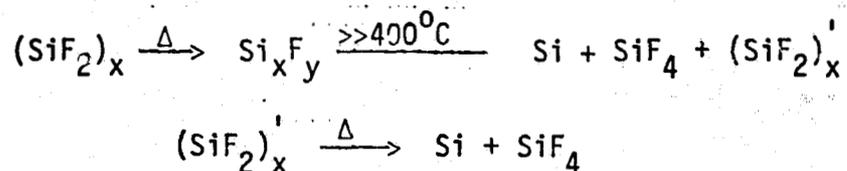
While it should be noted that optimization of the thermal disproportionation reaction apparatus would reduce the remaining unconverted fraction, $(SiF_2)'_x$, to a few percent, a series of experiments was undertaken to study the chemistry of both the $(SiF_2)_x$ and volatile products liberated from these during thermal conversion and also the polymer formed $((SiF_2)'_x)$ from condensed homologues liberated during $(SiF_2)_x$ conversion. Mass spectral analysis of the homologues liberated from the reformed polymer was also conducted.

A system was designed utilizing the basic concepts of the condensation-disproportionation coil, while incorporating a high temperature zone for the residual polymer $(SiF_2)'_x$ disproportionation reaction. In this apparatus the volatile products of the oils generated on heating the $(SiF_2)_x$ at low temperatures (400^oC) were passed across a high temperature (750^oC - 950^oC) quartz hot zone where disproportionation into silicon occurred. The apparatus

Table 2.2-7   STOICHIOMETRY

FLOW = 0.24 g/min.

Run	Run Time	Moles Si Formed After Conversion	Moles SiF_4 Liberated During Conversion	$\dfrac{\text{Moles } SiF_4}{\text{Moles Si}}$
11	60 min.	0.043 moles	0.036 moles	0.84
12	60	0.079	0.076	0.96
13	60	0.061	0.059	0.97
15	45	0.043	0.044	1.02
			Mean =	0.95

42

consisted of 2 identical polymer trapping vessels directly adjacent to a region capable of being heated to $850^{\circ}C$, Figure 2.2.6(a) and 2.2.6(b). These two units were connected by a 16 inch quartz homologue transport tube heated to $220^{\circ}C$. Polymer formation was allowed to occur in one half of the unit and subsequent thermal conversion forced volatiles past a quartz surface heated to $850^{\circ}C$. Thermal disproportionation of Si_xF_y homologues into silicon occurred in the $850^{\circ}C$ zone while the unconverted 20% - 40% was transported across the $220^{\circ}C$ zone into the 2nd condensation unit. Subsequent thermal conversion of the residue polymer, $(SiF_2)'_x$, formed from condensed unconverted Si_xF_y homologues forced the homologues past a 2nd $850^{\circ}C$ quartz surface affecting disproportionation into silicon and SiF_4.

In these experiments SiF_4 was passed across a 15 inch zone of mg silicon heated at $1350^{\circ}C$ at a flow of 0.24 gms SiF_4 per minute. Formation of polymer from SiF_2 took place (trap 1,) at $-78^{\circ}C$ in a isopropyl dry ice slush bath, unreacted SiF_4 was collected. Subsequent to polymer formation, the slush bath was replaced with a heating mantle, and a high resistance furnace heating element was wrapped around the 4" long constriction adjacent to the polymerization trap and connected to a 140 V/10A Variac transformer. This hot collar region was heated to $850^{\circ}C$ before power was applied to the heating mantle surrounding the condensation trap. The temperature of the condensation trap was raised to $400^{\circ}C$ at a heating rate of $10^{\circ}C$/minute with disproportionation of the oils into silicon in the hot zone occurring over temperature range $200^{\circ}C$ to $400^{\circ}C$. An identical procedure was followed to effect thermal disproportionation of the residual polymer $(SiF_2)'_x$ formed from unconverted homologues. High efficiencies of residue $(SiF_2)'_x$ disproportionation into silicon were realized on this apparatus.

Under these reaction conditions no evidence was observed of oil formation from condensed volatiles in the horizontal homologue transport region. This apparatus and reaction technique were used to obtain mass spectral data correlating species liberated during thermal conversion with pressure and temperature. Further, data from this apparatus was collected leading to calculations of % SiF_4 conversion (reaction between SiF_4 and mg Si), % homologue conversion, overall silicon to silicon yield, and residue conversion efficiencies.

43
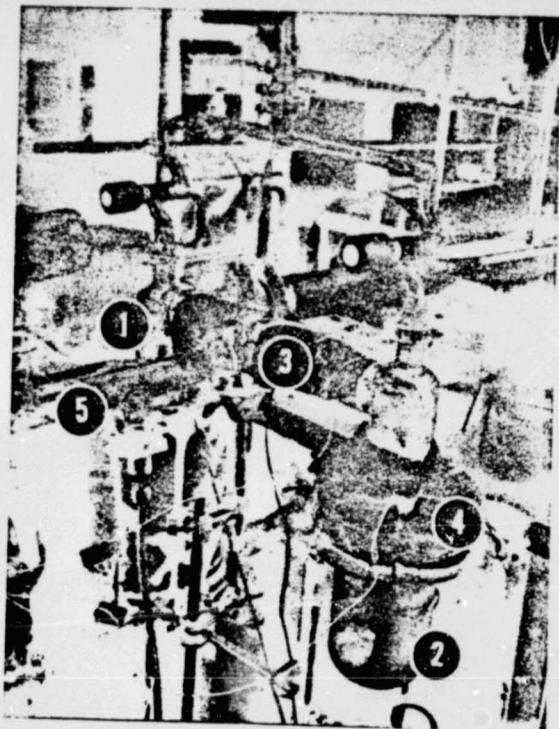
Figure 1a. Homologue Residue Conversion Unit.

1. Polymer trap 1
2. Polymer trap 2
3. Homologue transport region
4. Hot collar region
5. Mass spectrometer inlet.

Figure 1b. Homologue Residue Conversion Unit.

1. Polymer trap 1
2. Polymer trap 2
3. Homologue transport region
4. Hot collar region
5. Mass spectrometer inlet.
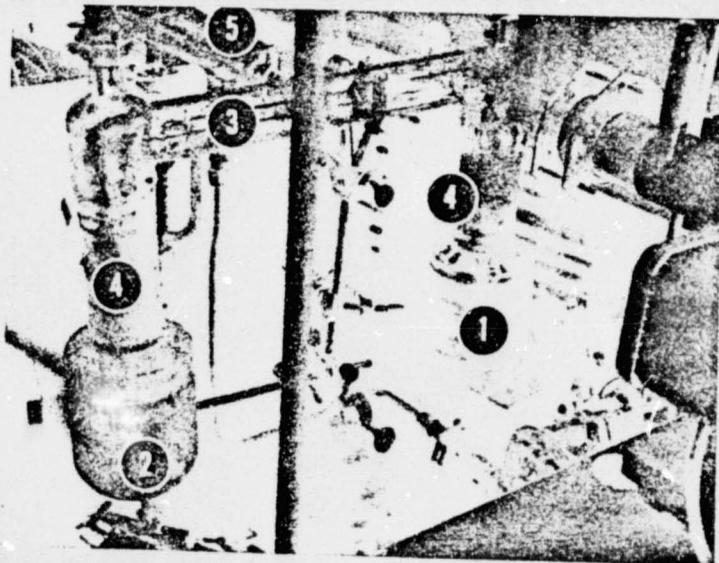
2.2.4.2 Results

2.2.4.2.1 Spectral Analysis of Si_xF_y

Table 2.2-8 presents data regarding the gas phase composition of homologues liberated during conversion of $(SiF_2)_x$ and $(SiF_2)'_x$. Here it will be noted that both the original polymer and the residue polymer formed from volatiles liberated during the thermal conversion of $(SiF_2)_x$ liberated a series of homologues of similar composition. However, the small concentration of oxygen containing species liberated from $(SiF_2)_x$ were not observed during the thermal conversion of the residue polymer $(SiF_2)'_x$. The relative intensities of the major species liberated during thermal conversion of $(SiF_2)_x$ have been previously reported. However, due to the very low intensity of the peaks above m/e 200 with respect to m/e 85, integration of homologues presented in Table 2.2-8 was not undertaken. The mass spectral data clearly indicate that $(SiF_2)_x$ and $(SiF_2)'_x$ undergo thermal conversion in a similar manner and liberate essentially the same series of volatile homologues silicon fluoride compounds.

2.2.4.2.2 Homologue Conversion Experiments

Data correlating homologue efficiency with residence time of Si_xF_y species in a non-optimized thermal conversion unit has shown that conversion efficiencies of 60% to 80% can be achieved. A series of experiments was undertaken to study the thermal disproportionation of the polymer $(SiF_2)'_x$ formed from condensed volatiles liberated during the conversion of $(SiF_2)_x$.

Table 2.2-9 presents data leading to an overall polymer conversion efficiency calculation. Here, from weights of SiF_4 liberated and weights of polymer formed and converted, the efficiencies of the conversion of $(SiF_2)_x$ and $(SiF_2)'_x$ into silicon was obtained. It will be noted that the conversion efficiency for stage 1 is 77%. This correlates extremely well with the data presented in Section 2.1. Furthermore, a 91% conversion efficiency for the residue $(SiF_2)'_x$ polymer was achieved. Due to the fact that conversion efficiency was observed to be inversely proportional to residence time, this high conversion efficiency is consistent with results showing a direct

45

Table 2.2-8 Si_xF_y MASS SPECTRAL DATA COMPARISON

MASS NUMBER	ASSIGNMENT		ORIGINAL POLYMER	$(SiF_2)_n'$
	x	y		
47	1	1		
66	1	2		
85	1	3		
113	2	3		
132	2	4		
151	2	5		
167	Si_2OF_5			NO
195	Si_3OF_5			NO
198	3	6		
222	3	7		
236	3	8		
264	4	8		
283	4	9		
292	5	8		
302	4	10		
311	5	9		
330	5	10		
349	5	11		
377	6	11		
396	6	12		
415	6	13		
462	7	14		
481	7	15		
528	8	16		
547	8	17		
575	9	17		
594	9	18		
660	10	20		
726	11	22		

Except where stated (No), all ions of
the above mass numbers were observed.

46

TABLE 2.3

RESIDUE $(SI_XF_Y)'$ CONVERSION BASED ON INDIVIDUAL STAGE CALCULATION

No. 1

$$(SIF_2)_X \quad \xrightarrow[1]{\Delta} \quad SI + SIF_4 \uparrow + (SI_XF_Y)' \quad \xrightarrow[2]{\Delta} \quad SI + SIF_4 \uparrow$$
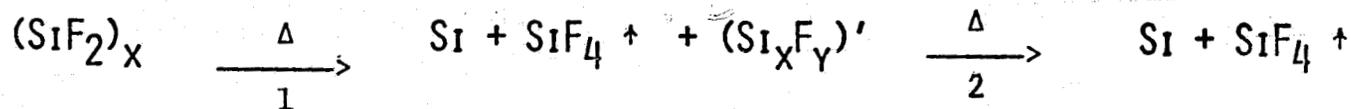
STAGE 1 - CONVERSION

GMS POLYMER FORMED	GMS POLYMER CONVERTED	GMS RESIDUE FORMED	%CONVERSION STAGE 1
14.13 G.	10.81 G.	3.32 G.	77%

STAGE 2 - CONVERSION

GMS RESIDUE FORMED	GMS RESIDUE CONVERTED	%CONVERSION
3.32 G.	3.02	91%

OVERALL POLYMER CONVERSION

OVERALL CONVERSION = 0.77 + (0.91 x 0.23) = 98%

relationship between residence time and conversion efficiency of $(SiF_2)_x$ polymer into silicon.

Table 2.2-10 presents data showing conversion efficiencies of polymer into silicon for two experiments using the double condensation-disproportionation unit to convert both $(SiF_2)_x$ and $(SiF_2)_x$ into silicon. Here it will be noted that an overall mean polymer conversion efficiency of 95.7% was achieved.

The results from these studies clearly show that conversion of the Si_xF_y homologues into silicon was possible and that high conversion efficiencies were achieved. An increase in throughput, however, was required, and effort was directed towards disproportionation on substrates with increased surface area, specifically a silicon packed fixed bed.

2.2.5   Thermal Disproportionation on Si Packed Beds

2.2.5.1 Experimental

After the establishment of homologue conversion efficiency on heated quartz surfaces, disproportionation on substrates with greater surface area was studied. The increased surface of the substrate gave the potential for greater homologue throughput for fixed conversion efficiency. A fixed bed packed with chunks of semiconductor grade silicon was chosen.

Preliminary packed bed studies indicated that homologue residence time within the packed bed was an important parameter affecting conversion efficiency. The correlation of system pressure variation with temperature of homologue conversion clearly indicated that, when the entire polymer mass was heated with a conventional trap heater, the homologues were rapidly forced through the disproportionation zone.

This results in a residence time which depends upon the heating rate at the homologue liberation-temperature. While this may be advantageous under certain conditions, e.g., rapid liberation of homologues leading to reduced process cycle time, it limited the capability of studying the disproportionation bed parameters exclusively. Consequently, a technique involving unidirectional heating of a uniformly distributed polymer film was developed (Figures 2.2.7(a)

Table 2.2-10

RESIDUE $(Si_xF_y)'$ CONVERSION BASED ON POLYMER INPUT / OUTPUT

	GMS POLYMER FORMED	GMS POLYMER + RESIDUE CONVERTED	OVERALL POLYMER % CONVERSION
NO. 1	14.1 G.	13.8 G.	98%
NO. 2	15.4 G.	14.9	97%
			97.5%
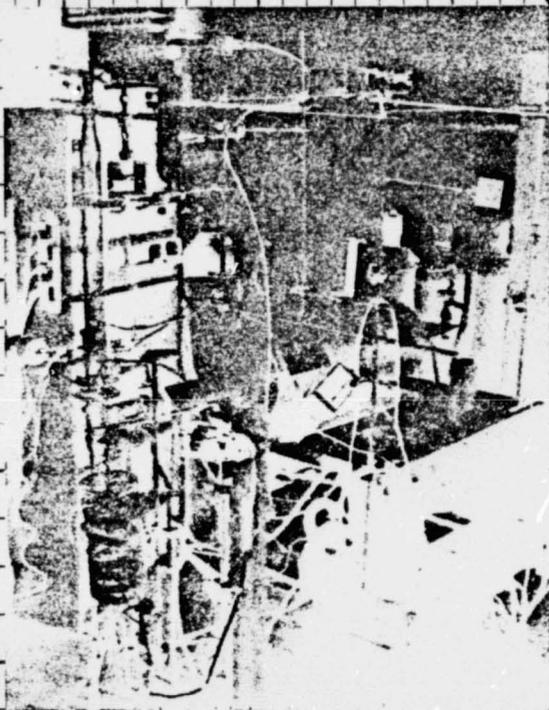
Figure 2a. Apparatus used for thermal disproportionation of packed Si beds.

POSTCARD

No. 6¾ ENVELOPE

Figure 2b. Closeup view of disproportionation apparatus.
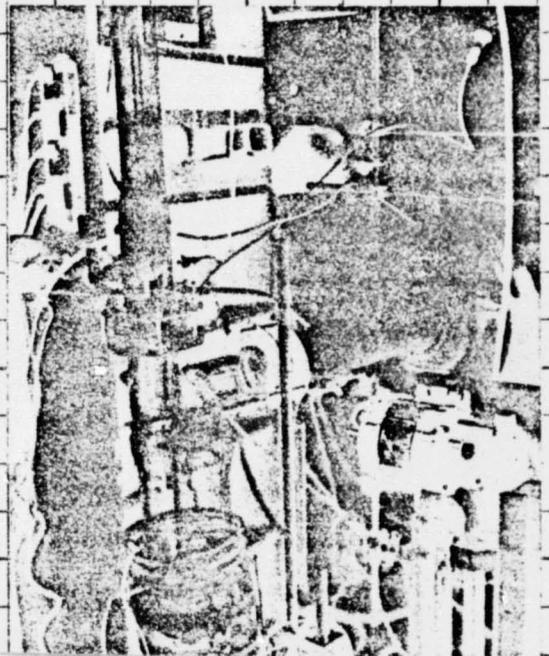
ORIGINAL PAGE IS
OF POOR QUALITY

and 2.2.7(b). A constant system pressure of 1-3 torr resulting from uniform homologue volatilization was achieved. This constant homologue pressure corresponded to a constant concentration of homologues entering the disproportionation bed during the course of the conversion of polymer into silicon. Briefly, the apparatus consisted of a movable ring heater which traversed the condensation trap at a uniform rate and allowed a constant concentration of homologues to reach the bed throughout the course of the experiment.

In order to eliminate reaction step 1 and 2 variations, an arbitrary set of reaction conditions was chosen. SiF_2 generator conditions consisted of a 1000 gm charge of 1-2 cm particle size mg Si heated to $1350^{o}C$. SiF_4 at a rate of 0.25 gm/min was passed through the heated Si charge resulting in an 800 micron downstream pressure. The disproportionation bed work utilized a bed consisting of a 1.5 inch column of 1-2 cm Si particles located directly above the condensation trap and heated to either $500^{o}C$ or $850^{o}C$. The length of the Si packed column was 16 inches, 8 inches and 4 inches.

Studies of polymer condensation temperatures aimed at achieving a uniform liberation rate indicated that $-78^{o}C$ trapping of SiF_2 to form $(SiF_2)_x$ polymer led to a uniform and reproducible distribution of polymer within the condensation trap. Lower temperature cooling, e.g., $-196^{o}C$ led to uneven polymer distribution and to non-reproducible Si_xF_y liberation upon heating.

For the purposes of bed disproportionation studies, a standard homologue liberation rate of 0.4 gms homologues per minute was used. This rate of homologue liberation is comparable with the rate of SiF_4 flow across the Si bed in reaction step 1.

Hence, with $-78^{o}C$ condensation and a uniform heating rate as obtained with the unidirectional elevator heater, a constant fraction of Si_xF_y homologues was reproducibly injected into the disproportionation bed. This permited evaluation of bed efficiency in the absence of reaction variations previous to thermal disproportionation.

2.2.5.2 Results and Discussion

The goal of this aspect of the Si/SiF_4 transport process investigation

was to study factors affecting the thermal disproportionation of Si_xF_y (x ≥2 to 11) into silicon on silicon packed beds.

Figure 2.2.8 is a histogram of the percent polymer unliberated from the bulk of polymer formed at the termination of the liberation procedure. While this unliberated fraction does not imply any physical or chemical maximum liberation capacity it does indicate that a known fraction of homologues was being liberated within a constant time period. Further, and equally important, it shows that downstream variations in bed parameters e.g., bed length and bed temperature did not affect the liberation reactions (step 3) as expected.

$$(SiF_2)_n \longrightarrow Si_xF_y \qquad\qquad \text{Step 3}$$

Figure 2.2.9 is a graph of % polymer conversion efficiency based on polymer input to the conversion bed versus conversion bed length for disproportionation at 850°C and 500°C. Table 2.2-11 gives the data in tabular form. The data obtained was subjected to a kinetic analysis in terms of a steady state integral plug flow reactor.

The expression for the rate of reaction in an integral reactor is

$$(-r_A) = \frac{dX_A}{d(V/F_{Ao})} \qquad\qquad (7)$$

thus a plot of X_A vs. V/F_{Ao} will have a slope at X_{Ai}

$$\text{slope } X_{Ai} = (-r_{Ai}) = \left[\frac{dX_A}{d(V/F_{Ao})}\right]_{X_{Ai}} \qquad (8)$$

and since $C_A = C_{Ao}(1-X_A)$
where C_A = concentration of A in moles ℓ^{-1}, a graph of $(-r_{Ai})$ vs. C_{Ai} can be plotted and the order of reaction with respect to A obtained via

$$(-r_A) = -\frac{dC_A}{dt} = kC_A^n \qquad\qquad (9)$$

52
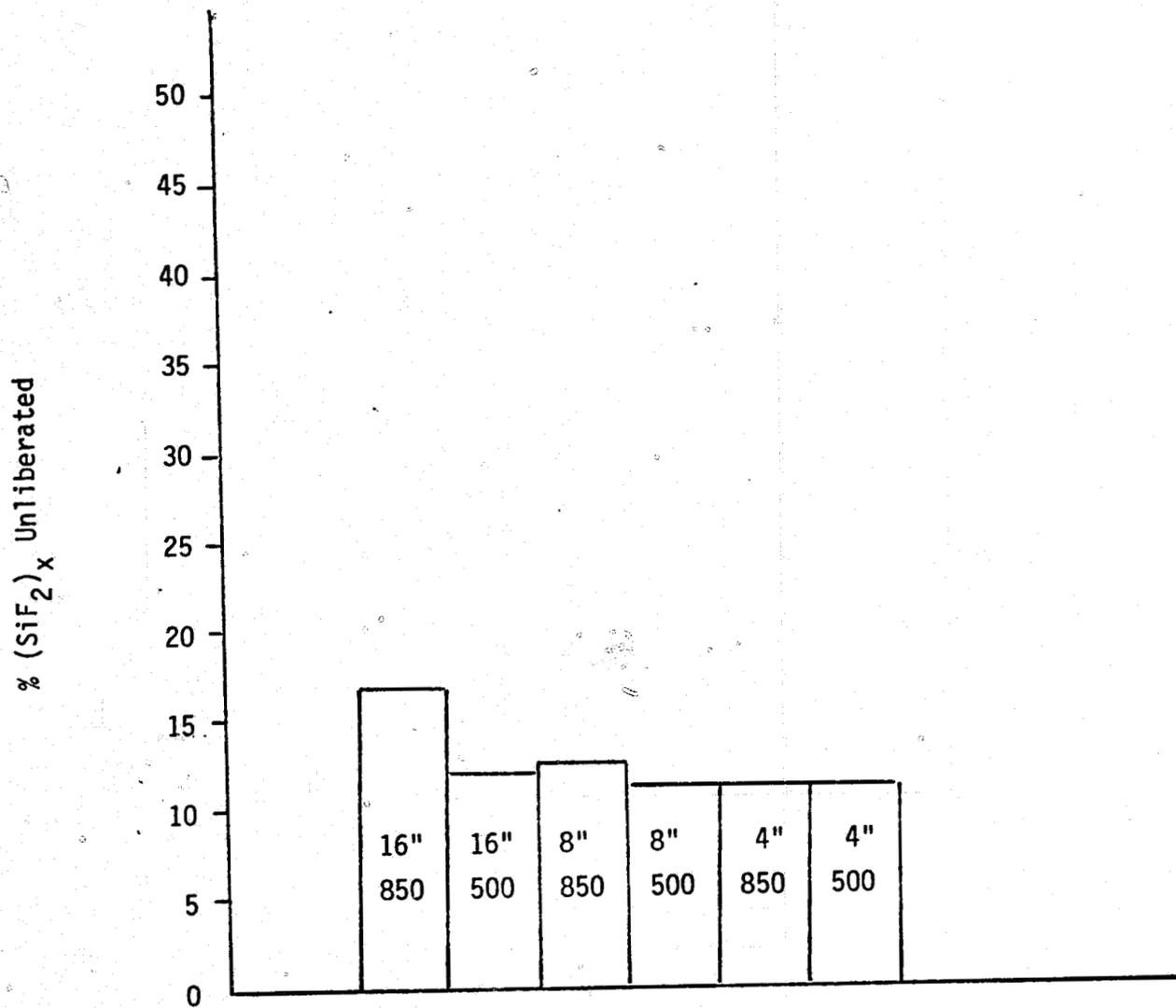
Figure 2.2.8 % $(SiF_2)_x$ Unliberated
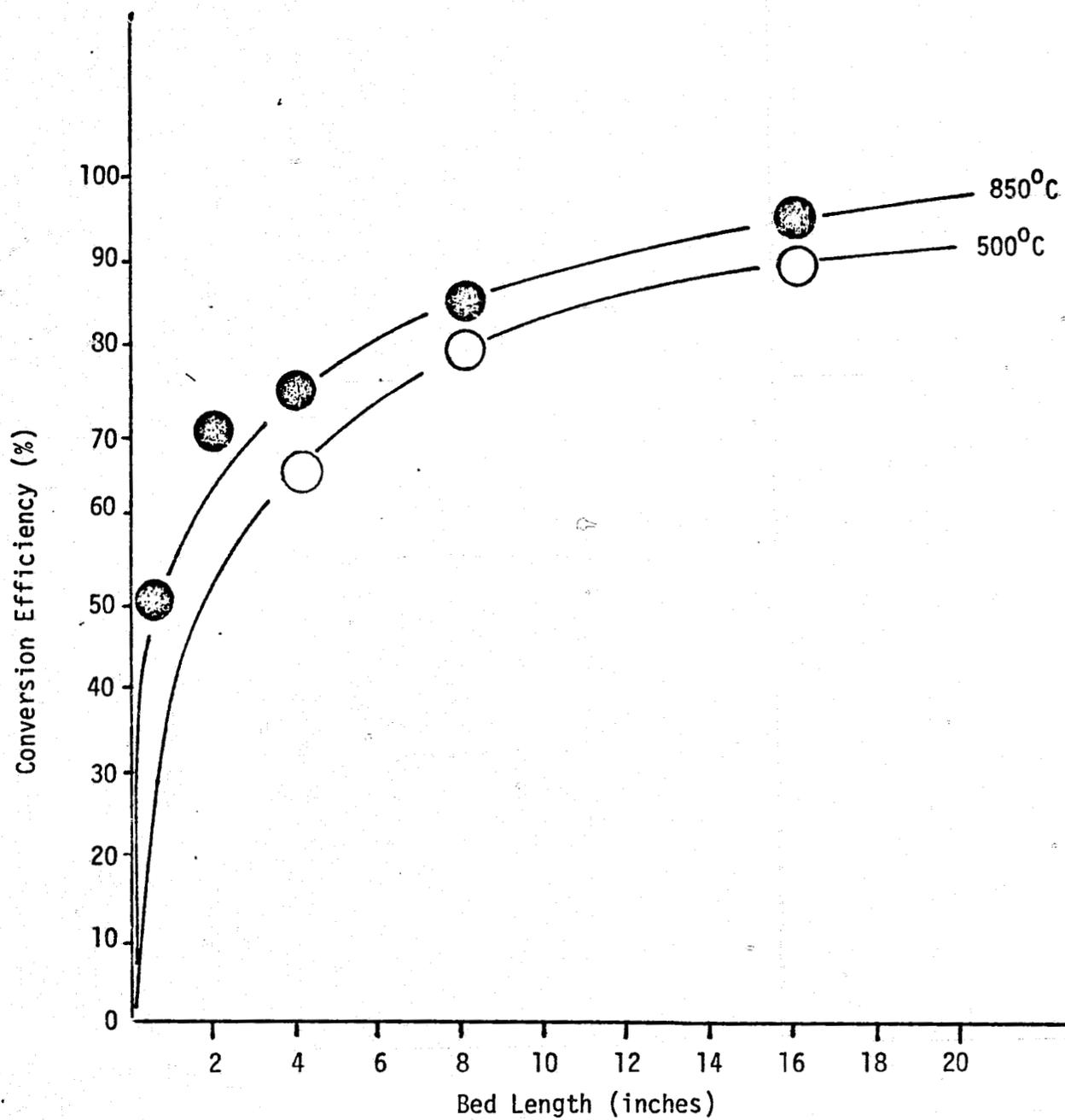
Figure 2.2.9 Conversion efficiency vs. bed length

where k is the rate constant, C_A is the molar concentration of A, and n is the order.   Finally,

$$\log (-r_A) = \log k + n \log C_A \qquad (10)$$

a plot of $\log (-r_A)$ vs. $\log C_A$ has a slope equal to n, the order of reaction, and an intercept equal to $\log k$, the log of the rate constant.

The following is a kinetic analysis of the data collected on thermal disproportionation of homologues liberated from the $(SiF_2)_x$ polymer.

Table 2.2-11 Data correlating Si bed length and
conversion efficiency.

Bed Length (in)	Conversion Efficiency 850°C	Conversion Efficiency 500°C
0.5	0.50	
2.0	0.70	
4.0	0.74	0.65
8.0	0.85	0.80
16.0	0.95	0.87

The mean value of the pressure measured at a point midway between the disproportionation bed and the condensation/liberation trap was

$$\bar{P} = 0.87 \text{ torr} \qquad \sigma = 0.16 \text{ torr}$$
$$\bar{P} = 1.14 \times 10^{-3} \text{ ats.}$$

Table 2.2-12 and 2.2-13 present X_A and V/F_{Ao} for various bed lengths leading to a graph of X_A vs. V/F_{Ao} as required by equation 11. Figures 2.2.10 and 2.2.11 are graphs of X_A vs. V/F_{Ao} for 850°C and 500°C conversions respectively. The slopes of the lines at X_{Ai} are equal to $(-r_{Ai})$ as expressed in equation 8.

55

Figure 2.2.10 X_A vs. V/F_{Ao} (850°C)

X_A vs. V/F_{Ao}

850°C (dashed line)
500°C (solid line)
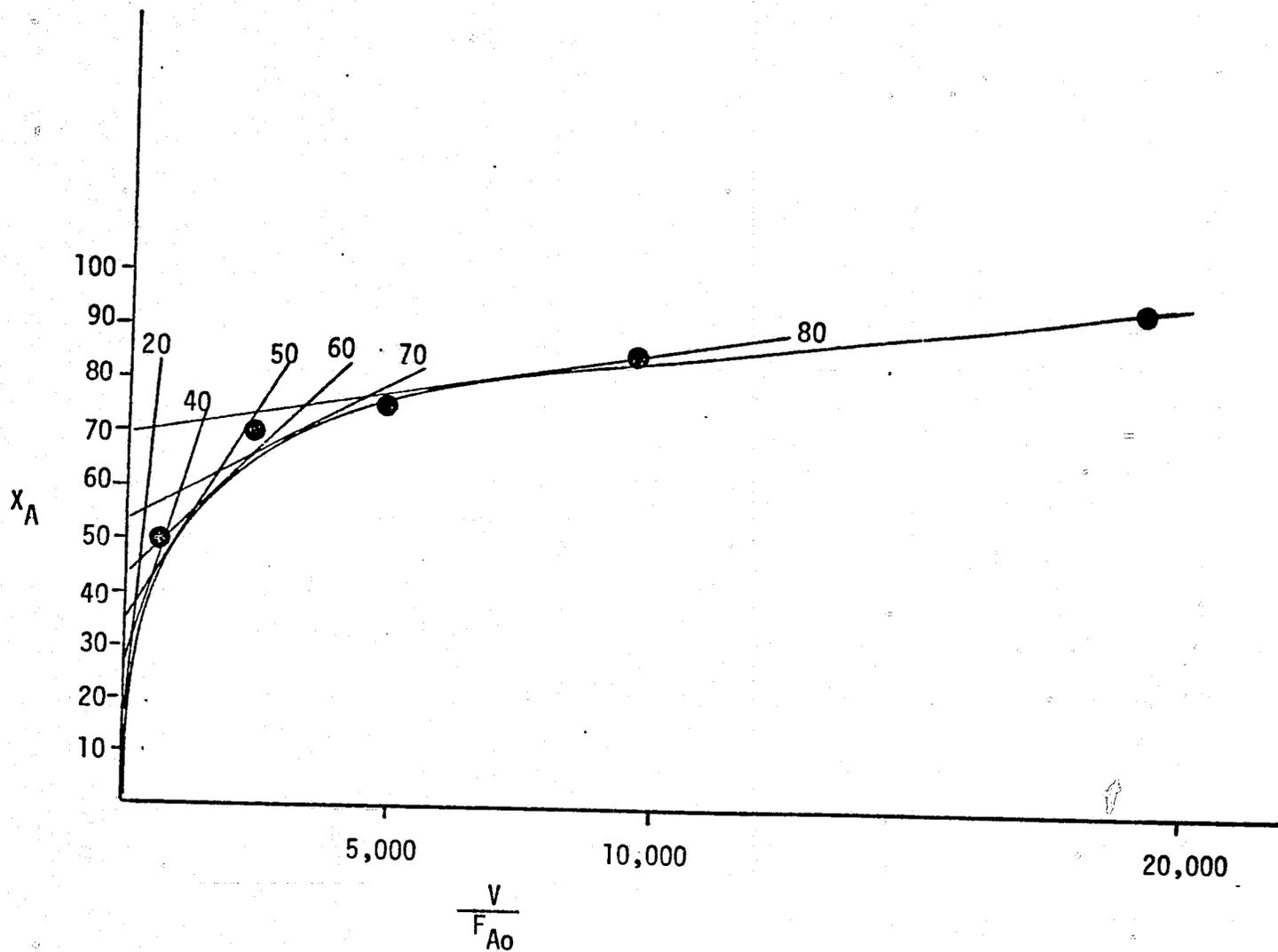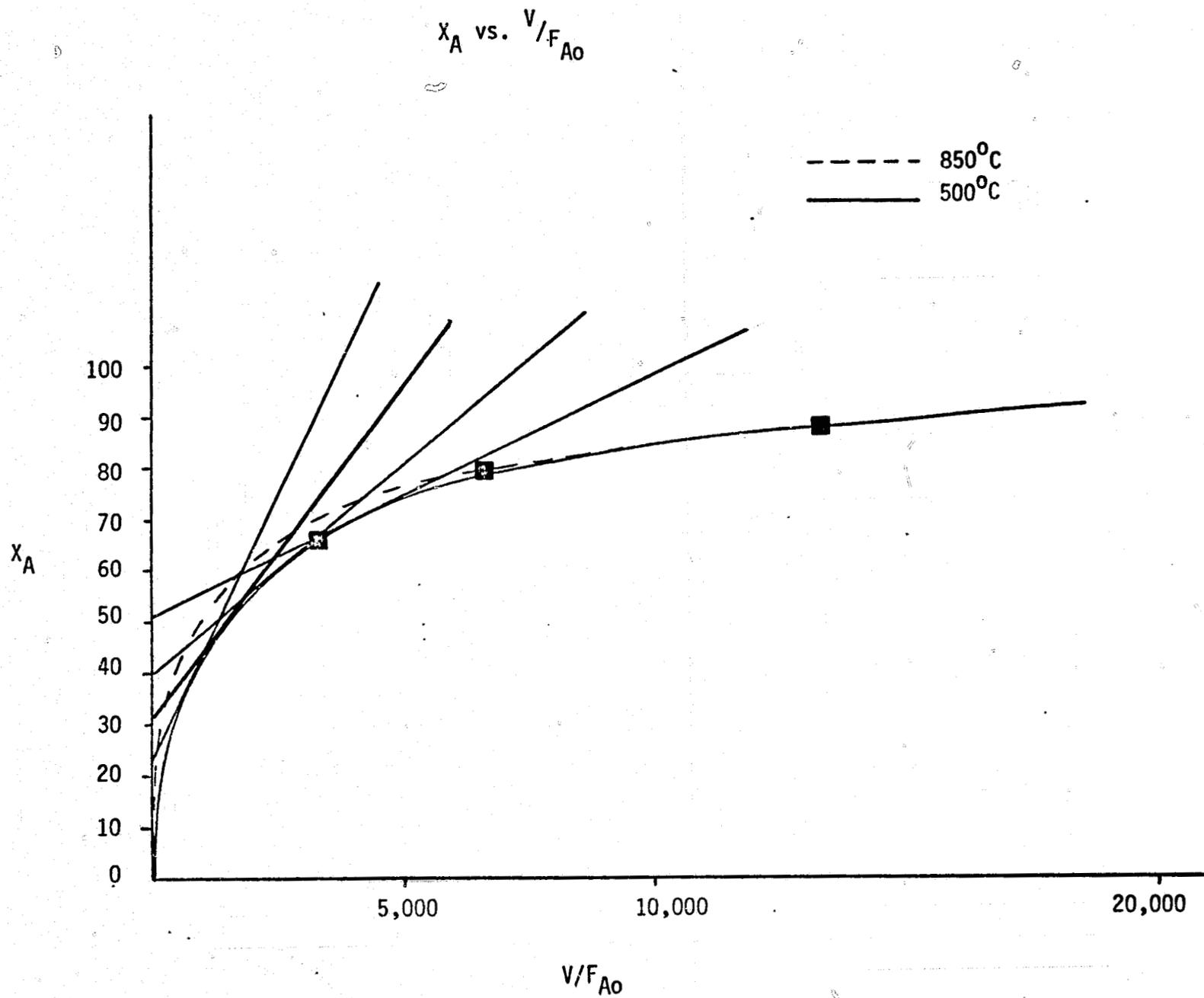
Figure 2.2.11 X_A vs. V/F_{Ao} (850°C & 500°C)

Tables 2.2-14 and 2.2-15 present values of $(-r_A)$ for various X_A for 850°C and 500°C conversions, making use of the expression $C_{A_0} = (1-X_{Ai})$ we may obtain C_{Ai} at $(-r_{Ai})$ for X_{Ai}.

Table 2.2-12 Data correlating bed length and V/F_{Ao} for conversions conducted at 850°C.

Bed Length	$V(\ell) \pm 2.6\%$	V/F_{Ao} (ℓ hr mol^{-1})	X_A
16	0.5676	19203.6	0.95
8	0.2825	9557	0.85
4	0.1429	4835	0.74
2	0.0693	2345	0.70
0.5	0.0173	585.3	0.50

Table 2.2-13 Data correlating bed length and V/F_{Ao} for conversions conducted at 500°C.

Bed Length (in)	$V(1) \pm 2.6\%$	V/F_{Ao} (1 hr mol^{-1})	X_A
16	0.5676	1.33×10^4	0.87
8	0.2825	6.62×10^3	0.80
4	0.1429	3.34×10^3	0.65

Table 2.2-14 Data correlating $1-X_A$ and C_A.

X_A	slope = $(-r_A)$ = $dX_A/d(V/F_{Ao})$ (moles ℓ^{-1} hr^{-1})	$(1-X_A)$	C_A M hr^{-1}
0.2	0.124	0.8	9.92×10^{-6}
0.3	0.065	0.7	8.68×10^{-6}
0.4	0.035	0.6	7.44×10^{-6}
0.5	0.0167	0.5	6.2×10^{-6}
0.6	0.0097	0.4	9.96×10^{-6}
0.7	0.0049	0.3	3.72×10^{-6}
0.74	0.0038	0.26	3.22×10^{-6}
0.79	0.00172	0.21	2.604×10^{-6}
0.8	0.00158	0.2	2.48×10^{-6}

Table 2.2-15 Data correlating $1-X_A$ and C_A ($500^\circ C$)

X_A	$(-r_A)$ (moles 1^{-1} hr^{-1})	$1 - X_A$	C_A M hr^{-1}
0.4	0.0204	0.60	$7.44 - 10^{-6}$
0.5	0.0131	0.50	$6.2 - 10^{-6}$
0.6	0.0075	0.40	$4.96 - 10^{-6}$
0.70	0.0043	0.30	$3.72 - 10^{-6}$

By making use of equations 10 and 11 it can be seen that a plot of log ($-r_A$) vs. log C_A should be a straight line of slope n; where n is equal to the order of the reaction with respect to C_A. Figure 2.2.12 is a graph of log ($-r_A$) vs. log C_A for the 850°C and 500°C conversions. The slope of the line for the 850°C conversion is:

$$n = slope = 2.98$$
$$\log_{10}k = intercept - 13.86$$
$$k = 1.67 \times 10^{14} \ M^{-2} \ hr^{-1} \quad \text{Correlation coefficient} = 0.993$$

A kinetic analysis of homologue conversion on a silicon packed bed in terms of an integral plug flow reactor has shown that our data is internally consistent and elucidates the relationship between bed length, residence time, conversion efficiency and reaction order.

2.2.6 Thermal Disproportionation on Low Pressure Fluidized Beds

2.2.6.1 Experimental

In order to achieve greater throughput, experimentation was directed toward development and utilization of a low pressure fluidized disproportionation bed.

In our initial fluidized bed experiments, a small Pyrex model was constructed (see Figure 2.2.13) and operated to determine flow rates and pressure drops associated with low pressure silicon bed fluidization. It was found that for a 1" diameter bed, flow rates of 400 - 900 sccm were required for fluidization of silicon particles of 0.6 mm. Furthermore, pressure drops of only 3-10 torr were observed per inch of bed height. Bed heights of 1", 3" and 4" resulted in minimum pressure drops of 3, 10, and 15 torr respectively for fluidization.

The experimental set up is shown in Figure 2.2.14. Polymeric $(SiF_2)_x$ was condensed at -78°C in trap No. 2 from gaseous SiF_2 emerging from the stage 1 reactor (No. 1). SiF_2 was generated in the previously described manner. Liberation of gaseous homologues from $(SiF_2)_x$ polymer was achieved by passing the heated elevator (No. 3) at a fixed rate across the polymer film deposited on the inside of trap No. 2. Concurrent with liberation of homologues from the polymer, helium was passed through the stage 1 reactor and thereby heated to

Figure 2.2.12 $(-r_A)$ vs. C_A

To Vacuum Pump

Particulate Baffle

Pressure
Gauge

Plate
Distributor

Bed Container Tube

ORIGINAL PAGE IS
OF POOR QUALITY

Particle Inlet

To Vacuum
Pump

Fluid Bed

Pressure
Gauge

Flow Control

Venturi Distributor
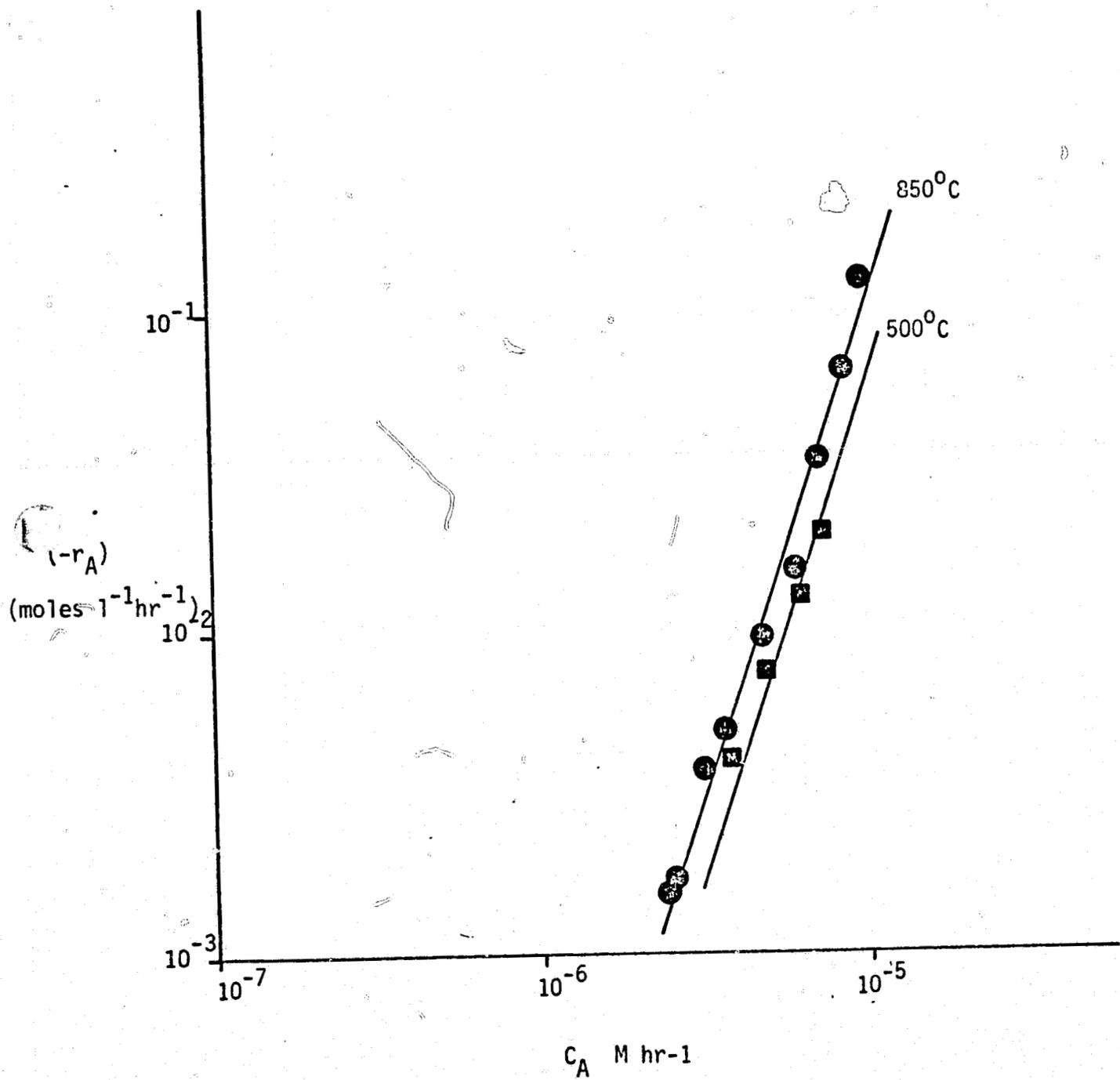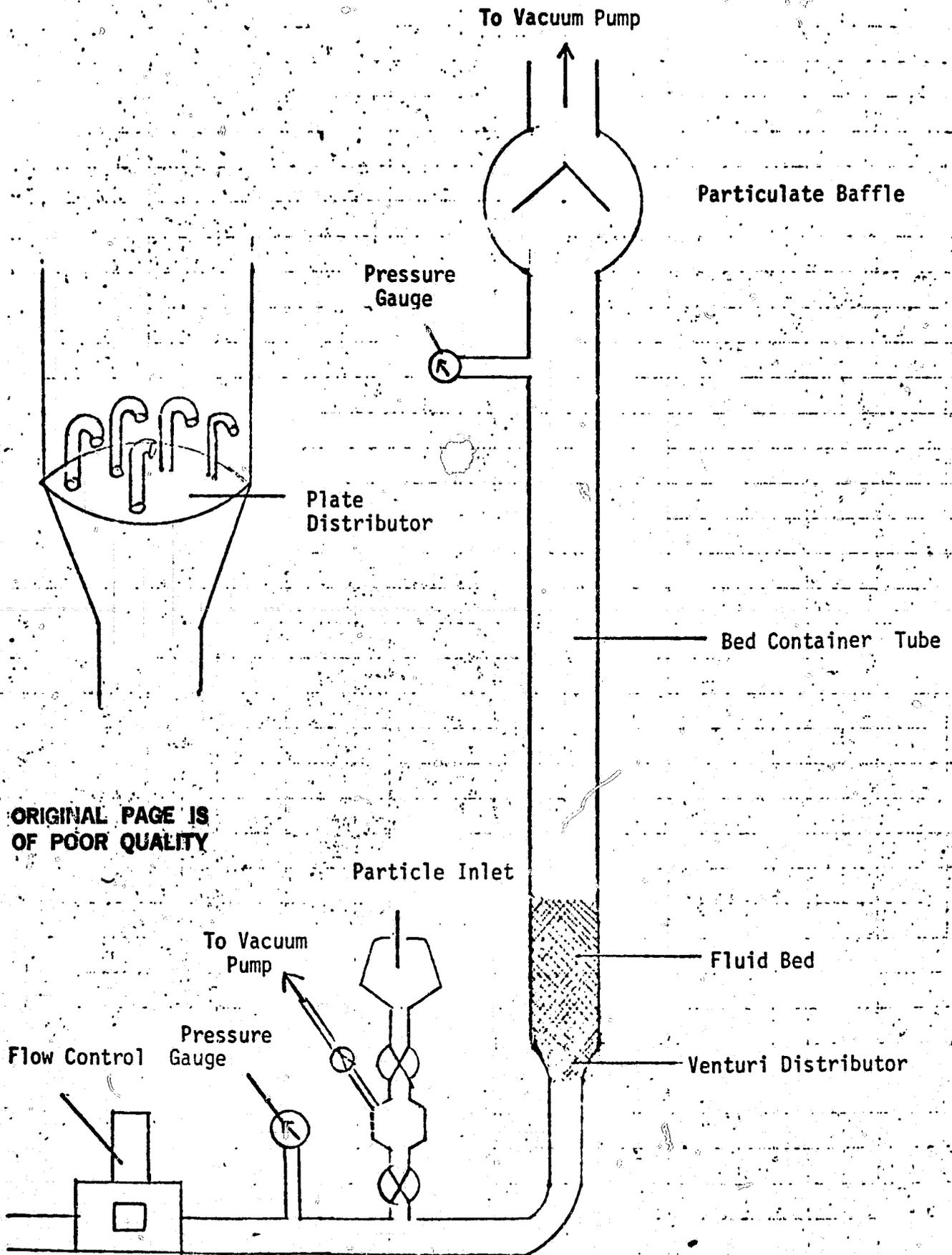
Figure 2.2.13   Preliminary fluidized bed design.
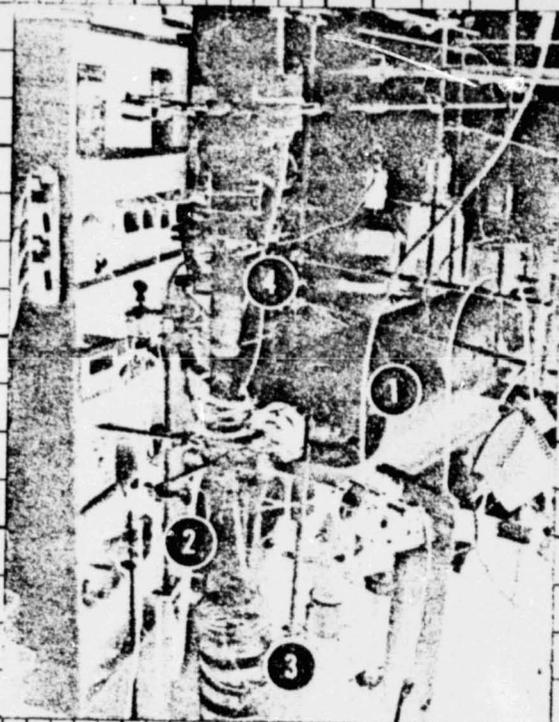
POSTCARD

No. 6¾ ENVELOPE

Figure 8. Experimental setup for fluidized bed experiments.

No. 10 ENVELOPE

15

approximately 500°C. From there it was injected into trap No. 2 effectively sweeping the homologues into the fluidized bed. The vacuum system was backed by an Edwards 23 cfm roughing pump. This pumping capacity was found to be necessary for fluidization of the described beds at low pressure.

The bed itself consisted of a 2 inch ID by 14 inch long quartz vessel packed with 0.589 mm to 1.40 mm silicon particles. The bed was heated to 800°C by an external clam shell heater. The function of the fluidized bed was to affect interaction between the hot silicon particles and gaseous homologues resulting in thermal disproportionation of the latter onto the silicon particles.

2.2.6.2 Results and Discussion

Table 2.2-16 presents the basic parameters affecting the onset of fluidization for the best observed fluidization for a particular bed length at room temperature. Silicon bed lengths were varied from 6 x 2 inches to 1.5 x 2 inches. It will be noted that in all cases fluidization occurred at upstream pressure equal to or less than 20 torr.

Table 2.2-16

Bed length (inches)	Pressure		He flow slm
	upstream (torr)	downstream (torr)	
1.5	15	15	0.5
2	18	15	1.25
3	16	5	0.4
4	18	5	0.4
5	18	2	0.35
6	18	5	0.31

One experimental disproportionation was successfully carried out. In this experiment 34.7 gms of polymer were condensed from SiF_2 while 25.5 gms of the polymer $(SiF_2)_x$ was converted into homologues during liberation and swept into the fluidized bed. This was a low liberation efficiency. However, a 74% conversion efficiency was achieved on this preliminary experiment, the calculation being based on the total weight of unconverted homologues that did not undergo thermal disproportionation following injection onto the fluidized bed.

2.2.7   Pneumatic Lifter as a Silicon Harvester

2.2.7.1 Experimental

Experiments were conducted to ascertain the potential of converting the Si_xF_y homologues into silicon by thermal disproportionation of the homologues on a low pressure pneumatic lifter. The goal in these experiments was to demonstrate the capability of pneumatically lifting silicon particles through a reaction zone containing Si_xF_y homologues.

Figure 2.2.15 illustrates the experimental appratus used to define operational parameters for a low pressure pneumatic lifting reactor. Silicon particles (<0.60 mm diameter) were placed in the hopper and the entire apparatus pumped down to 1 torr.

Injection of carrier gas at the carrier gas inlet (see Table 2.2-17 for gas flows and pressures) affects a slight pressure drop across the Si particle hopper. This results in silicon being fed from the hopper to the lifting tube through the silicon feed tube. Silicon particle feed rate was controlled by the pressure drop within the silicon particle hopper. Following injection into the lifting tube, the silicon particles are pneumatically lifted up the tube and collected in the particle collector.

Column 1, Table 2.2-17 gives the conditions of CO_2 carrier gas flow, Si feed rate, calculated resultant pressures, and calculated particle velocities derived from previous experimental testing with helium. Column 2, Table 2.2-17 presents the experimental data obtained from initial low pressure particle lifting experiments. Note the good correlation between calculated upstream pressure and the experimental value.

Vacuum/Pressure
Gauge Pump

4. Particle collector

5. Carrier gas

1. Si particle hopper

3. Lifting tube
(reaction zone)

2. Si feed tube

Carrier gas inlet/pressure gauge

Figure 2.2.15 Pneumatic lifter.

66
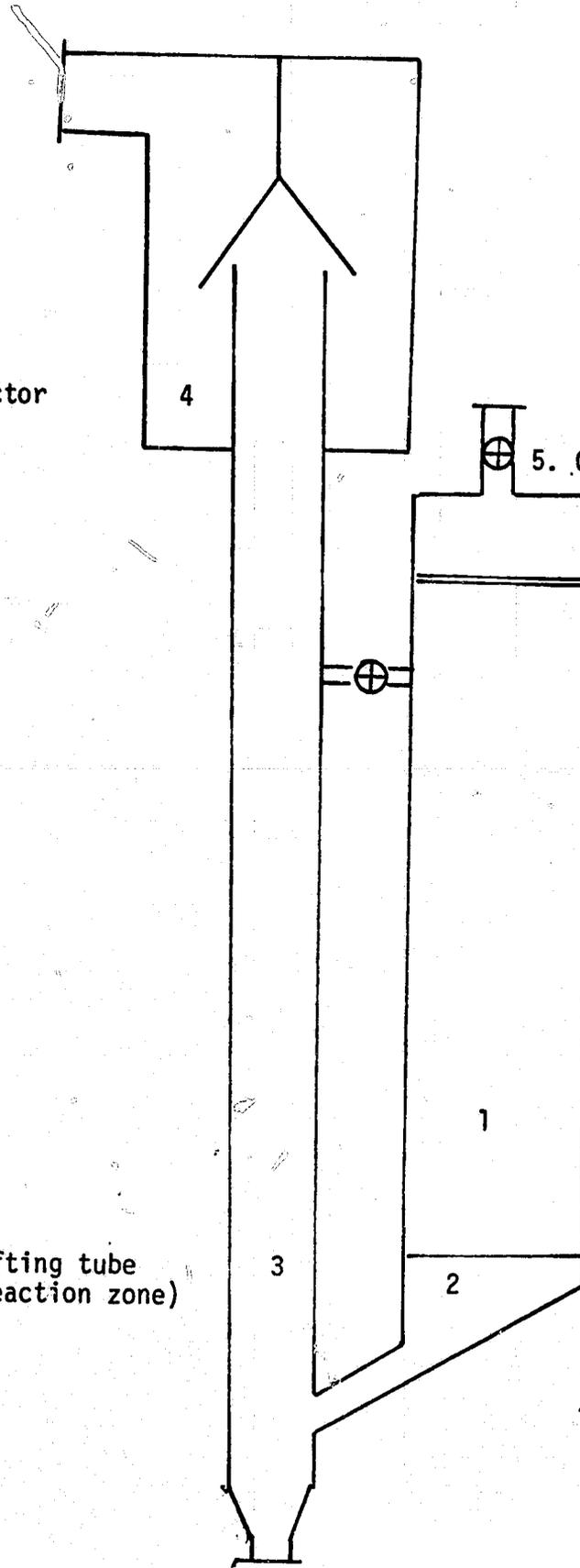
Table 2.2-17

	Calc. 1	Exper. 2
Gas	CO_2	CO_2
Temperature ^oC	21°	21°
Pressure Torr	97	75
Flow ($S\ell_{min}^{-1}$)	5.45	5.45
Particle Size	0.08-0.25	<0.60
Tube dia., inch	0.75	0.75
Velocity cm/min.	14,910	>14,910
Solids Flow g/min.	109	109

Figure 2.2-16 is a schematic diagram of a low pressure pneumatic lifting reactor which makes use of a recharging silicon hopper. Here heated silicon particles are transported up through the riser tube (3) where they react with reactant gases (Si_xF_y homologues). Following reaction within the riser tube, the silicon particles are dumped onto the top of the silicon hopper where they are heated to reaction temperature prior to reinjection into the gas stream. Fines are collected in the particle collector and product collected at an appropriate location within the hopper.

The silicon feed system in the apparatus depicted in Figure 2.2.16 consists of a J valve arrangement. A pressure differential across the bed caused by helium injection at the J valve forces silicon particles into the main riser tube where they are mixed with the reactant gases.

Table 2.2-18 presents operational parameter data for the recharging pneumatic lifting reactor.

Both reactor setups were backed by a 23 cfm Welch vacuum pump. Low pressure pneumatic lifting of solid chemical reactants through a reaction zone was satisfactorily demonstrated.

2.2.8   Discussion and Conclusions: From Si_xF_y Homologue Conversion Experiments

2.2.8.1 Residence Time vs. Conversion Efficiency Correlations

Previous sections have discussed the conversion efficiencies of Si_xF_y homologues on silicon packed beds and on fluidized beds containing silicon particles. A kinetic analysis of the homologue conversion in terms of a steady state integral plug flow reactor was presented. From these data correlations between homologue residence time within the reaction zone and conversion efficiency can be derived. These correlations are presented in Table 2.2-19 and Figure 2.2.17. Here it will be noted that for similar residence times within the reaction zone, comparable conversion efficiencies are obtained for the various types of disproportionation reactors. The calculated residence time versus expected conversion efficiency for the projected one kilogram per hour mini-plant pneumatic riser with gas velocity of 20 ft. sec^{-1} is shown.

4. Particle collector

1. Silicon particle hopper

3. Lifting tube
reaction zone

2. J valve

Carrier gas inlet

Carrier gas inlet
reactant gas inlet
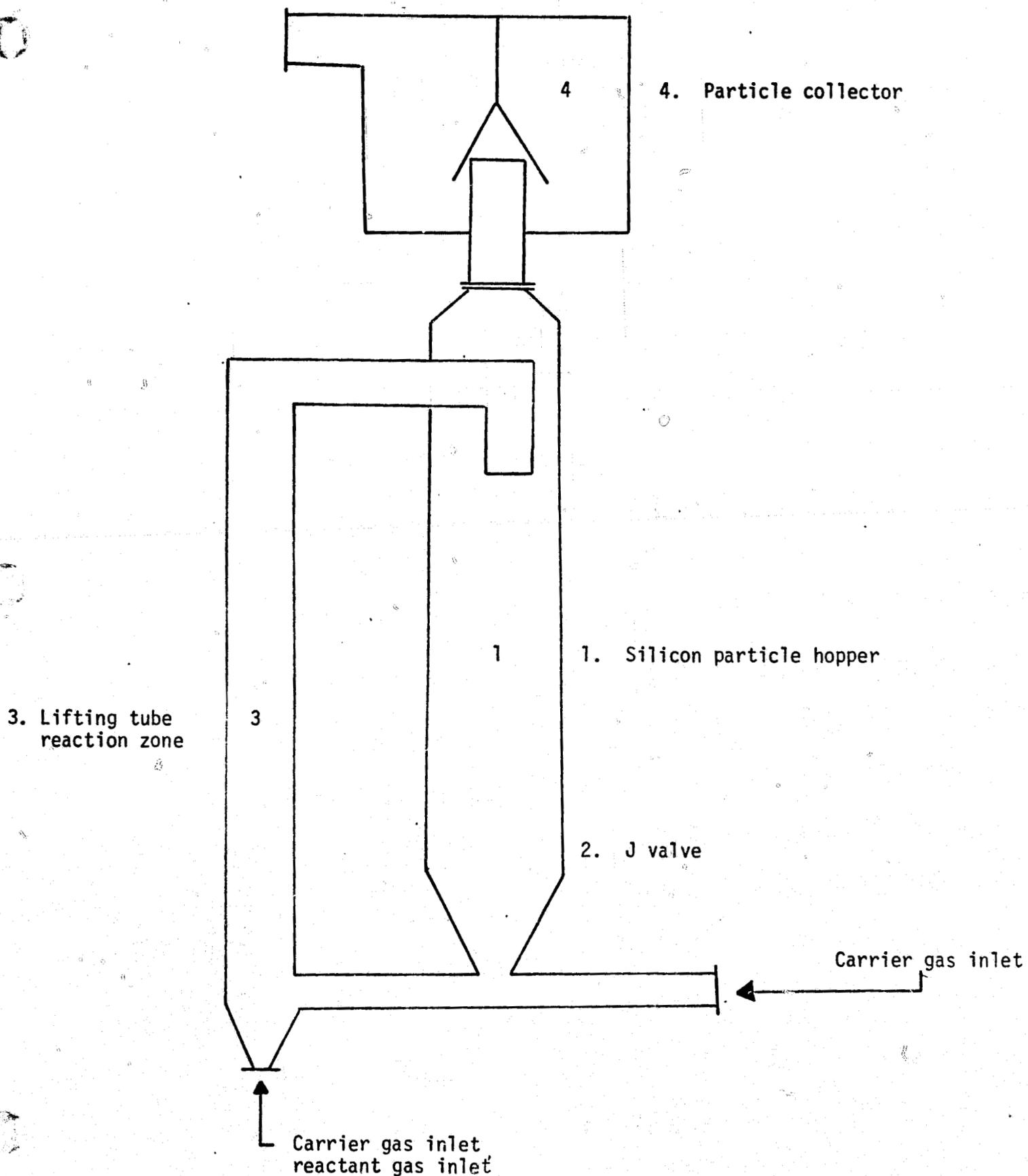
Figure 2.2.16

Table 2.2-18

	Series A	Series B
Gas	He	He/Si_nF_{2n+2}
Temperature $^\circ C$	21°	550°
Pressure (torr)	80	80
Flow std. ℓ (min^{-1}) (carrier)	0.3	0.4
Particle Size (mm)	0.60-1.5	0.60-1.5
Tube Diameter	0.75	0.75

Table 2.2-19

Data for conversion efficiency vs. residence time

Bed	Bed Length (in)	Conversion (%)	Residence Time (sec)
Packed	16	95	0.72
	8	85	0.355
	4	74	0.177
Fluidized	4	74	0.24
Lifter	21.4 ft.		1.06
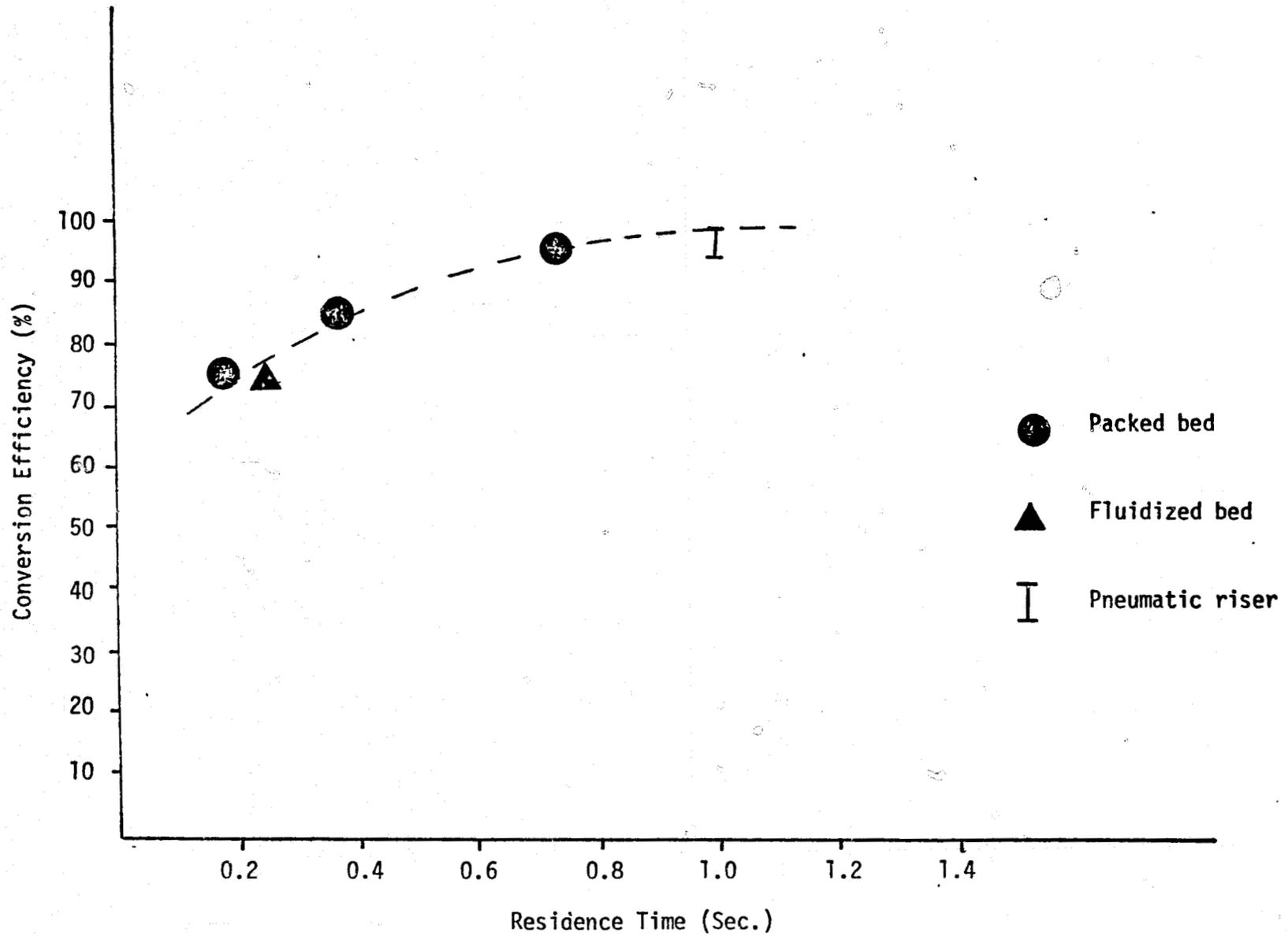
Figure 2.2.17

However, results from experiments conducted since termination of the Motorola-JPL/DOE contract indicate that the projected residence time versus conversion efficiency correlation for the pneumatic riser is very conservative and may give high conversion efficiency at residence times considerably less than one second.

Thermal disproportionation of Si_xF_y homologues on various types of conversion apparatus has been conducted. These studies have shown that high conversion efficiencies and high throughputs of homologues are feasible. It is concluded based on our work that conversion of the $(SiF_2)_x$ polymer to silicon is a viable process in terms of both throughput and conversion efficiencies as presented.

2.3 Chemical Process Feasibility Via the Near-Continuous Apparatus

2.3.1 Introduction

During the initial year of the contract numerous experiments were conducted which were directed toward long run times (1/4 - 4 hours) at silicon transport purification rates of 5-20 g/hr. The objectives of these preliminary experiments were to: produce silicon for evaluation, study and improve the transport rates and to improve the yield. These studies were termed chemistry feasibility studies.

Typical silicon yield data from these transport experiments are tabulated in Table 2.3-1. In Figure 2.3.1 can be found a diagram of the apparatus used in these initial experiments. During these runs the highest silicon transport rates were obtained when the $(SiF_2)_x$ polymer was converted under helium at a pressure slightly greater than one atmosphere at temperatures from 200 to $400^{\circ}C$. Maximum run times of 4 hours were achieved with a maximum silicon transport rate of 22 gm/hr. The silicon from these preliminary experiments was in the form of flakes and very fine grain powders.

During the course of these experiments it became apparent that an apparatus design change would be necessary if higher throughputs were to be achieved with less downtime between runs. Furthermore, new silicon harvesting technologies required testing before the process could be scaled to an engineering demonstration stage.

Thus, an apparatus of the near-continuous (N-C) design was proposed and built.

2.3.2 Experimental

Figure 2.3.2 is a schematic diagram of the near-continuous apparatus. The apparatus is a system standing about 8' high and occupying a floor space of ~2' x 3'. It was designed to approximate a continuously operating production system. During a typical 1 hour run the system draws a total of

Table 2.3-1. Preliminary silicon preparation experiments

RUN #	DATE	LENGTH OF RUN (HRS)	SiF_4 FLOW $CM^3/MIN.$ @ $21^{\circ}C$ & 1 ATM	CONVERSION ATMOSPHERE	Si COLLECTED (G)	YIELD (%)
P-16	1/19/77	0.5	426	Vacuum	4.30	29.0
P-17	1/21	0.5	426	He	9.04	61.0
P-18	1/23	1.0	426	He	17.95	60.6
P-22	2/11	2.0	426	He	31.7	53.5
P-23	2/15	4.0	426	He	54.7	50.4
P-24	2/23	4.0	559	He	~88	52.5

75

To Vacuum Pump

High Temperature Furnace

Mullite Tube

mg Si Charge

Baffle

Liq N$_2$ Trap

-78°C Trap

Valves

SiF$_4$

Mass Flow Meter
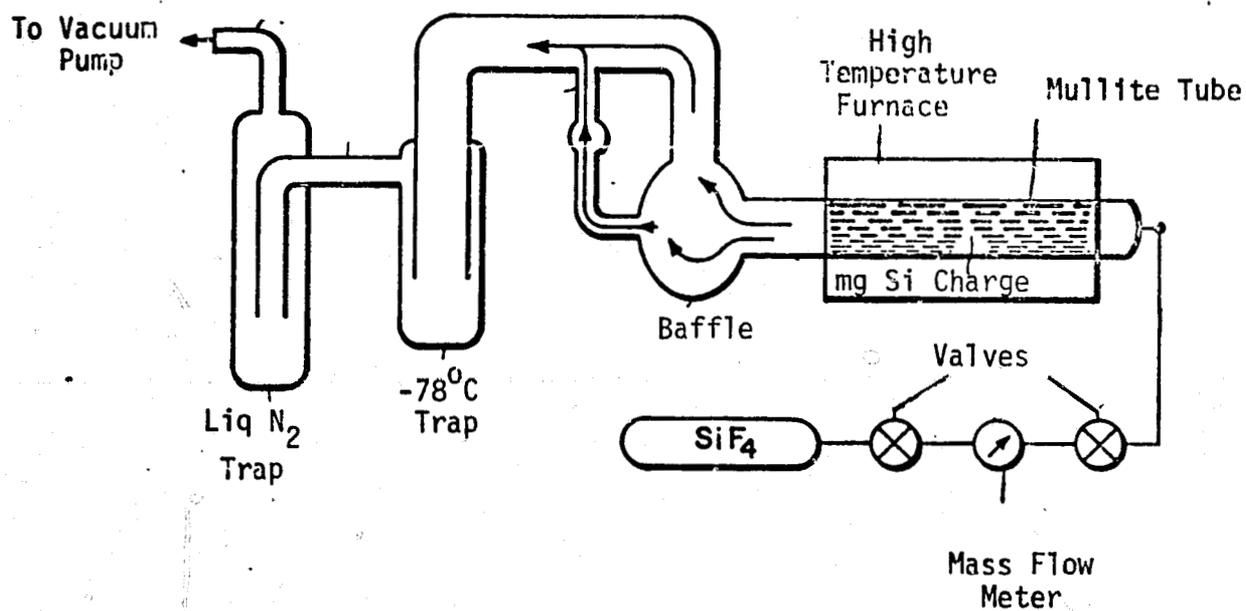
Figure 2.3.1. Schematic of the silicon purification apparatus used in the chemistry studies before construction of the N-C apparatus.
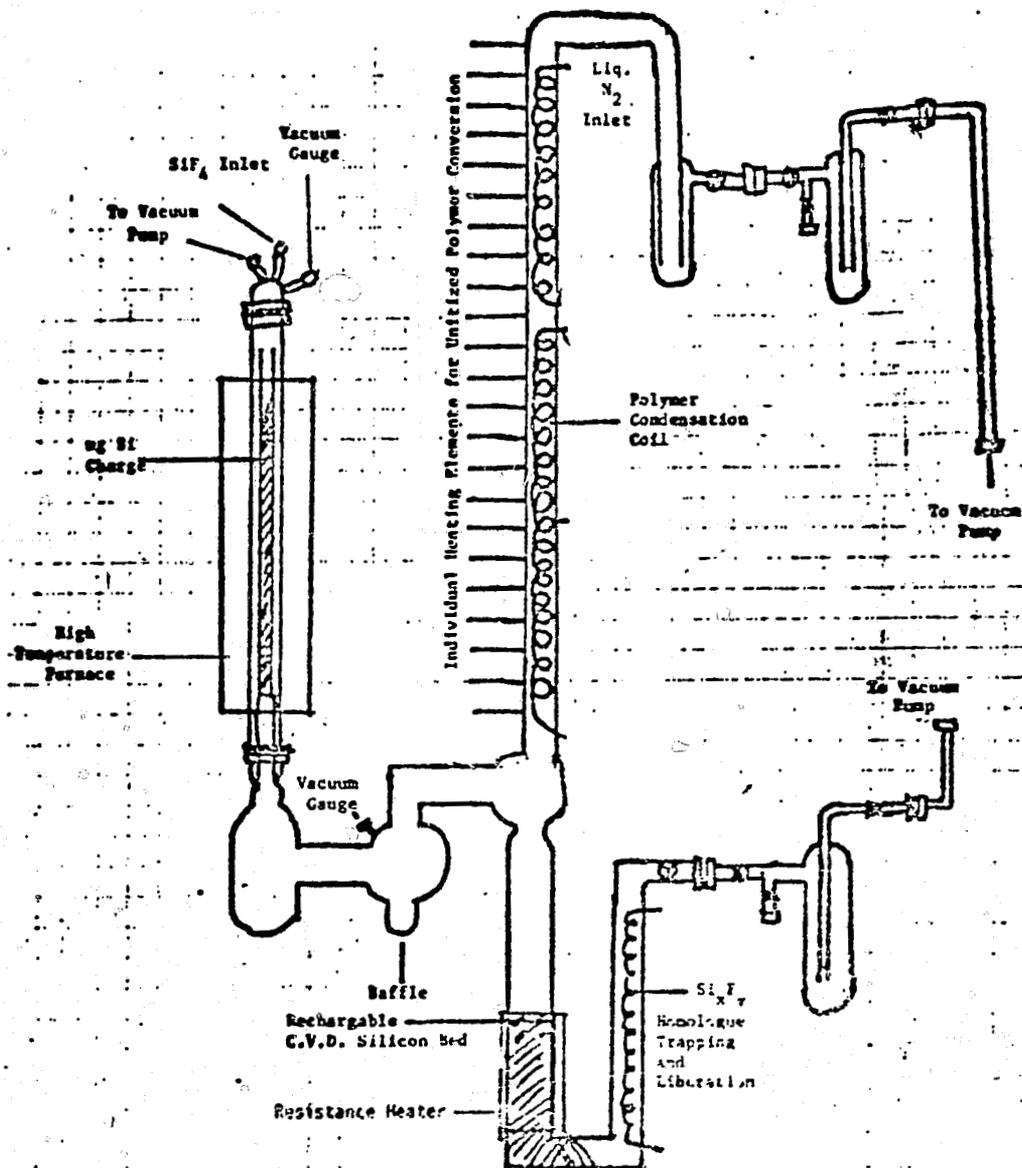
Figure 2.3.2. Depicted above is the near-continuous apparatus as
modified for silicon purification experiments. The
apparatus includes a vertical reaction furnace, re-
chargable C.V.D. Si_xF_y disproportionation bed and
unitized SiF_2 polymer condensation/liberation coil.

~10 KVA and consumes ~30 liters of liquid N_2. The following describes the individual parts in more detail.

2.3.2.1 SiF_4 Inlet System

A solid state torsion balance from Synthatron Corp. (Edgewater, N.J.) was employed to determine the weight of large SiF_4 cylinders to within ± 0.5 gm. The weight of the cylinder is tared to zero at the start of a run. At the finish, the weight of SiF_4 delivered is read directly. During typical 1 hour runs at flows of ~300 gm SiF_4/hr., the ± 0.5 gm precision represents an accuracy of better than 0.2%. A photograph of the apparatus is shown in Figure 2.3.3.

The SiF_4 flows out of the cylinder through a pressure regulator (~10 psi), through a Matheson mass flow controller, and into the N.C. apparatus. The flow controller is used to regulate the rate of flow, and the scale is used to monitor the flow. The pressure of the SiF_4 inlet is monitored via a combination low presure gauges (Hastings 0-800 torr and 0-10 torr).

2.3.2.2 Step 1 Reactor

In Figure 2.3.4 is illustrated the step 1 reactor. In essence the reactor is a 1" I.D. quartz tube, containing mg Si, enclosed in a Mullite tube which withstands the pressure differential at 1350°C. The vacuum seals are made with Viton o-rings. The reaction tube is placed in a vertical mounted Marshall furnace with the temperature monitored by an external Pt/Rh thermocouple (Type R).

The primary difference between this reactor and earlier models used in the preliminary studies is that it has a vertical configuration, which facilitates silicon recharging and minimizes tunneling through the bed.

The mg Si charge consisted of Union Carbide Corp. silicon (5-15 mesh) which had been mixed with 1% (by weight) of high purity quartz sand (Thermal American Fused Quartz). The 400 gm charge is supported by 40 gm of silicon
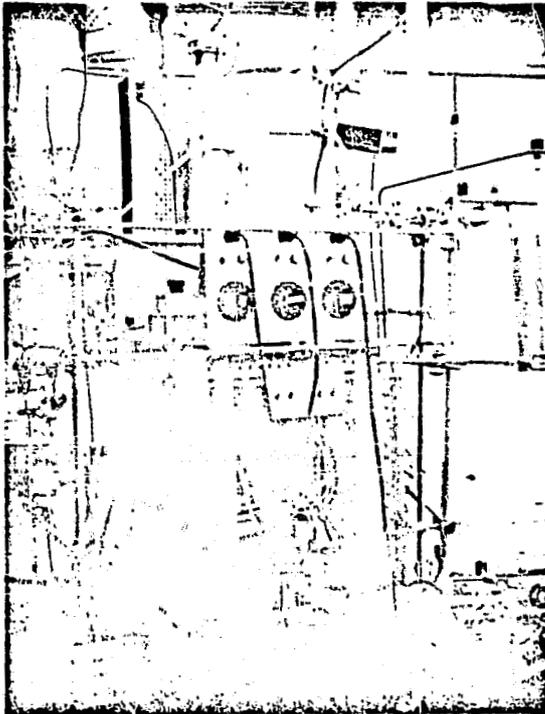
Figure 2.3.3   In the photo above is shown the
near-continuous silicon purification apparatus
with modifications incorporated.
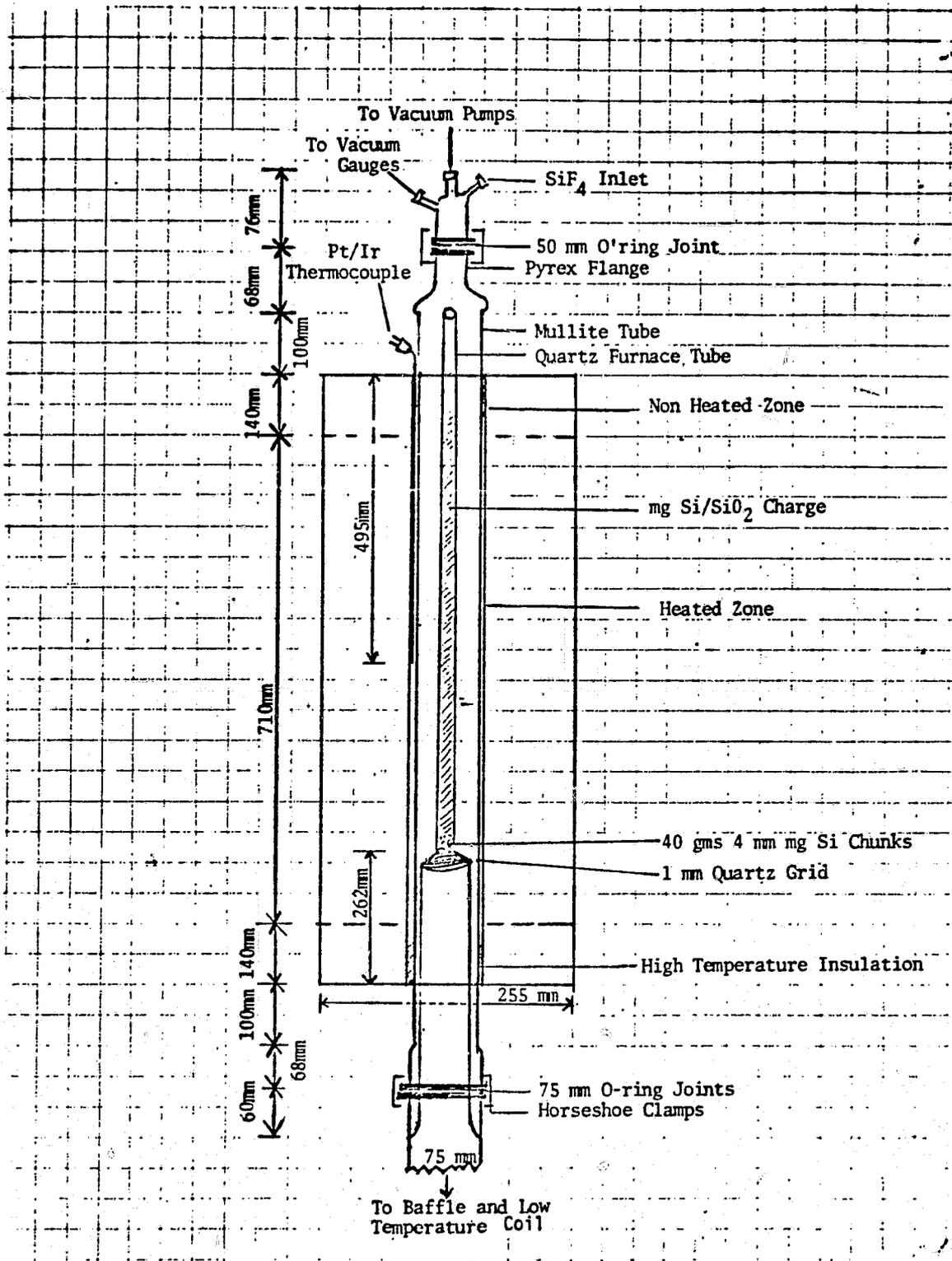
Figure 2.3.4. Depicted above is a sketch of the step 1 reactor in the near-continuous apparatus.

chunks (10 mm) in turn supported on a quartz grid.

2.3.2.3 Particulate Baffle

The particulate baffle shown in Figure 2.3.2 was incorporated into the system to remove free flowing particulates in the SiF_2 gas stream. These particles originate as unreacted mg Si or as small flakes of impure silicon which have deposited downstream from the step 1 reactor in a temperature zone near $600^{\circ}C$. Emission spec. analysis verified that both of these materials contained high levels of metallic impurities. An additional function of the baffle was to help provide a cooler area for the condensation/nucleation of non-volatile impurities distilling from the step 1 reactor.

2.3.2.4 Low Temperature Condensation Coil

In Figure 2.3.5 is shown the low temperature condensation coil. This part of the system is a 3" diameter quartz assembly with 4 internal quartz coils constructed from 10 mm diameter tubing. The inlets and outlets on the coils are fabricated with a built-in internal thermocouple well.

During the course of the experiments liquid N_2 was fed into the apparatus from a 160 liter tank. The liquid N_2 flowing through the bottom three coils was mixed with room temperature N_2 to increase the temperature to about $-100^{\circ}C$. Liquid N_2 was fed directly into the top coil. In the series of experiments in which the ΔH of polymerization was measured for $(SiF_2)_x$, the exhaust N_2 flow was monitored via a rotameter. The rotameter was connected to the coils through a 30 foot piece of tubing which allowed the temperature of the N_2 exhaust to equilibrate to near room temperature $(25^{\circ}C)$ before entering the rotameter. Consequently no temperature correction was made in the calculation of the volume of N_2 exhaust. The calculated surface areas of the low temperature coils are listed in Figure 2.3.5.

After the N_2 had been flowing through the coil about 5 minutes and the temperature had stabilized, SiF_4 flow was begun into the stage 1 reactor zone, initiating the formation of a SiF_2/SiF_4 mixture. This was fed to the low temperature coils. The majority of the SiF_2 polymerized on contact with

Liq N_2 Inlet

To Traps and Pump

N_2
Inlet

114.6 in^2

67.9 in^2

94.2 in^2

N_2 Exhaust

104.3
in^2

N_2 Flow Meter

T

SiF_4 + SiF_2

To Traps and Vacuum Pump

$Si_x F_y$ Recycle

Si Bed
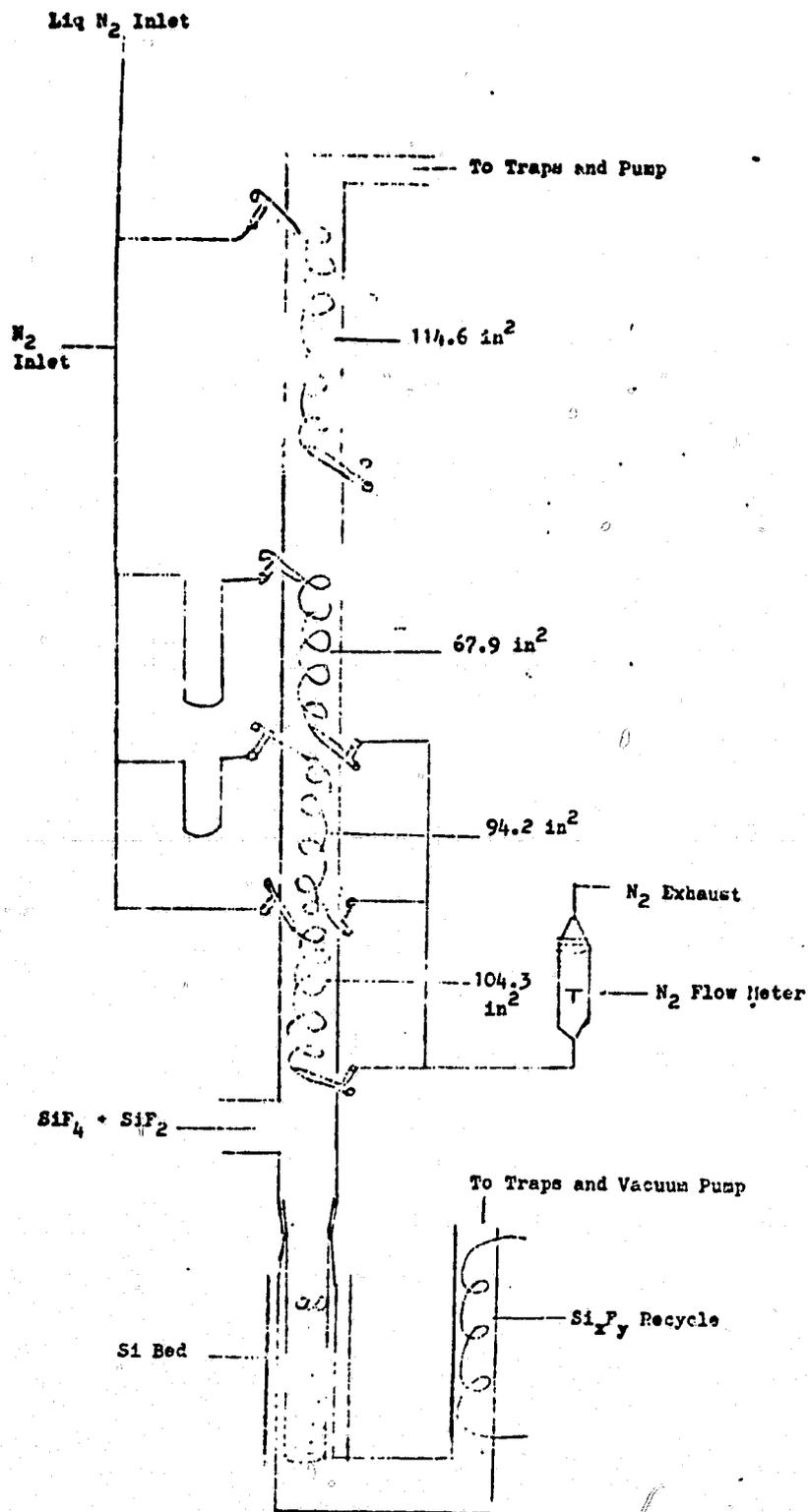
Figure 2.3.5 Schematic of N-C condensation coil.

the first coil. Residual SiF_2 ($\sim$2-10%) and unreacted SiF_4 (20-40% of
the process stream) condensed on the top (liquid N_2) coil.

At the completion of an experiment the SiF_4 flow was discontinued,
followed by termination of the N_2 flows. The $(SiF_2)_x$ polymer and SiF_4
condensation zones were allowed to warm to ambient. The process was ac-
companied by volatilization of unreacted SiF_4 which distilled into re-
movable weighed condensation traps. The completion of the distillation
processes was signaled by the return of the system to the initial background
pressure. A pressure recorder was used to more clearly define the necessary
pressure. The trap containing the unreacted SiF_4 was removed and weighed
(without warming) on an automatic Mettler open pan balance. The net SiF_4
reacted (i.e., SiF_4 delivered minus SiF_4 recovered), divided by the SiF_4
delivered, yielded step 1 reaction efficiency.

2.3.2.5 Silicon Harvesting

Figures 2.3.6 and 2.3.7 are sketches of the silicon harvesting bed
assembly. The bed is located directly below the low temperature coil.
During operation it is heated to $\sim$800°C with accompanying cooling of the
Si_xF_y recycle coil (see Figure 2.3.2). To begin the harvesting operation
the $(SiF_2)_x$ polymer on the coils is heated by external unitized heating.
In the unitized heating process small sections are sequentially heated
starting at the bottom, leaving previously heated section hot. A maximum
temperature of about 350-375°C is reached during this procedure. During the
process the $(SiF_2)_x$ polymer is converted into lower molecular weight Si_xF_y
homologues which distill from the hot zone and through the hot harvesting bed.
At Si_xF_y partial pressures above $\sim$7 torr the following homogeneous side re-
action appears to occur which yields a fine silicon powder.

$$Si_xF_y \xrightarrow[\text{7 torr}]{>300^OC} \frac{X}{2} \ Si + \frac{X}{2} \ SiF_4 \qquad \qquad \text{Step 3b}$$
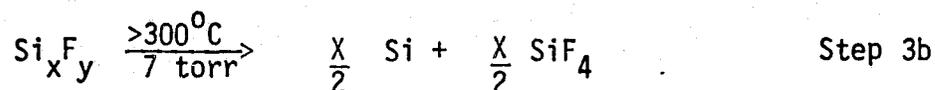
The remaining Si_xF_y homologues break down yielding CVD silicon directly on-
to the silicon in the harvesting bed.

Figure 2.3.6 In the figure above is sketched the entire quartz flange assembly. The assembly is composed of 4" quartz flanges (see Fig. 2.3.8), connecting quartz tubing (sizes 95/100 mm and 76/80 mm), and Kimax metal flanges with appropriate bolts, nuts, springs and washers. The flanges are sealed via a duplex Gore-Tex Teflon sealant/Viton o-ring method.

Figure 2.3.7   Shown above is the removable silicon harvestor. It is comprised of a Quartz sleeve insert containing the silicon bed which seals with Gore-Tex Teflon Joint Sealant. The bed is removed by opening the seal (see Figure 2.3.6) located above the bed and pulling the bed via the hook eyes. The Si bed is heated with a resistance furnace (not shown).

At the completion of a run the SiF_4 is distilled into a removable trap and weighed. The weight of the SiF_4 liberated from the $(SiF_2)_x$ polymer is used to calculate the mass of silicon transported.

$$(SiF_2)_x \longrightarrow \frac{X}{2} Si + \frac{X}{2} SiF_4 \tag{11}$$
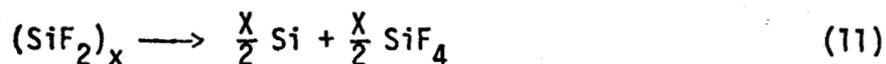
Si_xF_y homologues which distilled through the harvester bed without conversion and are collected on the Si_xF_y recycle coil are recycled as follows. The low temperature coil is cooled and the harvester bed is heated as before, followed by external heating of the Si_xF_y recycle zone to 350°C. The Si_xF_y homologues distill back through the bed. We have observed that as much as ∼98% of the Si_xF_y recycled was converted into Si and SiF_4 on the second pass. The SiF_4 liberated is trapped and weighed.

Silicon removal from the harvester is accomplished by backfilling the system with argon to atmospheric pressure and opening the 4" flange seal above the harvester (see Figure 2.3.7). The removable quartz harvester bed is then withdrawn. The harvester bed is inverted and the silicon chunks and powder are poured into a quartz crucible. The Si chunks are separated from the powder by screening and are returned to the harvester which is reassembled. The harvested silicon is stored under argon for subsequent analysis or crystal growth.

2.3.2.6 Quartz Flanges and Seals

The 4" conical flanges were purchased from Thermal American Fused Quartz Co. with o-ring groove ground to a depth of 0.055" (see Figure 2.3.8). The Parker Viton o-rings were size 2-157. The Gore-Tex joint sealant (100% virgin TFE fluorocarbon) was supplied by Quadna (Tucson, Az.). Each flange assembly consists of two 4 inch quartz flanges (Thermal American Fuzed Quartz Co.) with o-ring grooves. To isolate the Viton o-rings from the Si_xF_y homologues, a quartz sleeve was attached to the upstream quartz flange and extends past the seal. Furthermore, a Teflon seal (Gortex Teflon Joint Sealant,

REVISIONS					
REV.	ECO NO.	CHANGE	DATE	BY	
A	T.4318	.06 DIM WAS .074 TO .080 4.47 DIA WAS 4.737 ±.023 "O" RING No. WAS 158	9-6-73	DJC	

BREAK CORNERS
APPROX. .005 R.

0° TO 5°
TYP.

±.025 DIA

4.47

4.00
REF.

63

63

32

.06

.118
TO
.123

SEE ENLARGED
VIEW

PARKER "O" RING 2-157 REF.

UNLESS OTHERWISE SPECIFIED,
TOLERANCES:
INCHES .XX ±.02 .XXX ±.005
MILLIMETERS .X± — .XX± —
ANGULAR ± —
RMS ALL MACHINED
SURFACES.
FEATURE CONTROL SYMBOLS
PER ANSI Y14.5.
BREAK ALL SHARP EDGES AND
CORNERS, REMOVE BURRS.
UNDERLINED DIM NOT TO SCALE.
THIRD ANGLE ORTHOGRAPHIC
PROJECTION IS USED.

MATERIAL

HEAT TREAT

APPLIED FINISH

DRAWN BY Eileen CE   DATE 7-2-73

CHECKED BY   DATE

ENGR. APPROVAL   DATE

MOTOROLA INC.
Discrete Semiconductor Div.

TITLE: "O" RING GROOVE (4.00)
QUARTZ FLANGE
SOLAR SILICON PUR.

SIZE D   CODE IDENT. NO. 04713   DRAWING NO. GJ-04

SCALE NONE   WEIGHT —   SHEET 1 OF 1

NEXT ASSEMBLY | USED ON
APPLICATION

Figure 2.3.8 In the figure above is sketched the 4" I.D. conical quartz flange. The flange assembly
is shown in Figure 2.3.6.

1/8 inch) was placed inside the o-ring to further isolate the o-ring from Si_xF_y homologues. The Teflon Joint Sealant/Viton o-ring combination sealsata lower compression than a simple Teflon seal. The compression for the seal is supplied by a Kimax conical pipe flange coupling assembly equipped with eight bolts tightened to about 30 inch pounds.

2.3.2.7 Temperature and Pressure Monitoring

The temperatures in the step 1 reactor furnace and harvester bed were monitored by inserting a calibrated Pt/Rh (type "R") thermocouple between the furnace and the reactor tube. On those occasions when an internal probe was used, uranium glass graded seals were made to the platinum leads for sealing.

Temperature measurements in the $(SiF_2)_x$ polymer condensation area were made with Iron/Constantan thermocouples (type J). Special thermocouple wells were built into the center of the apparatus so that internal temperatures could be measured. In addition to monitoring the temperature with calibrated Doric Trendicator 400A Type J and R digital readouts, the temperatures were also recorded on multichannel Rustrak miniature temperature recorders. It was found that, after calibration, accuracies of $\pm 1^\circ C$ (limitation of reading the chart paper) were readily obtained on these low cost instruments.

Pressure measurements were made with calibrated Hastings vacuum gauges (e.g., DV-4D and DV-800) and were recorded on a Hastings MRV-4 vacuum recorder.

2.3.3 Results and Discussion

In the previous section, the N.C. apparatus was described in detail in additon to a description of the operational procedures of the system. In the present section results will be presented and their significance discussed for the following types of experiments.

i) Calibration experiments on s.g. silicon.

ii) Silicon sample production runs from mg silicon.

iii) Si_xF_y recycle experiments.

iv) ΔH of polymerization and heat transfer calculations

2.3.3.1 Calibration Experiments on Semiconductor Grade Silicon

The purpose of the calibration experiments was to identify the impurities which are introduced into the silicon product from the N.C. apparatus and SiF_4 reactant. Thus semiconductor grade silicon (~65 ohm cm) was crushed and loaded into the reactor. Six runs were made and the silicon harvested after the third and sixth runs. The operational parameters observed during the runs are contained in Table 2.3-2. During these runs (N.C. 70 to N.C-75), total downstream pressures of 0.5 torr were considered nominal and the SiF_4 flow was adjusted to maintain that pressure. The following is a discussion of observations made during these runs.

i) Step 1

Throughout this series, step 1 conversion efficiencies remained very constant. Our work to date has demonstrated that the step 1 conversion ef- ficiencies are directly dependent upon the reaction temperature and SiF_4 reaction pressure when a sufficiently long residence time is provided to ensure equilibrium. A more thorough discussion of the thermodynamics of step 1 can be found in Appendix I.

ii) Step 2

In this series of experiments the temperature of the gaseous N_2 coolant was set at -130°C for adequate cooling during polymer formation. If a coolant with a higher heat capacity were used such as liquid freon, then polymer formation could be accomplished with coolant temperatures at -70° to -80°C. The length of run was limited to 1 hour. Earlier runs (N.C. 33 and N.C.-40) demonstrated that the quantity of polymer (~800 gm) formed during a two hour run was sufficient to shear the inner coil as the

Table 2.3-2. Operational parameters observed during runs NC 70-75

RUN NO.	RUN DATE	RUN LENGTH (MIN)	SiF_4[a] DELIVERED (GM)	STEP 1[a] EFFICIENCY (%)	SILICON[b] PURIFIED (GM)	SiF_4[a] RECOVERY (%)	SILICON[b] TRANSPORT RATE (GM/HR)
NC-70	11/6/78	12	61.0	59.2			43.0
NC-71	11/7	32	165.5	62.3	31.5	90.2	
NC-72	11/8	60	331	62.4	51.8	95.7	51.8
Si_xF_y Recycle ———————					1.0 gm	94.1%Avg[c]	48.6gm/hr Avg[c]
NC-73	11/9	60	323	63.2	48.5	92.3	48.5
Si_xF_y Recycle ———————					3.5 gm	96.4[c]	52.1[c]

Silicon Harvested 132 gms

NC-74	11/17	60	347	60.3	49.2	92.3	49.2
NC-75	11/20	60	329	63.3	50.7	93.9	50.7
Si_xF_y Recycle ———————					5.4	96.0 Avg[c]	52.7 Avg[c]

Silicon Harvested 104.2 gm;   TOTAL SILICON HARVESTED 236.2 gm

(a) Measured value; (b) Calculated value; (c) Includes Si_xF_y recycle.

polymer expanded during warming. To date no such problems have occurred during 1 hour runs.

iii) Step 3

Unitized heating of the $(SiF_2)_x$ polymer and conversion into Si_xF_y homologues was adopted to uniformly convert the polymer into volatile compounds. In our earlier runs, before unitized heating, the entire mass of polymer was heated slowly. It was found that at a temperature between 200-250°C all of the polymer rapidly converted into volatile species, which sharply increased the pressure. In subsequent calorimetry studies, it was found that the polymer undergoes two exothermic conversions, the largest being near 280°C.[9]

iv) Step 4

A packed bed silicon harvesting arrangement was incorporated into the N.C. apparatus because of its simplicity and ease of operation. Two drawbacks are the small fixed amount of free volume and its tendency to clog as it is filled. The quantity of silicon which clogged the bed was found to be about 10% of the total mass of the bed. Thus, after 2 or 3 one hour runs the harvester required opening, powder removal, and reassembly.

Of the silicon harvested from the 3 one hour runs, typically about 50 gm of silicon was in the form of powder, another 75 gm was chemically vapor deposited on the bed and 25 gm lost as blowby thru the bed or because it never reached the bed. However no permanent layers of silicon or polymer were observed to form in the low temperature coil area.

A mass balance for silicon and for SiF_4 during the sg silicon runs is as follows.

Silicon Mass Balance

Step 1 reactor (observed)		Step 1 reactor (calculated)	
Silicon charge	520.8 gm	gm SiF_4 reacted	967.6 gm
Silicon unreacted	237.5 gm	mole SiF_4 reacted	9.30 moles
Silicon consumed	283.3 gm	Silicon consumed	260.4 gm

Silicon Harvest (observed)   Calculated

    Si + Harvester Total = 2454.5   gm SiF$_4$ recovered   897.2 gm

    Harvester Tare   = 2218.3   Moles SiF$_4$ 8.63 moles

    Obs. Silicon Harvest   236.2 gm   Calc. Silicon Harvest 241.5 gm

Si Mass Balance Efficiency = $\frac{236.2}{283.3}$ x 100% = 83.4%

Si F$_4$ Mass Balance

    Total SiF$_4$ in   =   1556.5

    Total SiF$_4$ unreacted   =   587.4

    Total SiF$_4$ off polymer conversion =   897.2

    Total SiF$_4$ out (587.4 + 897.2)   =   1484.6

Overall:

    SiF$_4$ mass balance efficiency 95.4%

    Over the course of about 100 experimental runs on the near-continuous reactor, typical Si transport efficiencies of ~80% were observed. The other 20% forms a metallic deposit downstream from the step 1 reactor in the 500-700°C region and an orange powdery scale which accumulates in the baffle region. The percentages of silicon deposited in these regions appears to be dependent upon the partial pressure of SiF$_2$, residence time of SiF$_2$ in the region, surface area and surface temperature. At 200°C or above, material lost in this region is minimized. For example, in earlier experiments the surface temperature in the baffle region was allowed to stay at ambient and up to 50% of the (SiF$_2$)$_x$ polymer and Si$_x$F$_y$ homologues deposited in this region. This reduced silicon transport rates and efficiencies.

    Under heated baffle conditions, SiF$_4$ mass balances, unlike Si balances, are quite high. Typical values range from 95-98%. A small amount of SiF$_4$ is lost by incorporation into the orange powdery scale. In addition, a small amount may be lost by not condensing in the liquid N$_2$ traps.

    v) Silicon Purity

    Polycrystalline silicon ingots were pulled from the remaining reactor charge and from the transported silicon charge. Resistivities were measured on both materials. The following is a summary of the results.

Sg Silicon Charge　　　　　　　　　　　　　　　　　　　　　**Silicon Harvested**

　　　　　　　　　　　　　　　　　("N" type)
　　Resistivity of Si charge before = 65Ωcm　　　Resistivity 5-7 Ωcm ("P")
　　Resistivity of Si charge after = 5-7 "

These results suggest that some "N" dopant is coming from the inlet SiF_4 or stage 1 reactor and the "P" dopant is introduced downstream in the N.C. apparatus or in the handling of harvested product.

2.3.3.2 Silicon Sample Production from Mg Silicon.

The purpose of these runs was to produce silicon samples for demonstration of purification and feasibility of the process. In Table 2.3-3 are shown operation parameters for a series of 5 consecutive runs. The following mass balances were observed.

(i) Silicon Mass Balances (NC 85-89)

Silicon In

Step 1 Reactor (observed)　　　　　　　　　Step 1 Reactor (calculated)

　　mg Si charge　　.380.0 gm
　　Final Wt.　　　　150.5 gm　　　　　　　Total Si reacted 200.9 gm in 4 hrs

　　Weight Lost　　　229.5 gm

Silicon Out

Observed　　　　　　　　　　　　　　　　Calculated

　　First harvest　82 gm　　　　　　　　　= 178.5 gm
　　Second harvest　84 gm

　　Total Si out　166 gm (56.5 gm powder + 109.5 gm CVD)

Overall Si Transport Efficiency

Observed　　　　　　　　　　　　　　　　Calculated

$$\frac{\text{Silicon out}}{\text{Silicon reacted}} \quad \frac{166}{229.5} \times 100\% = 72.3\%$$　　　$$\frac{\text{Silicon out}}{\text{Silicon reacted}} \quad \frac{178.5}{200.9} \times 100\% = 88.9$$

Table 2.3-3. Operational parameters observed during runs NC 85-89

RUN NO.	RUN DATE	RUN LENGTH (MIN)	SiF_4[a] DELIVERED (GM)	STEP 1[a] EFFICIENCY (%)	SILICON[b] PURIFIED (GM)	SiF_4[a] RECOVERY (%)	SILICON[b] TRANSPORT RATE (GM/HR)
NC-85	1/12/79	60	267	47.8	30.8	95.1	30.8
NC-86	1/13	60	289	49.9	37.9	98.8	37.9
NC-87	1/14	60	282	51.8	38.4	98.8	38.4
Si_xF_y Recycle					0.5		

Silicon Harvested: 82 gm

| NC-88 | 1/16 | 82 | 406 | 57.6 | 58.0 | 95.5 | 42.4 |
| NC-89 | 1/17 | 100 | 390 | 64.0 | 65.3 | 98.2 | 39.2 |

Silicon Harvested: 84 gm   TOTAL SILICON HARVESTED 166 gm

(a) Measured value

(b) Calculated value

(ii) SiF_4 Mass Balance (NC 81-84)

SiF_4 in	SiF_4 unreacted	SiF_4 from conversion	SiF_4 total
1279 gm SiF_4	533.4 gm	665.1	1198.5

$$SiF_4 \text{ Mass Balance} = \frac{1198.5}{1279.0} \times 100\% = 98.7\%$$

The total quantity of silicon harvested was 166 gm; 56.5 gm powder and 109.5 gm C.V.D. SSMS analysis (sample # NC87 & 79, Table 2.3-3) and electrical evaluations were conducted on silicon obtained from the powder after crystal growth. Resistivities varied between the two batches of silicon and between the seed and tang end of the ingot. Typical seed end measurements varied between 0.1 and 25 ohm-cm, with tang end at 0.3 to 0.6 ohm cm, n-type.

The 1400 gm silicon (sg poly) bed containing the 109.5 gm C.V.D. silicon was also used for crystal growth. Wafers cut from the seed and tang had resistivities of 8.6 ohm cm ("P" type) and 7.0 ("N" type) respectively. The remainder of the ingot and silicon wafers were sent to JPL for fulfillment of the silicon sample requirement.

In Table 2.3-4 are listed the parameters of the first 40 runs on the near-continuous apparatus. The transport rates have increased from ~5 to ~50 gm/hr, with 75 gm/hr as a maximum rate observed. Two hour runs have been conducted; however, under the overloaded conditions, the low temperature coil may fail. Overall silicon mass balances are ~80% whereas SiF_4 mass balances are ~95-97%.

2.3.3.3 Si_xF_y Recycle Experiments

One of the early chemical process problems concerned the maximum efficiency of conversion of the $(SiF_2)_x$ polymer or Si_xF_y homologues into silicon. Specifically, "was a thermally stable silicon containing compound formed from the $(SiF_2)_x$ polymer which would not convert into silicon thus

95

Table 2.3-4 Summary of data from the first 40 runs on the near-continuous apparatus.

Run No.	Run Date	Run Time (Min)	SiF₄ Delivered (gm)	SiF₄ Unreacted (gm)	Step 1(a) Conversion (%)	SiF₄ from Conversion (gm)	Silicon (b) Purified (gm)	Transport Rate (gm/hr)	SiF₄ (c) Recovery (%)
NC-1	9/9/77	60	31.7	10.4	67.2	6.9	1.86	1.86	54.3
NC-2	"	60	31.7	3.9	87.7	20.7	5.6	5.6	74.8
NC-3	10/6	60	129.6	26.4	79.6	41.6	11.2	11.2	52.5
NC-4	"	15	32.4	5.9	81.8	3.7	1.0	4.0	29.6
NC-5	"	15	32.4	20.5	36.7	9.8	2.6	10.6	93.5
NC-6	"	\-\- SiₓFy recycle (from NC-3-5)				20.7	5.6	\-\-	.66.2 (overall)
NC-7	7	15	32.4	8.0	75.3	9.0	2.4	9.6	52.4
NC-8	"	60	129.6	38.8	69.4	59.5	16.0	16.0	75.8
NC-9	"	\-\- SiₓFy recycle (from NC-7 & 8)				35.1	9.45	\-\-	92.8 (overall)
NC-10	19	30	96.0	35.1	63.4	48.1	12.95	25.9	87.2
NC-11	20	30	96.0	35.9	62.6	37.8	10.18	20.4	76.8
NC-12	"	25	80.0	29.6	63.0	12.0	3.23	6.5	52.0
NC-13	21	30	96.0	45.9	52.2	43.3	11.66	23.3	92.9
NC-14	"	\-\- SiₓFy recycle (from NC-13-13)				53.6	14.43	\-\-	92.8 (overall)
NC-15	11/28	30	100	33.2	66.8	16.9	4.6	9.2	50.1
NC-16	"	30	100	29.0	71.0	16.7	4.5	9.0	45.7
NC-17	"	60	200	58.6	70.7	45.5	12.3	12.3	52.1
NC-18	"	60	200	53.3	70.9	89.8	24.2	24.2	71.6
NC-19	"	60	200	67.7	66.1	64.5	17.4	17.4	66.1
NC-20	29	120	400	130.9	67.1	157.2	42.3	21.2	72.0
NC-21	30	120	400	191.4	52.2	95.6	25.7	12.7	71.8
NC-22	12/1	\-\- SiₓFy recycle (from NC-16-21)				172.8	46.6	\-\-	76.8 (overall)
NC-23	1/23/78	30	101	50.3	50.2	27.0	7.3	14.3	76.5
NC-24	25	60	202	86.0	57.4	81.8	22.0	22.0	83.0
NC-25	26	60	202	71.2	64.8	126.2	34.0	34.0	97.7
NC-26	28	60	202	95.1	52.9	109.5	29.5	29.5	101
NC-27	28	\-\- SiₓFy recycle (from NC-23-26)				47.2	12.7	\-\-	98.2 (overall)
NC-28	3/30	30	133	94.3	29.1	12.7	3.4	13.6	80.5
NC-29	"	15	110	50.8	53.8	(COIL CRACKED UPON WARMING)			
NC-30	4/6	15	70.5	46.2	34.5	10.2	2.0	11.2	80.0
NC-31	7	15	41.0	13.0	68.2	24.7	6.7	13.3	92.0
NC-32	10	120	607	158.8	73.8	419.5	112.9	56.5	95.3 (e)
NC-33	11	120	562	(COIL CRACKED UPON WARMING)					
NC-34	5/10	15	50.0	21.3	57.4				
NC-35	"	15	72.5	33.6	53.7	96.7	26.0	34.7	93.1
NC-36	11	15	79.5	37.4	52.9				
NC-37	12	120	661	268.6	59.4	379.8	102.3	51.1	98.1
NC-38 (f)	15	120	639.5	243.3	62.0	395.5	106.5	53.2	99.9 (d)
NC-39 (f)	24	120	611	212.7	65.2	362.2	97.5	48.8	94.0 (e)
NC-40	25	120	632.5	(COIL CRACKED UPON WARMING)					

(a) Bed parameters (mg Si): Diameter 1"; Length 53.5 cm; Temperature $1330^\circ C$ inlet, 1350 (center), 1300 outlet; particle size 5-20 mesh mg Si; Weight 396 gm mg Si + 4.0 gm SiO_2.
(b) Calculated value.
(c) Measured value.
(d) Includes SiₓFy recycle.
(e) SiₓFy recycle will increase this value 3-6%.
(f) Inlet pressure at start of run NC-38 was 155 torr, run NC-39 was 300 torr; inlet pressure at finish of run NC-38 equaled 98 torr, run #2 equaled 99 torr; downstream pressures of 0.50 and 0.55 torr were observed for runs NC-38 and 39 respectively.

reducing the overall transport efficiency?" The solution to the problem became apparent by recycling the Si_xF_y homologues (see Table 2.3-4).

Runs NC-6, 9, 14, 22 and 27 represent Si_xF_y recycle runs. Si_xF_y recycle is accomplished by redistilling the Si_xF_y homologues through the silicon harvesting bed which is maintained at $\sim 800^\circ C$. After run NC-27, Si_xF_y recycle was not deemed necessary because of the high observed polymer conversion efficiencies ($\geq 95\%$ on the first pass) during the unitized polymer conversion to decomposition of the higher homologues into SiF_4 and silicon before reaching the harvestor bed. Furthermore, as the bed fills with silicon (less free void space through the bed) the Si_xF_y partial pressure increases above 10 torr which leads to higher homologue conversion efficiencies. For example, in runs NC-23 through 26, NC-30 through 33 and NC-34 through 38 the increasing conversion efficiency trend is readily apparent. After runs NC-26, 29, 33, 38, and 40, the silicon was harvested and the bed replaced.

2.3.3.4 Heat Transfer Coefficient (U) and ΔH Heat of Polymerization of $(SiF_2)_x$

Seven calorimetry experiments were conducted on the N-C apparatus and the calculated values for U, the heat transfer coefficient, and ΔH, the heat of polymerization of $(SiF_2)_x$ are found in Table 2.3-5. Values ranging from -12 to -24.8 kcal/mole were observed for the ΔH polymerization of $(SiF_2)_x$. These values are below the value of -37.3 kcal/mole used in the energy balance for scale up purposes.

The values calculated for U (see Table 2.3-5) range between 3 and 8 Btu/hr-ft^2-$^\circ$F.

It should be noted that the effect of nitrogen coolant flow indicates that it is limiting the heat transfer rate.   Thus, we would expect higher U in the mini-plant where the liquid freon coolant will have a much higher heat transfer coefficient than the gaseous N_2 coolant.

Table 2.3-5. Heat transfer coefficient and heat of
polymerization of $(SiF_2)_x$

Run No.	N_2 Coolant Flow Rate	Overall Heat Transfer Coefficient U, Btu/hr-ft^2-$^\circ$F	Heat of Polymerization $-\Delta H^*$, kcal/mole SiF_2
63	1.37	3.4	12.0
64	1.37	3.4	11.5
65	1.67	3.7	18.2
66	1.37	3.3	18.2
67	1.57	3.8	19.9
68	2.17	8.2	23.6
69	2.0	6.5	24.8

*Not corrected for sensible heat of SiF_4 and SiF_2

98

2.4   Product Analysis

2.4.1   Introduction

In the early stages of this project, a concentrated attempt was made to determine if chemical methods could be used to characterize the silicon product other than by growing crystals. The results of that effort were used as a guide to interpretation of the subsequent analytical results.

In this section the concept of semiconductor silicon will be discussed along with work done to establish chemical techniques and criteria. Comparison of chemical techniques with crystal growth as evaluation tools and the chronological evolution of SiF_2 transported product purity are presented.

2.4.2   Working Definition of Semiconductor Grade Silicon

A number of aspects must be considered when defining semiconductor grade (sg) silicon. The most important would seem to be, what the properties of the silicon are when you pull a crystal and make a device. Crystal pulling can also be a major aspect in the total sg silicon purification process. In this step, impurities which have small distribution coefficieints ($<10^{-2}$) are effectively eliminated from the solid silicon. Conversely, sg silicon which has not been purified by crystal pulling or float zone refining often contains relatively high concentrations of materials with small distribution coefficients.

Initially we adopted the following as a working definition. Using spark source mass spectroscopy (ssms) as the analytical tool, sampling matrix was employed to compare the SiF_4 transport poly directly with samples of commercially available sg poly. This would allow the development of the process in the most efficient manner and permit the most rapid evaluation.

2.4.3   Spark Source Mass Spectroscopy (SSMS)

In order to employ ssms as a valid evaluation technique, a data base was to be established by analyzing several samples of commercially available

semiconductor grade polycrystalline silicon by ssms. Data obtained for SiF_4 transport silicon were to be compared to this baseline data for evaluation.

A major problem occurred with this plan. Data obtained from analyses by an outside service lab[*] indicated much larger concentrations of impurities than found by electrical or other analytical methods on commercial polysilicon. This led to suspension of further product analysis until adequate comparative standards were obtained to establish the limitations of the ssms technique in a service lab. environment. To this end a sample exchange was begun with other investigators in Task I who were using ssms as a primary analytical tool This allowed cross checking and led to working standards which helped resolve the reliability problems.

Before these results are discussed,a description of the ssms analytical technique for powder samples is necessary. In the following sections the form of the samples for ssms is:

i) Most of each SiF_2 transport Si sample was in the form of small grain powder (1 to 5 micron).

ii) All sg poly samples are large single pieces of Si made up of small single crystals.

iii) Crystal samples were used as single pieces.

2.4.3.1 SSMS Techniques for Analysis of Powder Samples

The procedure for handling and analyzing powder samples of Si was developed at Accu-Lab. Research, Inc. It is as follows:

i) The sample is ground in a high purity quartz vial until it is a fine powder. Subsequently both BN and SiC mortar and pestle sets were used to grind material. BN was the most satisfactory for all elements except boron.

[*]Accu-Lab. Research Inc., Wheat Ridge, CO

TABLE 2.4-1

COMPARISON OF SSMS DATA FOR ANALYSIS OF DOW CORNING COMMERCIAL SG POLY SILCON FROM DIFFERENT LABS. (ppm wt.)

| | Service Lab | | Monsanto | |
	15	16	35 a	35 b
B	N.D. 4E-3		N.D. 1.1E-3	N.D. 9.6E-4
C			--	--
N	--		--	--
O	--		5.3E-1	1.5E-1
F	1.7E-1	N.D. 2.1E-2	6.0E-1	2.0E-1
Na	1.6E-2	1.4E-2	3.8E-2	6.5E-3
Mg	1.6E-2	6E-3	NR	ND 2.4E-3
Al	8.7E-2	1.7E-1	NR	" 2.3E-2
P	1.4E-1	3.7E-1	NR	" 2.3E-2
S	2.4E-2	1.2E-2	NR	" 1.2E-2
Cl	8.1E-2	1.9E-2	1.3E-1	4.0E-2
K	3.7E-1	2.3E-2	3.6E-1	4.0E-3
Ca	2.3E-1	5E-1	off scale EST	1.4E-2
Ti	2.1E-2	6.3E-2	3.6	1.5E-2
V	ND 5E-2	ND 5E-2	NR	ND 4.1E-3
Cr	ND 2.3E-2	7.5E-2	NR	2.5E-2
Mn	3.9E-1	1.0	NR	ND 7.4E-3
Fe	1.7E-1	1.3	NR	" 1.0E-1
Ni	2.9E-1	1.5	NR	" 1.4E-1
Cu	2.3E-1	8E-2	NR	" 1.7E-2
Zn	2.4E-2	6.7E-2	ND 7.2E-3	" 5.5E-3
Ga		ND 5E-2	NR	" 4.4E-3
Ge		"	ND 1.4E-2	" 1.2E-2
Zr		"	ND 6.0E-2	" 5.7E-2
Mo		"	ND 5.2E-2	" 4.2E-2
Ag		"		ND 2.8E-2
Sn		"		3.1E-2
Sb		"		3.0E-2
Te		"		6.6E-2
Bn		"		2.9E-2
W		"		1.1E-1
Pb		"		7.6E-2
Bi		"		4.0E-2

N.D. = not detected--numberical value is the detection limit

N.R. = not reported

101

ii) The powder is slurried with an equal weight of high purity
graphite in distilled acetone until thoroughly mixed. The
graphite ratio was determined to give good results in the
pressing operation.

iii) The dried mixture is pressed into the shape of the electrode
in a high purity polyethylene form. Under pressure the form
liquifies. Thus a uniform hydrostatic pressure performs the
compaction operation. Very small samples ($\sim$10 mg) are mounted
so that the sample is in the tip of the electrode.

iv) The electrodes are mounted in the ssms and standard analysis is
conducted.

2.4.3.2 SSMS Sample Exchange

A sample of Dow Corning polysilicon was sent to Monsanto for ssms
(sample #35). This sample was part of the same piece as samples 15 and 16
analyzed by the service lab. Table 2.4-1 lists the element by element con-
centration data obtained by the two different labs. Samples 15 and 16 were
submitted separately and not identified as the same material. Sample runs
35a and 35b were run on a single sample. It was dismounted and shaped between
runs. In Table 2.4-2 are listed the results for two single crystal samples
from the Monsanto group. It is again apparent that for some elements (i.e.,
Na, K, Ca and Mn in this case) the reproducibility is not good. since the
highest readings appear to be associated with the same sample (C-1-A) it may
point to a problem in the sample handling procedure. For the elements most common
in mg silicon the agreement is very good (Fe, Al, Mg, Ti, Cr and Ni).

The data from samples 15 and 16 (Table 2.4-1) tend to indicate poor
reproducibility. However, a closer examination of 35a and 35b shows that other
factors may be very critical in determining the reliability of the analysis for
each individual sample. Figure 2.4.1 is a schematic diagram of a cross section
of a polycrystalline sample. The composition of the interior of the grain will

TABLE 2.4-2

Comparison of SSMS analyses from Service Lab.
and reported data for Monsanto samples

	Sample C-10-B-1		Sample C-1-A	
ELEMENT	SERVICE LAB.	REPORTED[15]	SERVICE LAB.	REPORTED[15]
Be	<31 ppba	NR[1]	<31 ppba	NR
B	16	180 ppba	104	120 ppba
C	670	540	12600	96
O	NR[1]	78000	NR	49
F	59	50	59	24
Na	145	9	330	6
Mg	ND[2] 58	ND 2	ND 58	ND 2
Al	53000	40000	31	" 23
P	ND 45	ND 25	ND 45	" 17
S	ND 44	ND 12	ND 44	15
Cl	<8	9	8	11
K	58	3	600	2
Ca	63	7 estimated	450	9 estimated
Ti	<12	ND 2	<12	ND 2
V	ND 27	ND 2	ND 27	ND 1
Cr	<11	ND 2	<11	7
Mn	51	ND 3	820	ND 2
Fe	27	ND 39	55	ND 29
Ni	<170	ND 46	<140	ND 40
Cu	9	ND 5	<9	ND 4
Zn	ND 30	ND 2	ND 30	ND 1
Ga	ND 20	ND 1	ND 20	ND 1
Ge	ND 18	ND 3	ND 18	ND 2
Zr	ND 15	ND 11	ND 15	NR
Mo	ND 15	ND 8	ND 15	ND 6
Ag	ND 13	ND 4	ND 13	ND 3
Sn	ND 12	NR	ND 12	NR
Sb	ND 12	NR	ND 12	NR
Te	ND 11	NR	ND 11	NR
Ba	ND 10	NR	ND 10	NR
W	ND 8	NR	ND 8	NR
Pb	ND 8	NR	ND 8	NR
Bi	ND 7	NR	ND 7	NR

1　Not Reported

2　Not Detected - Reported detection limit
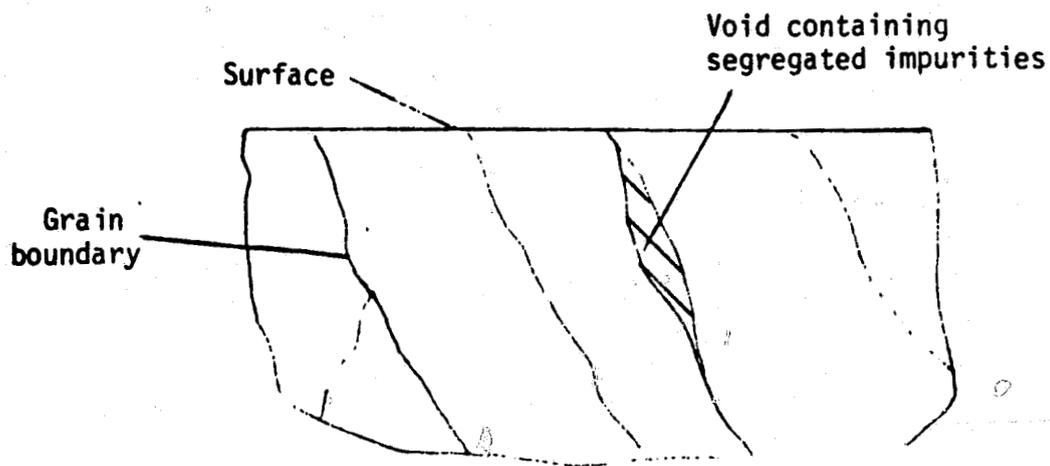
Figure 2.4.1 Schematic cross sectional diagram of a sample of commercial poly silicon SSMS sample showing the grain boundary and void structure which influences analytical results.
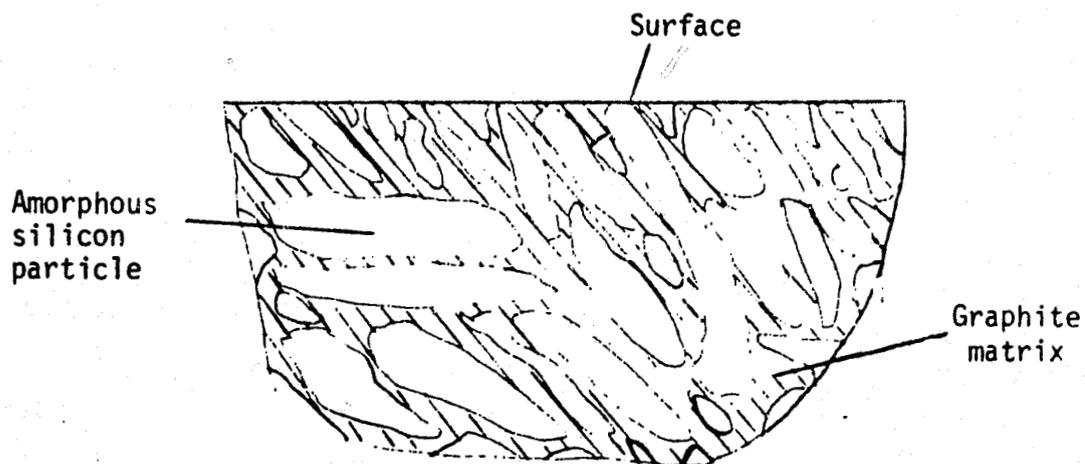
Figure 2.4.2 Schematic cross sectional diagram of a composite SSMS sample (SiF_2 poly and graphite). The large silicon particle surface to volume ratio which influences analytical results is illustrated.

be characteristic of bulk material. The relatively small surface area will have a minor effect. A very real problem arises in ssms when the discharge strikes a grain boundary or void. In these regions the apparent concentration of impurities may be much higher than the bulk due to surface absorption during manufacturing deposition and/or segregation effects. The data illustrates this effect very clearly for 35a) and b) particularly with respect to Ti and Ca. According to the Monsanto spectroscopist[9] a void or inclusion was struck by the arc during the analysis. These high concentration readings are reportedly typical when this occurs when sg polycrystalline material is analyzed. This may partially explain why when commercial sg poly is analyzed consistently high readings are obtained for some impurities while these same elements appear to be absent in single crystal material reported elsewhere. It should be noted that analytical data (electrical and chemical) available for commercial sg poly lots is often gathered on samples which have been subjected to float zone crystal growth which eliminates grain boundary/void problems.

The grain boundary/void problem must be considered whenever material other than single crystals is being analyzed. In the case of compacted composite samples such as the SiF_2 transported poly/carbon samples. This becomes a much more severe problem. Figure 2.4.2 illustrates that the much larger particle surface area may influence the ssms results because of absorbed material and segregation effects. Here the surface is not sputtered away as in the case of a single crystal sample, but as the sputtering of a composite electrode proceeds, new material is exposed to the arc which was in a surface state after the decomposition process. It is apparent that an understanding of the influence of surface cleaning, prior to compaction, on the resulting impurity analysis is necessary to correctly interpret the ssms data of compacted samples.

One of the first steps to the understanding of the effects of surface contamination was to eliminate the possible sources of impurities during sample preparation. It has been necessary therefore, to improve the reliability of the sample grinding procedure used in the fabrication of the composite graphite/silicon sample electrodes. At first the samples were ground in a ball mill. The sample was contained in a quartz vial with quartz balls which were used to pulverize the silicon. Occasionally the balls would chip or break up during

the operation. Contamination of the silicon samples was also probable for those samples for which no visual breakdown of the vial and balls was noted. Trace impurities present in quartz are at high enough levels to have placed some uncertainty in the ssms data. This problem was reduced by obtaining a boron carbide mortar and pestle set. Boron carbide is a preferred material for this process. Because of its hardness it will not contaminate silicon samples during grinding except possibly with boron.

Sample cleaning procedures were also evaluated to help reduce the surface contamination problem. Some impurities such as fluorine, alkali and earth metals can be removed from the surfaces of powder or flaked material at least partially by rinsing in D.I. water. Other impurities such as heavy metals can be removed by etches. Therefore some SiF_4 poly from a test run was divided into several lots and subjected to various cleaning procedures. Some preliminary results have been gathered by emission spec analysis. Table 2.4-3 lists the ES results. More complete data from ssms showed the same results.

Table 2.4-3 ES analysis data for samples prepared by SiF_2 transport which have been cleaned by various techniques (ppm wt.).

SAMPLE	CLEANING PROCEDURE	Al	Mn	Mg	Cu
46	As prepared	800 $\pm$200	2 $\pm$1	$\leq$1	3 $\pm$1
47	D.I. H_2O rinse	"	"	"	"
48	HF:HNO_3 etch D.I. H_2O rinse	"	"	"	"
49	H_2SO_4:H_2O_2 etch D.I. H_2O rinse	"	"	"	7 $\pm$2

In Table 2.4-4 are summarized the apparent reliability limits for all of the samples which were exchanged. Again, for the most common mg Si contaminants, the reliability limits are in good agreement. For others such as Ca, Na, Mn, K, etc. there is very poor agreement. For those samples where agreement in reliability limits is good, such as Fe and Zn, the reliability limit is clear, ∿50 and ∿40 ppba respectively. Where agreement is poor such as for Mn, reliability is questionable and each analysis must be evaluated independently in context.

It should be noted that this is a technique which analyzes a small portion of the sample; therefore, non homogeneity in the distribution of the impurity in the sample can lead to misleading concentration values. This was clearly illustrated by a previously reported sample and should be considered whenever anomolous data is generated.

2.4.3.3 Powder Sample Correction Factors

Since there is a distinct difference in ssms sample preparation between powder and single crystal samples, an experiment was run to further establish the reliability and accuracy of the ssms analyses which have been run on the SiF_4 transport product. The experiment was simply this: a sample of n-type single crystal silicon, which was analyzed on an in-house project, and was found to contain <.005 ppm wt. of boron, was resubmitted for analysis by the same technique as the powder samples. The sample was ground in a boron carbide and a silicon carbide mortar and pestle, slurried with distilled acetone and graphite, then compressed into electrodes. The result of this handling is shown in Table 2.4-5.

The first column is the result for the single crystal sample prior to grinding. The second column lists the results for the same material after handling in boron carbide, while the third lists the results after grinding in silicon carbide. Subtracting column 2 from column 1 gives a correction factor (Δ) which can be used to give a more realistic measure of the purity of the powder product which has been prepared in BC apparatus. Similarly, a Δ for SiC was calculated. These factors are quite high for several of the elements

Table 2.4-4 Apparent detection limits for service lab ssms analysis for various samples which were run as single pieces.

Element	Dow Corning Commercial Poly	Dow Corning Single Crystal	Monsanto Single Crystal C-10-B-1	C-1-A
B	10.5 ppba	∿ 50 ppba	(1)	(2)
C		5000	700 ppba	12,600 ppba
F	250	1000	60	60
Na	17		150	350
Mg	18	70	nd 58	nd 58
Al	175		(1)	35
P	350		nd 45	nd 45
S	21		nd 44	nd 44
Cl	63	5000	10	10
K	300		60	600
Ca	350		65	500
Ti	35	nd 30	<12	<12
V	nd 28	nd 30	nd 27	nd 27
Cr	nd 14		<11	<11
Mn	200	60	51	820
Fe	50		30	60
Ni	140		<170	<140
Cu	35	40	10	10
Zn	30	nd 50	nd 30	nd 30
Ga	nd 20		nd 20	nd 20
Ge	nd 18		nd 18	nd 18
Zr	nd 15	nd 50	nd 15	nd 15
Mo	nd 15		nd 15	nd 15
Ag	nd 13		nd 13	nd 13
Sn	nd 12		nd 12	nd 12
Sb	nd 12		nd 12	nd 12
Te	nd 11		nd 11	nd 11
Ba	nd 10		nd 10	nd 10
W	nd 8		nd 8	nd 8
Pb	nd 8		nd 8	nd 8
Bi	nd 7		nd 7	nd 7

1) Al and B doped
2) B doped

ND = not detected by either lab: highest reliability limit listed.

Table 2.4-5 SSMS results for semiconductor grade single crystal sample prepared by various methods. Growth specimens slurried with graphite and compacted into electrodes. (ppm wt)

	Single Crystal	Ground in BC	Ground in SiC	Δ_{BC} (Column 2 – Column 1)	Δ_{SiC} (Column 3 – Column 1)
B	<.005	7.4	2.0	7.4	2.0
F	--	48	130	48	130
Na	--	<6.0	<6.0	<6.0	<6.0
Mg	--	<1.2	4.7	<1.2	4.7
Al	.03	0.61	99	.58	99
P	.16	3.2	2.9	3.0	2.7
S	--	3.9	14	3.9	14
Cl	<.01	4.2	14	4.2	14
K	.21	<1.0	1.9	<1.0	1.7
Ca	.20	.61	1.3	.41	1.1
Ti	<.02	.03	3.5	.01	3.5
V	--	--	.26	--	.26
Cr	--	--	1.5	--	1.5
Mn	.46	.02	1.4	-.44	.9
Fe	<.09	1.3	56	1.2	56
Ni	1.5	--	<.29	-1.5	-1.2
Cu	.01	.30	5.5	.3	5.5
Zn	--	--	.60	--	.6
Sr	--	.03	.08	.03	.08
Zr	--	--	2.3	--	2.3
Nb	--	--	.51	--	.51
Mo	--	<.11	.90	<.11	.90
Cd	<.16	--	<.13	-<.16	--
Sn	--	<.09	.88	<.09	.88
Ba	--	5.9	1.4	5.9	1.4
La	--	<.04	<.04	<.04	<.04
HF	--	--	<.22	--	<.22
W	--	--	4.8	--	4.8
Pb	--	<.07	<.07	<.07	<.07

of primary concern such as B, P, Fe and Al. It is recognized that since these Δ values are the results of only one experiment they are not to be taken as anything but indications of contamination during sample preparation.

Table 2.4-6 lists the results obtained for a sample after the correction factor has been used to compensate for handling contamination. Column 1 is the Δ factor. The second column is the result for 77-215-38-8 after standard processing and the third for the same sample after correction.

Some observations can be made:

i) BC mortar and pestle sets contaminate less than SiC sets.

ii) The SiF_2 transport product analyses reported to date may in fact indicate contamination which is not real, but an artifact of the ssms analytical procedure, the real impurity concentration being much lower than reported.

iii) SSMS analysis of powder samples may not be at all reliable in determining powder purity and its usefulness as input material for crystal growth. The only apparently valid test is actual crystal growth coupled with subsequent solid state material evaluation.

2.4.4 Emission Spectroscopy

In-house emission spectroscopy (ES) analysis facilities have been extensively utilized in this project as a semiquantitative tool for evaluation. The detection limits are much higher than for ssms, but are adequate for coarse evaluation for many impurity elements. Phosphorus is one element, however, for which ES is not useful.

2.4.5 Comparison of ES and SSMS Analyses

To verify that ES is an adequate screening process, a comparison of results from ES and ssms are listed in Table 2.4-7. Only five elemental impurities were detected by ES; they are Mg, Al, Ca, Mn and Cu. No Fe was detected. Metals such as Fe, Al and Mn are compared to 1, 10, 100, 1000 ppm wt.

TABLE 2.4-6

SSMS results for single crystal and slurried samples. (ppm wt)

	Δ	.77-215-38-8 as received	77-215-38-8 Corrected
B	7.4	4.3	--
F	48	250	200
Na	<6.0	<6.0	--
Mg	<1.2	<1.2	--
Al	.58	3.0	2.4
P	3.0	3.2	.2
S	3.9	8.4	4.5
Cl	4.2	74	70
K	<1.0	4.3	3.3
Ca	.41	4.6	4.2
Ti	.01	.10	.09
V	--	.02	.02
Cr	--	2.1	2.1
Mn	-.44	.03	--
Fe	1.2	2.0	.8
Ni	-1.5	.16	--
Cu	.3	1.1	.8
Zn	--	.75	.75
Mo	<.11	1.1	1.0
Cd	-<.16	.15	--
Sn	<.09	.11	.02
Ba	5.9	.59	--
La	<.04	.06	.02
Sr	.03	--	--
Pb	<.07	<.07	--

TABLE 2.4-7

Comparison of ES and SSMS data for SiF_4 transport poly. Run 2-11-77 trap 2, concentrations in ppm wt.

ELEMENT	SAMPLE 79 (ES)	SAMPLE 85 (SSMS)
B	NR*	4.3***
F	NR	>0.5%
Na	ND** (500 ppm wt d.l.)	<17
Mg	<1	<5
Al	1-10	1.3
P	NR	10
S	NR	11
Cl	NR	0.21
K	ND (500 ppm wt d.l.)	3.8
Ca	1	6.8
Ti	ND	0.23
Cr	ND	0.33
Mn	<1	1.2
Fe	ND	5.7
Ni	ND	0.05
Cu	<1	0.19
W	ND	1.6
Zn	ND	0.29

ALL OTHER ELEMENTS <0.2 ppm wt.

*Not Reported

**Not Detected - usually detection limit <<1 ppm wt.

***Sample Ground in BN mortor and pestal

112

standards. Often metals are detected, but have characteristic emissions less intense than the 1 ppm wt. standard. Thus, for Fe to be undetected, its concentration in the sample must be <<1 ppm wt. This is true for many other metals except for the alkali metals which have higher detection limits.

The ssms analysis agrees quite well with ES reports. In most cases metals undetected in ES show up in low concentrations by ssms. Calcium is slightly higher in ssms and ES. The presence of iron at 5.7 ppm by wt. as reported by ssms is surprising and may imply Fe contamination of the sample during grinding or compounding when the electrode is prepared.

2.4.6   mg Silicon Bed Depletion and Impurity Distribution

Of critical importance in this type of study is the characterization of the separation of the impurities and the locations in the system where they are concentrated. First are described the analyses for a depleted mg Si bed used in an early near-continuous experiment. Data from an earlier batch run where deposits in various parts of the system were taken as samples is discussed in terms of impurity distribution.

2.4.6.1 mg Si Charge Depletion

A set of samples from a partially depleted reactor bed of mg Si was analysed by ES, Table 2.4-8. This bed was used for near-continuous run #3. The first column (77-215-37-16) lists the results for a yellow deposit found on the inlet side of the bed outside the hot zone. The second column is for the inlet side of the bed. The third is from a position near the outlet of the bed. A deposit was formed downstream from the bed in a cooler region of the tube. The results for it are in the last column.

The deposit in the inlet side, column 1, may have been formed during the initial heat up of the system prior to the introduction of the SiF_4 flow. It contained high concentrations of several metals which may have volatilized. Sample 18 shows the previously established effect that long exposure to flowing SiF_4 has on mg Si. Fe, Mn, Cr, V and Ti concentrations increase indicating that as silicon is removed via SiF_2 these elements remain. Downstream (sample 20)

TABLE 2.4-8

ES Results for Samples Taken from a
Partially Depleted mg Silicon Bed (ppm wt.)
Series 77-215-37

Impurity	16	18	20	26
Fe	>1000	>1000	1000	3
Mn	1000	1000	100	10
Cr	1000	1000	100	--
Ca	1000	30	--	>1000
Mg	10	1	1	10
Ni	300	300	30	10
V	>1000	1000	100	--
Ti	1000	1000	100	3
Cu	1000	100	30	1
Zr	1000	300	300	--
Al	100	10	100	>1000
B	10	10	10	--
Co	300	100	10	--
Sr	--	--	--	100

this effect is less pronounced indicating less silicon removal in this portion of the reactor bed.

The last sample result shows that certain elements (Ca and Al) appear to form fluorides which condense in regions of the appropriate temperature range. Most of the other impurities are not introduced into the gas stream or pass into other regions of the reactor.

This substantiates earlier observations that the mg Si bed is depleted of silicon and metallic impurities are left behind and increase in concentration particularly on the upstream end.

2.4.6.2 Impurity Distribution Studies

Until the SiF_4 recycling work is completed, it is not possible to do a complete impurity mass balance on the SiF_2 polymer system. However, an impurity distribution study based only on the solid deposits from various parts of the system can be useful and instructive. Figure 2.4.3 shows the results of a preliminary study based on the emission spectroscopic analysis of samples taken from the system. The input material is typical mg silicon (column 1). The next three samples were taken from the charge after a long series of runs[10]. They were taken from locations in the charge as shown schematically in the figure. The next two samples are deposits formed in the furnace tube downstream from the hot zone. The baffle yielded the next sample. Samples number 69 and 68 are shown as the converted product formed from Traps 1 and 2 respectively.

From this data it can be seen where various impurities in the input charge material deposit. The three samples taken from the depleted charge itself show clearly that Fe, Cr, Mn, Ti, V and Ni are not transported to a large degree in the SiF_4 gas stream. As the input gas stream impinges on the charge, Si reacts and is carried away leaving the impurities to build up in concentration. The data from the second and third sample show little impurity build up apparently because the gas mixture reached a steady state in the first section of the reactor. Another group of elemental impurities including Ca, Mg and Cu are present in low levels in the input charge and appear to be little changed at this stage of charge depletion.

Element	INPUT mg Si	FURNACE (>1100 C)					BAFFLE (R.T.)	TRAP 1 (<-45 C)	TRAP 2
Fe	> 1000	> 1000	> 1000	> 1000	10	—	—	—	—
Al	100-1000	5	5	5	1	100-1000	> 1000	5	1
Cr	100-1000	> 100	50	50	—	—	—	—	—
Mn	100 ± 50	500	100	10	< 1	50-100	—	—	—
V	10-100	500	100	100	—	—	—	—	—
Ti	100 ± 50	1000	1000	1000	5	—	< 1	< 1	—
Ni	10-100	500	100	50	1	—	—	—	—
Ca	100-1000	1	1	5	5	10-100	—	1-10	1
Mg	10 ± 5	—	< 1	< 1	< 1	1-10	1000 ± 200	< 1	< 1
Cu	10 ± 5	5	5	5	1	10-100	1-10	< 1	< 1
Na	nd	—	—	—	—	—	> 500	—	—
Ga	nd	—	—	—	—	—	10 ± 5	—	—
B	nd	—	—	—	—	—	1-10	—	—
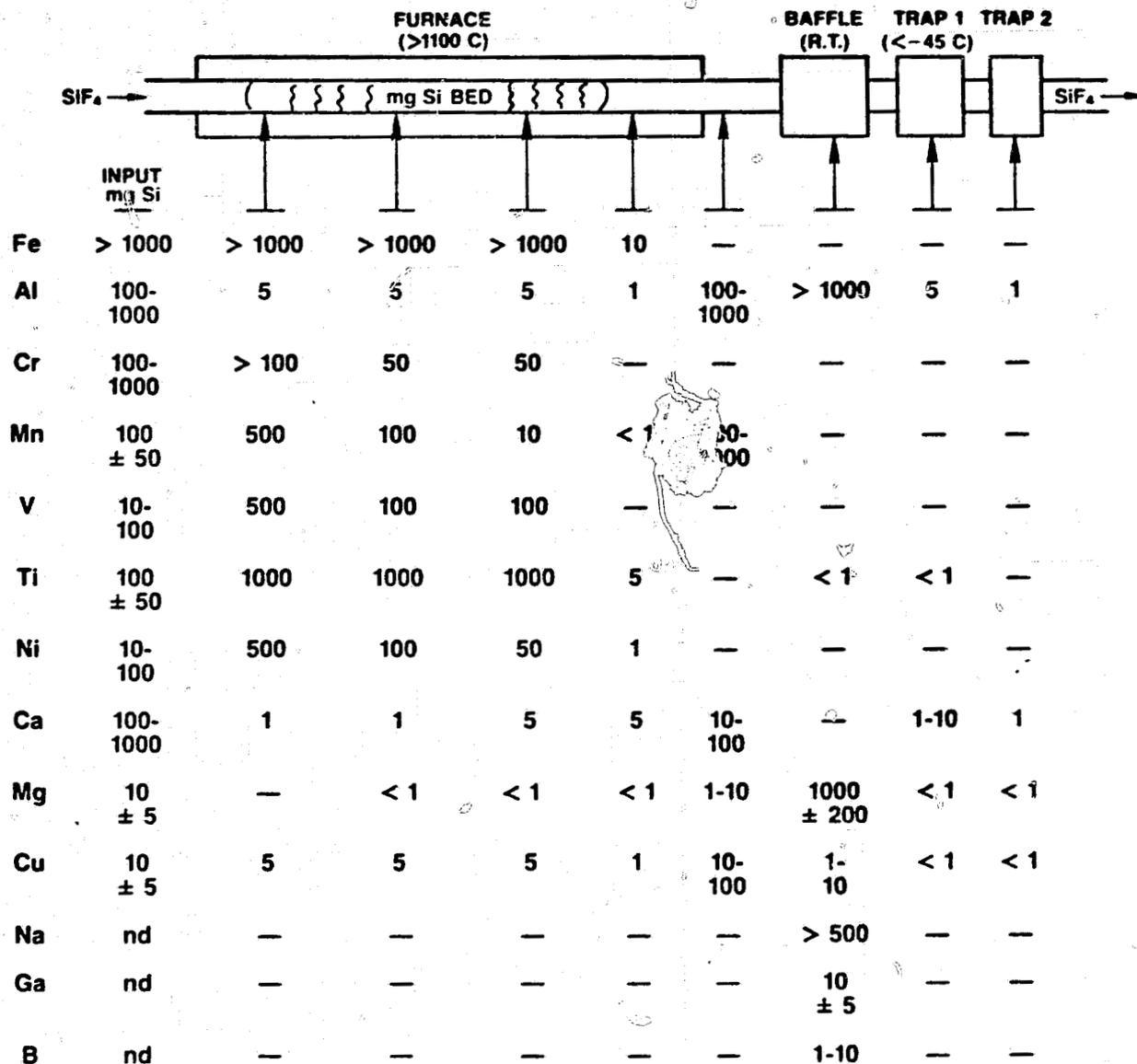
Figure 2.4.3   Emission spec. results for samples taken from various sections of the SiF$_2$ polymer transport system.   All concentrations are in ppm wt.

Of particular interest is the rapid depletion of Al from the charge. We propose that metallic Al impurities react very rapidly with SiF_4 to yield AlF_3, viz.,

$$3SiF_4 + 4Al \longrightarrow 3Si + 4AlF_3 \qquad (13)$$

Furthermore the mass spectral studies indicate that once the Al has been volatilized as AlF_3 it can undergo a reaction with the quartz liner to yield aluminum silicates such as $Al_6Si_2O_{11}$ and SiF_4. The major portion of these silicates remains as a coating on the quartz tube, but analysis of the deposits in the baffle also indicates that some is swept out of the tube and is trapped there under the batch mode conditions. High throughputs may alter these results.

This result indicates that a pretreatment of a fresh mg silicon charge with SiF_4 may be an effective way to reduce Al content in the mg silicon charge. The gas would then be recycled. This is consistent with predictions made on the basis of free energy change (ΔG) for reaction of SiF_4 with various impurities. Al and B are the only impurities of interest which have a negative ΔG, thus these are the major ones expected to be transported. In the case of boron, it is present in such low levels in these samples that the results do not clearly indicate the role boron is playing in the overall process. The growth of crystals from the product is the most reliable way to determine its effect. This is described in a later section.

The deposits between the hot zone and the product traps contain large amounts of impurities which form fluoride compounds of low and moderate volatility such as Al, Ca, Mn, Mg and Cu.

The baffle is used to trap particulates and condense some polymer enhancing impurity nucleation from the gas stream. Three elements, Na, Ca and B were detected in this area which were not detected even in the input material. These elements could be present below ES detection limits in the charge and be concentrated in the baffle deposit underscoring the need for this stage in the apparatus.

	(1)[a] mg Si	(2)[b] First Sample (76-33-14-22)	(3)[c] #62 (1-K-B)	(4)[c] #85	(5)[c] Kinetic Reactor (77-103-2-8)	(6)[a] (77-215-49-21)	(7)[d] #162 (Crystal)
Li	nd	.12	nd	nd	nd	nd	
Be	nd	nd	nd	nd	<.09	nd	
B	8	4.3	6.3	--	--	1.0	.30
F	--	>1%	1300	>.5	>1%	~.5%	.34
Na	--	45	~10	<17	--	~5	.10
Mg	--	7.7	~6	<5	--	--	nd
Al	1100	310	27.5	.7	6.3	--(e)	1.5
Si	Maj	Maj	Maj	Maj	Maj	Maj	Maj
P	14.3	680	15	7	--	22.3	3.7
S	--	22	2.2	7	3.3	--	nd
U	--	39	--	--	--	--	.48
K	--	57	~2	3	1.6	--	.36
Ca	9.9	350	4.5	6.4	12.6	~1	.36
Ti	79.5	4.3	.12	.22	.13	15	nd
V	45	<.01	nd	nd	nd	--	.01
Cr	16.5	1.4	.33	.33	.17	nd	nd
Mn	28	.20	~.5	.33	.17	nd	nd
Fe	800	8.4	--	~1.2	~1.0	--	.16
o	nd	<.02	nd	4.5	.3	--	.24
Ni	3.9	23	nd	nd	nd	nd	nd
Cu	6.5	3.7	nd	<1.0	--	nd	<.29
Zn	4.4	1.1	2.4	--	--	--	<.01
Ga	.12	nd	1.3	.29	--	--	nd
Sr	3.2	.37	nd	nd	nd	nd	nd
Zr	7.4	<.03	nd	.03	.41	.9	nd
Nb	--	nd	<.10	.05	nd	--	nd
Mo	--	nd	nd	.07	nd	nd	nd
Sn	--	1.3	.9	.6	--	--	nd
Ba	2.7	.57	nd	<.1	<.1	nd	.63
Pb	--	.85	nd	--	--	4.5	nd
U	nd	nd	nd	<.05	--	--	nd
Ru	nd	.02	nd	nd	<.06	nd	nd
Vt	3.3	<.62	nd	nd	nd	nd	nd
As	nd	nd	.43	<.28	nd	.25	nd
Se	nd	nd	nd	<.10	nd	nd	nd
Rb	nd	nd	nd	<.07	nd	nd	nd
Cd	nd	nd	nd	<.08	nd	nd	nd
C	--						<.16
							.64

(a) Ground in SiC

(b) Ground in quartz

(c) Ground in BC

(d) Not ground

(e) Note - based on small difference between large numbers

Recycling of the output gases will give information on the build up of highly volatile fluoride compounds in the gas stream. One pass through the reactor does not permit buildup to occur to the detection limits of GC/MS analysis.

2.4.7 Chronological Silicon Product Purity

Silicon has been made via SiF_2 transport under many different sets of conditions since the inception of this project. Initially, relatively simple batch reactors were used. Introduction of the baffle concept resulted in a lower aluminum content. During the kinetic studies, run under highly controlled conditions of low throughput, samples of very high quality were produced. Finally experiments designed to produce samples containing larger quantities of material at higher throughput and in a semi-continuous manner were conducted.

Throughout the evolution of the process many factors including reactor design and sample handling techniques have been incorporated to improve purity. Table 2.4-9 gives an indication of the changes in the character of the product. The first column is a typical mg Si ssms analysis. The second column lists the results for the first silicon product submitted for ssms analysis. Aluminum was reduced by a factor of three over mg Si, but clearly there was contamination by the system particularly in the case of P. Most other impurity levels were reduced.

Inclusion of the baffle design, a high temperature vacuum bake out cycle and elimination of P containing o-rings resulted in the sample depicted by column 3. Al and P concentrations were reduced dramatically while substantial decreases were registered for most other impurities. Perhaps the best sample produced in the large batch reactors is listed in column 4. The sample in column 5 was produced on a small reactor, under low throughput conditions during the kinetic studies. The reactor did not have a baffle, thus the Al content is higher than would be consistent with the levels of the other elements. The product was high density CVD Si rather than powder. Overall it was the best uncorrected sample analyzed by ssms.

With the increased emphasis on engineering studies, continuous operation and higher throughput, new reactors were designed which, while incorporating the concepts known to produce high purity, stressed the chemical process. Purity, while still adequate, fell in some respects. The results in column 6 illustrate this effect. The powder samples were fabricated into electrodes by methods described above. Thus, the results have been corrected for handling contamination.

The last column lists results for a crystal grown from product similar to, but not identical to, the sample from column 5. These results show the effective purification inherent in crystal growth. The resistivity of this crystal is 0.15 ohm cm n-type (corresponding to 1 ppma uncompensated P). Work on the removal or control of electrically active donors and acceptors could yield a product suitable for solar applications.

The analyses in Table 2.4-9 show that within the limits of ssms, our major tool for purity determination, the products produced and described in columns 5, 6 and 7 are not distinguishable from semiconductor grade samples analyzed by a service lab except for possibly phosphorus. Thus, within the constraints of our "working definition" of semiconductor grade silicon, our goals have been attained. Realistically however, further work is needed to affect removal of donors and acceptors to a lower level consistent with standard solar cell resistivities.

2.4.8   Evaluation of the SiF$_2$ Transport Product by Crystal Growth

Several samples from the near-continuous transport experiments were converted to single crystal for evaluation. Basically the process involved:

    a) harvesting the powder samples
    b) vacuum heat treatment at 800 to 1000°C
    c) compaction into pellets
    d) load/melt in an ADL Model HP crystal furnace
    e) crystal growth/slicing/evaluation.

Often in these experiments, the results of melt down were not simple. In most cases incomplete melt down or dross formation on the melt surface prevented crystal growth. The dross was analyzed by electron microprobe and Auger analysis. The results showed SiC formation from the graphite parts in the rf heated system. When this occurred the melt was solidified, etched to remove the crucible remains and remelted. In all cases the ingots were large grain polycrystalline. The results of some experiments are shown in Table 2.4-10. From the partial listing in the table it is clear that donors (phosphorus) dominate the product carrier type at about 1 ppma. Experiment 4) yielded an ingot which was compensated with the seed end being dominated by boron. Due to the smaller segregation coefficient for phosphorus (.35 versus .8 for boron), the P was concentrated in the melt thus dominating the tang portion of the ingot.

The ssms results for experiment 7) are presented in Table 2.4-9. The results show that for all elements except the primary dopants the process is effective in purification. However, further work on removal of B and P from the deposition gas stream is required to attain a high resistivity product.

2.4.9 Comments on Silicon Evaluation

In the preceding sections work on the evaluation of the SiF_2 transported Si product has been described. It can be summarized as follows: Within the constraints imposed by reliance on ssms as the primary evaluation tool, the SiF_2 transport process produces Si which approaches semiconductor grade quality.

Regarding ssms it has become apparent that the technique requires several prerequisites to be a reliable analytical tool for silicon in the ppba range. The first is the dedication of a machine to the analysis of high purity silicon with no other materials introduced. A second is reliable standards with a uniform distribution of impurity in the concentration range of interest. Third, a standardized sample preparation and cleaning procedure must be developed.

The first prerequisite can be attained only by a capital commitment. It is entirely a question of established need and capital. Few semiconductor companies will enter this field until the reliability of this technique for

Table 2.4-10 Results of crystal growth experiments.

SiF$_2$ Transport Conditions Bed Material/Product	1st Pull		2nd Pull		Type	Run Date/ Comments
	Seed	Tang	Seed	Tang		
1) mg bed/powder product	.08 Ωcm				N	4/11/77
2) mg bed/powder	.11				N	4/15/77
3) Combined salvaged charge material from above and 2 runs for which no ingots were produced			.10		N	4/22/77
4) mg bed/powder compacted with D.I. water - combined 2 salvaged runs			1.0 (P-type)	2-5 (N-type)		6/1/78
5) mg bed/powder 2 growth cycles			.23	.12	N	12/22/78
6) mg bed/powder	0.1-27 (N & P type)	.3-.6 (N-type)				1/17/79
7) mg bed/powder	.15				N	1/19/79

measuring concentrations for a variety of impurities in the ppb range is established. The need for sensitive analytical tools is not questioned. Judging from the reports of labs. where this first prerequisite has been met, it is apparent that background readings and "memory" can be reduced so that reliability and reproducibility are attained.

The development of reliable, well characterized standards is required before ssms (or any other technique) will be widely accepted. These must be readily available throughout the industry. Currently standards are not widely available. Segregation effects in crystal growth cause concentration gradients, precipitates and non-homogeneities which cause crystals to have variable composition from one region of the lattice to another. This of course produces variable analytical data and degrades the usefulness of the standards. A fairly long term R & D effort in the development of standards must be undertaken before widespread acceptance of ssms will occur.

Procedural techniques of preparation and cleaning present the least severe problem in ssms. Standard cleaning procedures currently state-of-the-art in the semcionductor industry can be implemented directly. This cleaning must be done just prior to analysis to remove contamination from packaging and shipping materials.

The above discussion has emphasized the necessary conditions to attain reliable ssms data at current technological development. This is not, however, adequate to completely analyze semiconductor grade silicon. The detection limits for such critical impurities as boron, phosphorus, aluminum, titanium, vanadium and arsenic are in the range of several ppba under the conditions described in the preceding sections.

Electrical evaluation of single crystals, long an established and reliable technique in the semiconductor industry, must be incorporated into any evaluation scheme for silicon. As emphasized above, ssms results indicate the SiF_2 product approaches semiconductor quality; however, it is clear from the in-house crystal growth evaluation that further work on the removal of B and P from the gas stream is required to ultimately attain that quality. Emphasis on crystal growth as an evaluation tool at the onset of this project would have highlighted this problem and been more instructive in guiding the course of the project toward attainment of the stated goals.

2.5   One Kg/Hr Mini-Plant Design

After the feasibility of the chemistry of the process was suf-
ficiently established, Phase II of the program was initiated in June
1978. The objective of the first six months of this phase was to design
and engineer a mini-plant to be capable of 1000 gm/hr. Its purpose would
be to collect critical engineering data on the feasibility and scale-up
of the process.

The firm of Raphael Katzen Associates International, Inc. (RKA),
of Cincinnati, Ohio, was retained as consultants to carry out the chemical
engineering, design, support, and costing for the mini-plant and other
scale-up projections. Since the full design report from RKA is being sub-
mitted to JPL at the same time as this final report, only those drawings
and descriptions relevant to an overall view of the engineering design will
be included herein.

The process as designed for the mini-plant covers all basic aspects
of the proposed commercial process including the initial SiF_4/Si reaction,
the impurity dropout baffle, the SiF_2 polymerizer, the homologue formation
and Si harvester, and the SiF_4 condenser with capability for batch recycle
of SiF_4.

2.5.1   Main Process

The process flow diagram is given in Figure 2.5.1 with the process
description as follows.

The reaction between metallurgical grade silicon and SiF_4 takes place
in Reactor R-101 at a temperature of 1,350°C and a pressure 0.5 torr. SiF_4
is introduced into the bottom of the reactor and travels up through the
bed support tube. It can be preheated in the bed support tube if the tube
extends up into the heated zone or it can be preheated in the lower portion
of the silicon bed. Metallurgical grade silicon is introduced into the re-
actor through a lock hopper on top of E-103. The bed in the reactor can be
operated in a fixed or fluid mode depending on the size of the silicon

		①	②	②A	③	④	⑤	⑥
Si			2.4	0.2				
SiF₄		10.3			2.1	2.1	2.1	
SiF₂					10.4	10.4		
SiₓFᵧ								
TOTAL - LB/HR		10.3	2.4	0.2	12.5	12.5	2.1	TRACE
TEMPERATURE-°F		25	25		1350	250	-30	-150
PRESSURE- TORR.		300	760		0.5	0.3	0.25	0.10

* = SLAG
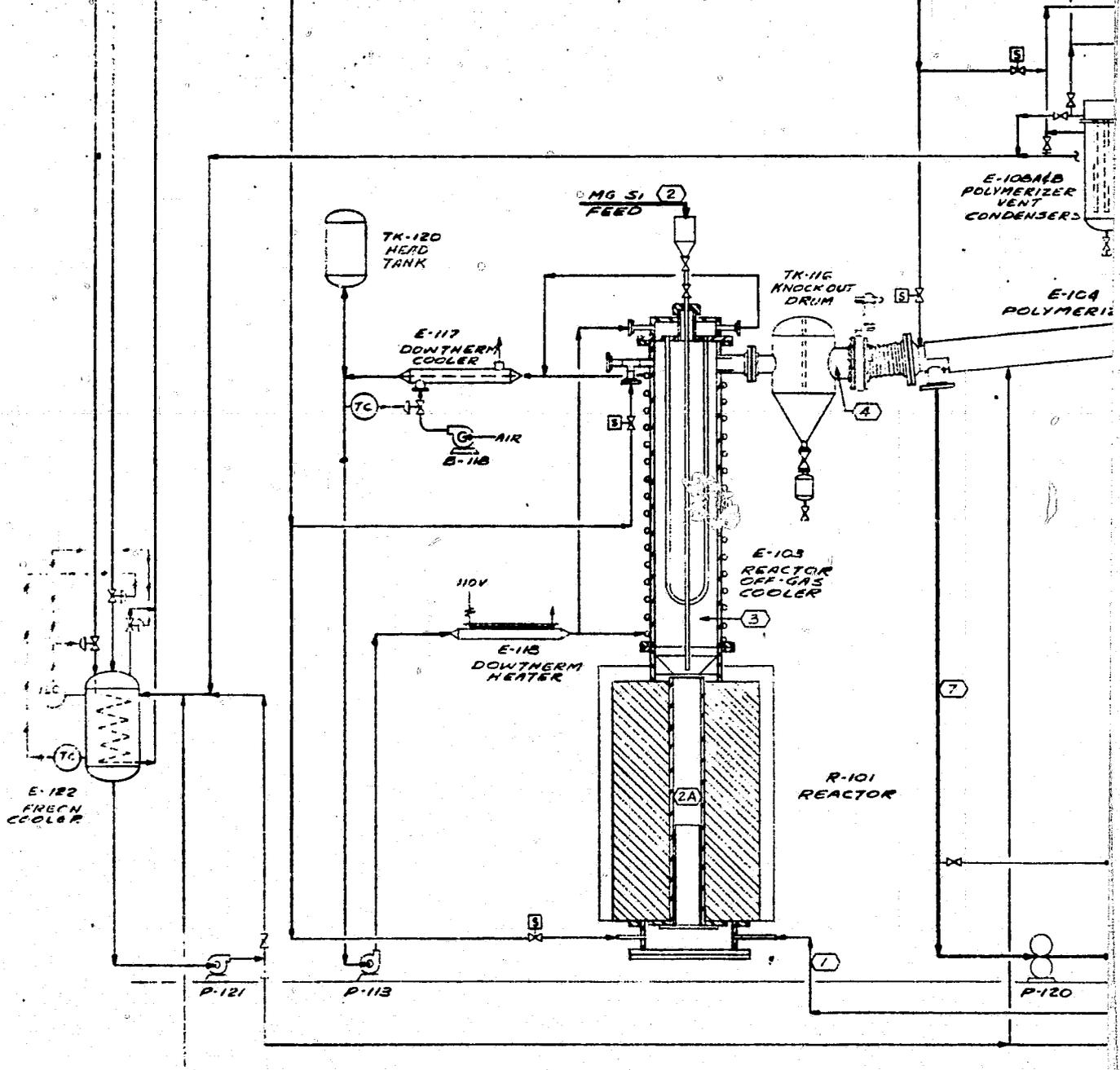
Figure 2.5.1 Process Flow Sheet.

PART I

	(8)	(9)	(10)	(11)	(12)
	1,295				2.2
		126.2	118	8.?	
10.4					
10.4	1,295	126.2	118	8.2	2.2
50	850	800	250	250	70
0.3	150	100	150	0.1	760

R-100 HARVESTER

E-110 SF RECYCLE COOLER

AIR

P-114 VACUUM PUMP

E-112 S.F₄ CONDENSER

E-111A&B HARVESTER VENT CONDENSER

AERATION GAS

PRODUCT

B-113

FREON HEATER

ORIGINAL PAGE IS OF POOR QUALITY

particles in the bed. All the reactor internals, including the reactor tube, bed support, heating elements and insulation are made from graphite. The reactor heating element is divided into three separately controlled sections.

The SiF_2 formed in the reactor and any unreacted SiF_4 flow upward into Cooler E-103. Dowtherm in the tubes and walls of E-103 cool the reactor off-gas from $1,350^{\circ}C$ to $250^{\circ}C$. Tank TK-116 is a baffled knockout drum which will remove most of the entrained particulate impurities coming from the reactor. The drum is fitted with a lock hopper to allow periodic removal of the collected solids.

Polymerizer E-104 is a jacketed. scraped surface exchanger. The gases are cooled from $250^{\circ}C$ to $-30^{\circ}C$ using Freon in the shell at $-80^{\circ}C$. The SiF_2 is condensed and polymerized on the walls of E-104. The scrapers remove the polymer deposit, which comes off in granular form. The condenser is sloped toward the gas inlet end. This causes the polymer granules to move countercurrent to the gas flow to the solids discharge nozzle. The jacket of E-104 is divided into several sections to allow flexibility in operating conditions. The remaining SiF_4 passes into Polymerizer Vent Condenser E-108 where it is condensed to a solid on surfaces cooled with liquid nitrogen.

The polymer falls from the polymerizer outlet into the suction hopper of Polymer Pump-120. This is a progressive cavity pump fitted with an Auger feed hopper. The hopper is electrically traced to warm and soften the granular polymer before it enters the pump.

The polymer is discharged into the vaporizer section of Harvester R-107. This is a bed of silicon granules fluidized by a recirculating SiF_4 gas stream. The inlet gas temperature is $250^{\circ}C$. Silicon addition and withdrawal hoppers are provided to allow inventory and particle size adjustment during operation. The polymer is converted to gaseous homologues and diluted in the vaporizer so that the homologue partial pressure is 5 torr. Gases leaving the vaporizer section then enter the riser portion of the harvester. The gases entrain hot silicon particles introduced near the bottom of the riser and carry the silicon up the riser. The heated silicon particles provide the heat and surface area necessary to decompose the homologues to silicon and SiF_4

and deposit the silicon on the particles. The silicon particles and the gas are separated in the upper portion of the harvester. The gas flows out through a baffle and is then cooled from approximately 800°C to 250°C in the air-cooled SiF$_4$ Recycle Cooler E-110. The net make of SiF$_4$ is removed from the recycle stream under pressure control and is condensed in Harvester Vent Condenser E-111 by liquid nitrogen. The bulk of the recycled SiF$_4$ is returned to the harvester by Blower B-113.

The silicon solids from the top of the harvester flow by gravity down through an electric heater and are returned to the bottom of the riser. A portion of the circulating silicon is removed from the bottom of the down-comer. Some of this material is product while the rest is crushed, etched to remove surface impurities, and returned to the top of the downcomer as seeds for silicon deposition.

As an alternate to the riser harvester, a fast fluidized bed with a recirculating gas stream could be used. This would require a different harvester vessel.

2.5.2 Vacuum Relief System

A header containing an inert gas at approximately 1 atm pressure provides a means of bringing the system up to atmospheric pressure in the event of a leak. It also provides an inert purge when the system is opened. The inert gas is manually controlled from a central point by solenoid valves at each purge gas inlet.

2.5.3 Dowtherm System

The cooling medium for Reactor Off-gas Cooler E-103 is liquid Dow-therm "A". Pump P-113 circulates Dowtherm at approximately 20 gpm through Dowtherm Heater E-118, through the Cooler, E-103, and then through an air-cooled Dowtherm Cooler E-117. Since the thermal load from the process is relatively small compared to the size of the Dowtherm system, it may be necessary to run E-118 continuously in order to provide the necessary temperature control in Cooler E-103.

2.5.4 SiF₄ Recycle System

The SiF_4 collected in Vent Condensers E-108 and E-111 is re-
turned to storage cyclinders for reuse as reactor feed. This recycle
is carried out in the following steps. When Condenser E-108A has ac-
cumulated a full load of SiF_4, the process is swung over to Condenser
E-108B. E-108A is valved off from the vacuum system and is connected
to SiF_4 Condenser E-112. A warm fluid (Freon at $-65^{\circ}C$) is introduced
to the coils and the pressure is brought up to approximately 35 psig.
Under these conditions, the SiF_4 liquefies and is then boiled out of
E-108A and recondensed in E-112 using refrigerant at $-80^{\circ}C$. The liquid
SiF_4 condensed in E-112 flows by gravity into a refrigerated storage
tank (TK-123A or B). These can be blown down to atmosphere at the
end of the boilout cycle as needed. If polymer accumulates on the
condensing surface of E-108A, connections are provided to allow melting out
the polymer with hot SiF_4 from the harvester recycle stream. When the
boilout cycle is complete, the exchanger is isolated from Condenser E-112
and the liquid nitrogen is put back into the coils. This will condense
the SiF_4 in the condenser and return it to a low pressure in preparation
for a new condensing cycle. Exchangers E-111A and B operate in a similar
manner.

2.5.5 Freon Refrigeration

To provide the intermediate temperature levels in the polymerizer
and SiF_4 condensers, Freon is cooled to $-80^{\circ}C$ with liquid nitrogen in Freon
Cooler E-122. Pump P-121 circulates the Freon to Polymerizer E-104 and SiF_4
Condenser E-112. The warmer Freon required for meltout of Condensers E-108
and E-111 is provided by the discharge from Condenser E-112. During melt-
out the Freon will flow from E-112, through Freon Heater E-124 to the units
being melted out. With this arrangement, meltout can be carried out regard-
less of the status of the rest of the process.

When the vent condensers are swung from condensing to meltout, the
fluid in the tubes is changed from liquid nitrogen to Freon. The gaseous

128

nitrogen left in the tubes will be carried back to Freon Cooler E-122 and vented from the system under pressure control. When the condensers are swung from Freon back to liquid nitrogen, the Freon will have to be blown back to E-122 with gaseous nitrogen before the liquid nitrogen is cut in.

2.5.6   Equipment Design

The basis for the design and sizing of the process equipment is briefly summarized in Table 2.5-1. The equipment cost derived from the list given in Table 2.5-2 is based mainly on cost estimates received from vendors. The eleven page instrument list is too extensive to be shown herein, but is in the RKA full design report.

A model of the mini-plant was put together by RKA to assist in the layout and the piping design. The model is laid out to fit into the proposed site of the unit in an existing empty structure at Motorola. Views of the layout from two different directions are given in Figure 2.5.2a and 2.5.2b.

2.5.7   Estimate

Using cost totals from the equipment and instrument lists and the piping design model, an estimate of the installed cost for the 1 kg/hr mini-plant has been made. The breakdown of the $812,000 installed cost is given in Table 2.5-3. Items in the estimate other than the equipment and instruments are judgments based on this particular plant. Conventional estimating factors used to generate an installed plant cost from the equipment and instrument costs were not used because of the small size of the plant and the small amount of piping required.

The relatively high cost of the plant per unit of output results from using commercial equipment, but on a small scale. This cost can be justified by the fact that the data obtained from this plant will be directly applicable to the design of a commercial plant.

Table 2.5-1 Equipment List - Mini-plant

MINI-PLANT EQUIPMENT DESIGN BASIS

Item	Description	Design Basis	Assumptions
E-103 Reactor Off-Gas Cooler	12" dia. x 67" 30 sq. ft on tubes and jacketed shell	$U=1.0$ Btu/hr ft^2 °F $Q=5,253$ Btu/hr	The liquid coolant will prevent corrosion of the metal surfaces by the hot gases.
E-104 Polymerizer	6" x 8" x 12' Vogt scraped surface unit, 17 sq. ft	$U_o=3.7$ Btu/hr ft^2 °F $Q=11,730$ Btu/hr	
E-105 Polymerizer Vent Condensers	12" dia. x 66" 25 sq. ft. in two panel coils and jacketed shell 2 required	See E-111	
E-111 Harvester Vent Condensers	12" dia. x 68" 25 sq. ft. in two panel coils and jacketed shell 2 required	2 hr. accumulation SiF_4 deposit 1/4"thick Feed rate=10.3 lb/hr	Specific gravity of solid SiF_4 is 1.58.
E-110 Recycle Cooler	Air cooled fin tubes Inconel tubes	$U_o=2.2$ Btu/hr ft^2 °F based on extended surface cooling gas from 800°C to 250°C $Q=30,180$ Btu/hr	
E-112 SiF_4 Condenser	U-tube condenser 16 sq. ft.	$U_o=50$ Btu/hr ft^2 °F	
B-113 SiF_4 Recycle Blower	85 acfm @ 150 torr 22" WG static (air equivalent) Inconel construction with magnetic drive	10.7" WG calculated @ 400 °C operating temperature	
R-101 Reactor	Fixed bed type Graphite construction	0.0369 kg/hr in^2 reaction area @ 80% conversion	
R-107 Harvester	Riser type reactor 800°C, 150 torr operating conditions Inconel shell with internal insulation and cast SiC abrasive lining	1 sec. residence time in reactor	

130

Table 2.5-2 Equipment List - Mini-plant

EQUIPMENT LIST
1 kg/hr Plant

Item No.	Description	Design Conditions	Materials of Construction	Estimated Total Cost
Exchangers				
E-103	Reactor Off-gas Cooler $Q = 5,253$ Btu/hr $A = 30$ ft^2	300°C Vacuum	304 SS	$ 7,960
E-104	Polymerizer Scraped Surface, double pipe exchanger $Q = 11,720$ Btu/hr $A = 17$ ft^2	-120°C	316 SS	12,000
E-108A&B	Polymerizer Vent Condensers $Q = 722$ Btu/hr (Cooling) $Q = 963$ Btu/hr (Meltout) $A = 24$ ft^2	-196°C 50 psig/ Vacuum	304 SS	12,050
E-110	Recycle Cooler Finned Hairpin, Air Cooled $Q = 30,180$ Btu/hr	900°C Vacuum	Inconel	2,000
E-111A&B	Harvester Vent Condensers $Q = 2,420$ Btu/hr (Cooling) $Q = 5,776$ Btu/hr (Meltout) $A = 24$ ft^2	-196°C 50 psig/ Vacuum	316 SS	12,080
E-112	SiF$_4$ Condenser $Q = 5,776$ Btu/hr $A = 16$ ft^2	-120°C 100 psig	304 SS	2,750
E-117	Dowtherm Cooler Air Cooled Fin Tube $Q = 5,253$ Btu/hr $A = 3$ ft^2	300°C 50 psig	C.S.	1,800
E-118	Dowtherm Heater (Electric)	300°C 50 psig	C.S.	$ 1,130
E-122	Freon Cooler Tank Coil $Q = 29,612$ Btu/hr $A = 4.5$ ft^2	-196°C	304 SS	3,000
E-124	Freon Heater (Electric)	-80°C 20 psig	304 SS	1,495
BLOWERS				
B-113	SiF$_4$ Recycle Blower 100 acfm	400°C	Inconel	30,000
B-118	Dowtherm Cooler Blower 300 acfm	Ambient	C.S.	1,200
REACTORS				
R-101	Reactor	1,350°C Vacuum	Graphite	90,000
R-107	Harvester	800°C Vacuum	Silicon Carbide	87,000
TANKS				
TK-120	Dowtherm Head Tank	300°C 50 psig	C.S.	2,000
TK-123A&B	SiF$_4$ Storage Tanks	-100°C 1,100 psig	304 SS	10,800

Table 2.5-2 (continued) Equipment List - Mini-plant

EQUIPMENT LIST

1 kg/hr Plant

Item No.	Description	Design Conditions	Materials of Construction	Estimated Total Cost
PUMPS				
P-114	Vacuum Pump 200 acfm	25°C Vacuum	C.S.	$ 7,000
P-119	Dowtherm Circulation Pump 20 gpm @ 50' TDH	300°C 50 psig	C.S.	800
P-120	Polymer Pump 10.4 lb/hr	200°C Vacuum	C.S. Teflon	3,300
P-121	Freon Circulation Pump 10 gpm @ 50' TDH	-120°C 20 psig	C.S.	800
F-125	Vacuum Pump Filter	Full vacuum 250°C	C.S.	710
			TOTAL	$ 289,905

132
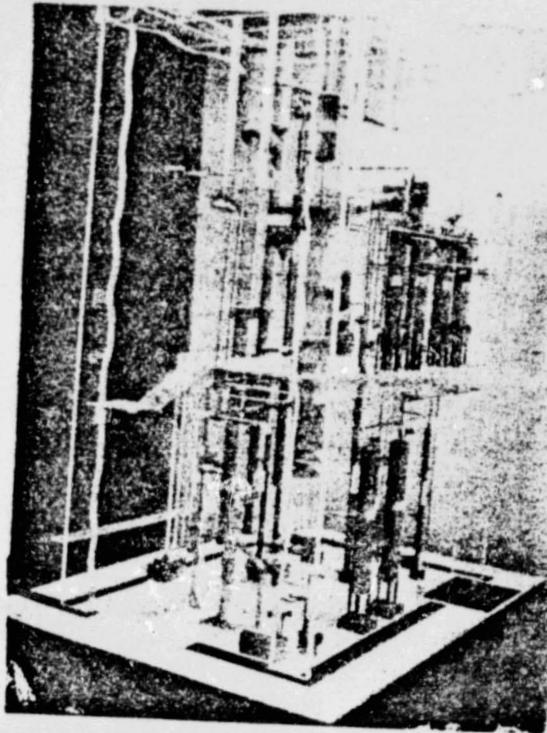
Figure 2.5.2a   Side angle view of mini-plant
model.
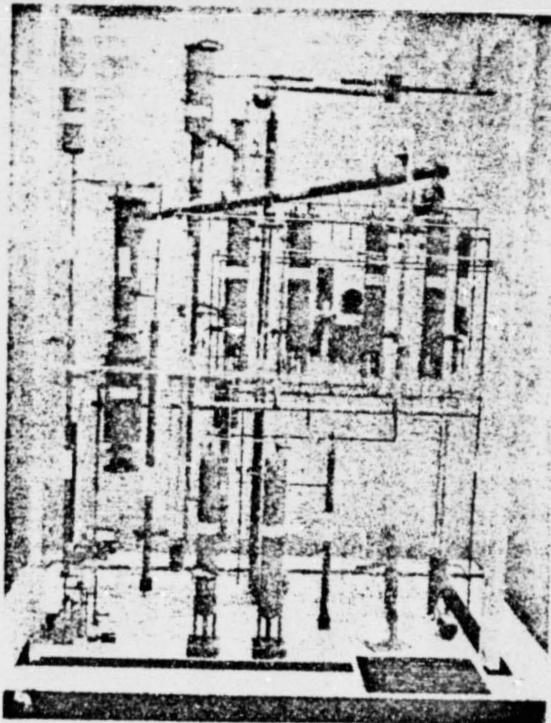
Figure 2.5.2b   Front view of mini-plant
model.

133

Table 2.5-3 Mini-plant Cost Estimate

1 kg/hr Plant Cost Estimate

DIRECT MATERIALS

Equipment $ 289,905

Field Materials

Piping	$ 38,000	
Electrical	14,000	
Instruments	71,250	
Insulation	10,000	
Painting	1,500	
		$ 134,750

TOTAL DIRECT MATERIALS $ 424,655

DIRECT LABOR

Equipment Installation $ 43,500

Installation of Field Materials

Piping	$ 40,000	
Electrical	15,000	
Instruments	15,000	
Insulation	20,000	
Painting	4,000	
		$ 94,000

TOTAL DIRECT LABOR $ 137,500

INDIRECT COST

Construction Overhead	$ 45,800
Contractor's Fee	18,000
Engineering	50,000

TOTAL INDIRECT	$ 113,800
STRUCTURE AND FOUNDATIONS	30,000
SUBTOTAL ESTIMATE	$ 705,955
CONTINGENCY	106,045
TOTAL ESTIMATE	$ 812,000

E-110
HARVESTER
RECYCLE COOLER

R-107
HARVESTER

R-104
POLYMERIZER

E-106 B
POLYMERIZER
VENT CONDENSER

E-105 C
REACTOR
OFF-GAS
COOLER

E-115
HARVESTER
VENT CONDENSER

R-101 C
REACTOR

E-112
S.P. CONDENSER

B-113
S.P. RECYCLE
BLOWER

P-120 C
POLYMER
PUMP

P-114
VACUUM
PUMP

TK-126
S.P.
STORAGE

E L E V A T I O N
SCALE

49
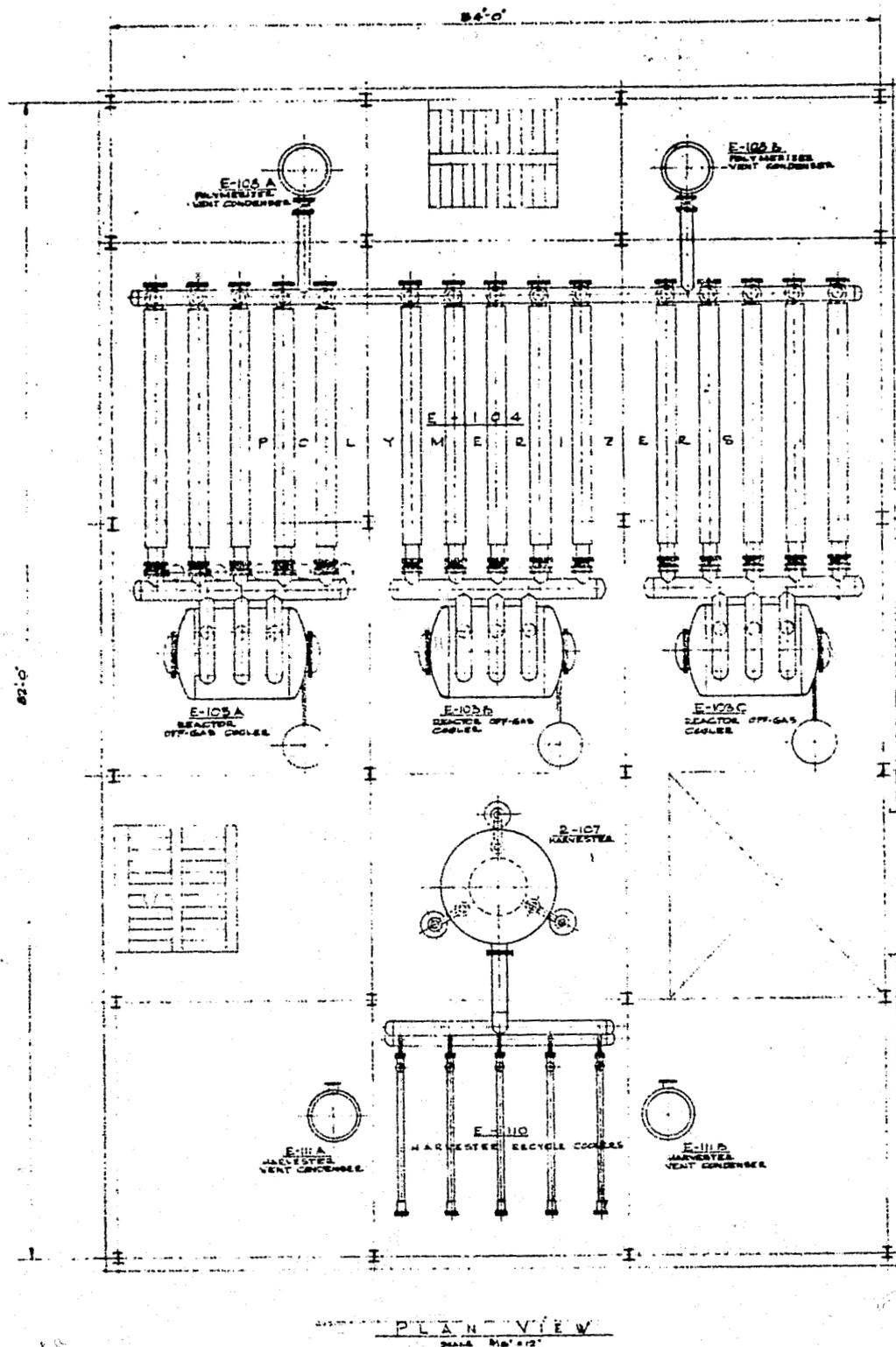
Figure 2.5.3 Conceptual layout of 100 MT/yr plant.

135

2.5.8 Design and Economics at Silicon Production Rates to 1000 Metric Tons per Year

A conceptual design was developed for a commercial plant producing 1,000 MT/yr of semiconductor grade silicon and the plant cost was estimated. The cost of a plant producing 330 Mt/yr was scaled from the 1,000 MT plant. This section gives a brief process description of the commercial plant as well as a summary of the assumptions and design basis used for the major equipment items in the commercial plant.

The operating conditions for the commercial plant were generally taken to be identical to those assumed for the mini-plant. The main exception to this is in the operating temperature of the harvester, which was assumed to be 600°C for the commercial plant, while the mini-plant is expected to be capable of running from 500 to 800°C if necessary.

The proposed layout for the 1,000 MT plant is given in Figure 2.5.3. Equipment numbering for the commercial plant is the same as that used in the mini-plant. Metallurgical grade silicon is metered by gravity through a small lock hopper from evacuated feed tanks to each of the three Fluid Bed Reactors, R-101A through C. Fresh silicon feed enters at one end and flows in approximately plug flow through the reactor. Unreacted silicon and ash continuously overflow the outlet weir and leave the reactor. SiF_2 produced in the reactor flows upward through Cooler, E-103. A header system on top of each cooler assures an even flow of gas over the plates and delivers the cooled gases to the five polymerizers associated with each reactor (15 total). SiF_4 leaving the polymerizers flows through headers to one of two Polymerizer Vent Condensers, E-108 A & B, where it is condensed to a solid with liquid nitrogen. Two 7,800 cfm vacuum pumps back up the condensers.

One polymer pump serves each set of five polymerizers. The three pumps discharge into the vaporizer on the single harvester.

Harvester R-107 uses a single riser scaled up directly from the one kg/hr mini-plant. Three solids downcomers and heaters are used to provide an even distribution of solids into the riser. Operation at 600°C

was assumed. The silicon produced at this temperature will contain a considerable amount of fluorine. A small post-treatment reactor will heat the product to 800°C to yield pure polycrystalline silicon.

The net SiF_4 made from the harvester will be condensed in Harvester Vent Condensers, E-111 A & B. Operation of these units is identical to Condensers, E-108 A & B, and they are backed up by the same vacuum pumps that serve the polymerizer condensers.

Table 2.5-4 gives a brief summary of the design basis and major assumptions used in sizing the major equipment for the 1,000 MT/yr commercial plant. Table 2.5-5 is an equipment list including estimated costs that comes to a total equipment cost of $2,382,300 which includes an offsite refrigeration package at $600,000.

The total capital cost for the 1000 MT/yr commercial plant is estimated by RKA at $6,160,000 as summarized in Table 2.5-6. Capital for a 330 MT/yr plant is given in Table 2.5-7.

In Quarterly Report No. 10, a Motorola generated equipment and capital cost was presented for that point in the project. Table 2.5-8 compares the investment costs as presented then in column 1 and the present RKA estimate in column 2. Note that the Motorola estimate did not include a capital figure but instead included both capital charges and operating charges under the utilities cost. The major reason for the lower RKA estimate is that they believe that the standard factors that had originally been used for installation, etc. per the standard format from Lamar were not applicable in this particular case where we have less piping, instrumentation, etc. than in a standard chemical plant or refinery. However, mindful of the fact that the resulting product cost is high due to the higher refrigerant and capital cost than the RKA estimate, the result from Quarterly Report No. 10 is given in Table 2.5-9 for a Si cost of $7.71/kg. Figure 2.5.4 from the same report shows the effect that more or less capital has on the Si cost for two SiF_4 costs. Note that the RKA capital estimate of $6,160,000 gives a Si product cost of under $7/kg.

Table 2.5-4   Equipment Design Basis - 1000 MT/yr Plant

EQUIPMENT DESIGN BASIS

Item	Description	Design Basis	Assumptions
E-103 Reactor Off- Gas Cooler	6'6" ϕ_2 7'T/T 443 ft^2 panel coil bundle in each 3 required	U_o=1.0Btu/hr ft^2 ^oF Q=210,000Btu/hr ea. Panels on 6" centers	—
E-104 Polymerizer	12"x14"x30' Vogt Scraped Surface Units, 94.2 ft^2/unit 15 required Equipped for use with direct refrigeration	U_o=3.7 $\frac{Btu}{hft^2F}$ Q=100,000 $\frac{Btu}{hr}$ ea	5 30' units in parallel will not have excessive pressure drop
E-108 Polymerizer Vent Con- densers	3' ϕ x 8' 293 ft^2 panel coil bundle in each 2 required	2 hr accumulation SiF_4 deposit ¼" thick Panels on 6" centers Feed rate = 263 lb/hr	specific gravity of solid SiF_4 is 1.58
E-111 Harvester Vent Con- densers	3 ϕ x 14' 1214 ft^2 panel coil bundle in each 2 required	2 hr accumulation feed rate = 1275 lb/hr panels on 3" centers SiF_4 deposit ¼" thick	specific gravity of solid SiF_4 is 1.58
E-110 Recycle Cooler	Air cooled Fin tubes Inconel tubes	U_o = 2.2 $\frac{Btu}{hr\ F\ ft^2}$ based on extended surface cooling gas from 600°C to 427°C Q=1.17 MM Btu/hr	
E-112 SiF_4 Con- denser	U-tube condenser 283 ft^2	U_o=50 $\frac{Btu}{hr\ ft^2}$ ^oF	

Table 2.5-4   (continued)

EQUIPMENT DESIGN BASIS

Item	Description	Design Basis	Assumptions
B-113 SiF$_4$ Recycle Blower	12000 acfm @ 27" WG static (air equivalent) Carpenter 20 construction with double mechanical seal	13" WG calculated 427°C operating temperature	Carpenter 20 alloy is satisfactory @ 427°C
R-101 Reactor	Fluid bed conveyor-type. Graphite 24 ft^2 surface 3 required	0.0369 kg/hr in^2 reaction rate @ 80% conversion	4-6" bed depth is sufficient
R-107 Harvester	Riser-type reactor 600°C, 150 torr operating conditions Inconel shell with SiC tile lining	Direct scaleup of 1 kg/hr unit 1 sec residence time in riser	1) Harvesting reaction will proceed satisfactorily at 600°C 2) Post treatment of Si product at 800°C will produce satisfactory material 3) Inconel can safely withstand process gases at 600°C.
Refrigeration Package	3 loop system producing liquid N$_2$ at -176°C, ethylene at -80°C, and 70 psig and ethylene at -65°C and -95 psia.	Heat loads 275,000 Btu/hr N$_2$ 147 MM Btu/hr ethylene @ -60°C 352,000 Btu/hr ethylene @ -65°C	

Table 2.5-5 Equipment List - 1000 MT/yr Plant

Item No.	Description	Design	Material	Estimated Item(s) Cost	Estimated Total Cost
Exchangers					
E-103 A-C	Rx offgas cooler $Q=210,000$ Btu/hr $A=443$ ft^2	300°C full vac	316 SS	42,300	126,900
E-104 A-O	Polymerizer $Q=100,000$ Btu/hr each 15 required $A=94.2$ ft^2 12" x 14" x 30' Vogt	-80°C full vac	316 SS	23,600	354,000
E-108 A-B	Polymerizer vent cond. $Q=250,000$ Btu/hr $A=275$ ft^2	-176°C full vac	316 SS	22,900	45,800
E-110 A-E	Harvester recycle cooler $Q=1.17$ MM Btu/hr $A=750$ ft^2 Brown Fin Tube	650°C full vac	Inconel 600	40,000	200,000
E-111 A & B	Harvester vent condenser $Q=210,000$ Btu/hr $A=1,241$ ft^2	-176°C full vac	316 SS	67,300	134,600
E-112	SiF_4 condenser $Q=220,000$ Btu/hr $A=283$ ft^2 Doyle & Roth VF125U2-12H 12' 3/4"O shell x 12' tubes	-80°C 70 psia	304 SS	7,300	7,300

140

Table 2.5-5 (continued)

Item No.	Description	Design	Material	Estimated Item(s) Cost	Estimated Total Cost
E-117	Dowtherm cooler Q=640,000 Btu/hr A=130 ft^2 Brown Fin Tube	300°C 50 psig	CS	4,300	4,300
E-118	Dowtherm heater 50 kw electric	300°C 50 psig	CS	10,000	10,000
Blowers					
B-113	SiF$_4$ recycle blower 12,000 cfm	482°C full vac	Carpenter 20	75,000	75,000
B-118	Air cooler blower 5,000 cfm 30 hp	Ambient	CS	3,000	3,000
Reactors					
R-101 A-C	Reactor	1350°C full vac	Graphite, 316 SS	150,000	450,000
R-107	Harvester	600°C full vac	Inconel 600 Silicon Carbide		165,000
R-124	Rust treatment reactor	800°C	Graphite	40,000	40,000
Tanks					
TK-120	Dowtherm head tank	250°C 50 psi	CS		8,000
TK-123	SiF$_4$ surge tank 2'ø x 16' T/T	43°C 1,000 psi	316 SS	44,400	44,400
TK-124 A,B,C	Silicon feed hoppers 3'ø x 6' T/T	full vac Ambient	CS	2,500	7,500
Pumps					
P-114 A-B	Vacuum pump 7,880 cfm Stokes model 1719			46,250	92,500
P-119	Dowtherm circulation pump 150 gpm @ 100' head	300°C 30 psig	CS	5,000	5,000
P-120 A-C	Polymer pump 433 lb/hr			3,330	10,000
	Off sites refrigeration package				600,000
			EQUIPMENT TOTAL		$2,382,300

Table 2.5-6 Capital Cost - 1000 MT/hr Plant

DIRECT MATERIALS

Equipment		$ 2,382,300	
Field Materials			
Piping	$ 310,000		
Electrical	215,000		
Instruments	105,000		
Insulation	81,000		
Painting	7,000		
		$ 718,000	
TOTAL DIRECT MATERIALS			$ 3,100,300

DIRECT LABOR

Equipment Installation		$ 198,000	
Installation of Field Materials			
Piping	$ 245,000		
Electrical	145,000		
Instruments	65,000		
Insulation	85,000		
Painting	18,000		
		$ 558,000	
TOTAL DIRECT LABOR			$ 756,000

INDIRECT COSTS

Construction Overhead	$ 250,000		
Contractor's Fee	79,000		
Engineering	550,000		
TOTAL INDIRECT COST			$ 879,000
BUILDING AND FOUNDATIONS			398,000
SUBTOTAL ESTIMATE			5,133,300
CONTINGENCY			1,026,700
TOTAL ESTIMATE			$6,160,000

Table 2.5-7 Capital Cost - 330 MT/yr Plant

DIRECT MATERIALS

Equipment	$1,294,230	
Field Materials		
Piping	143,000	
Electrical	98,400	
Instruments	66,310	
Insulation	35,800	
Painting	3,100	
	$ 346,610	
Total Direct Materials		$ 1,640,840

DIRECT LABOR

Equipment Installation	$ 89,400	
Installation of Field Materials		
Piping	113,000	
Electrical	66,300	
Instruments	44,400	
Insulation	37,600	
Painting	7,900	
	$ 269,200	
Total Direct Labor		$ 358,600

INDIRECT COSTS

Contractor's Overhead	$ 51,000	
Contractor's Fee	16,000	
Engineering	450,000	
Total Indirect Cost		$ 517,000
Building and Foundations		220,000
Subtotal Estimate		2,736,440
Contingency		547,300
TOTAL ESTIMATE		$ 3,383,740

143

Table 2.5-8   Investment Comparison

SiF_4 PURIFICATION PROCESS

CAPITAL COST ESTIMATE COMPARISON

1000 M TON/YR PLANT

	INVESTMENT $1,000,000	
	MOTOROLA	KATZEN
EQUIPMENT COST	1.46	1.78
REFRIGERATION	INCL. IN. OP. COST	0.60
INSTALLATION, ETC.	5.50	2.75
CONTINGENCY	2.09	1.03
TOTAL	9.05	6.16

Table 2.5-9   Total Si Product Cost

ESTIMATION OF TOTAL PRODUCT COST WITH Si_xF_y RECYCLE
($ PER KG SG Si PRODUCED)

1. **DIRECT MANUFACTURING**
   1. RAW MATLS MG SI 1.09 KG x $1.00/KG   **1.09**
      SIF$_4$ 0.24 KG x $1.00/LB x 2.2 LB/KG   0.54

   2. DIRECT OP. LABOR 10 MEN/SHIFT
      5 SKILLED @ 6.90/HR x .0372 = .26   **0.44**
      5 SEMI-SK @ 4.90/HR x .0372 = .18

   3. UTILITIES ELECTRICITY 13.8 KW-HR x $.03/KW-HR   0.41
      REFRIGERANT 0.00155 MM BTU x $85/MM BTU   0.13
      0.015 MM BTU x $24.4/MM BTU   0.37

   4. SUPERVISION/CLERICAL 15% OF 1.2   0.07

   5. MAINT. & REPAIRS 10% OF FIXED CAPITAL($9.1 MM)   0.91

   6. OPERATING SUPPLIES 20% OF 1.5   0.18

   7. LABORATORY CHARGE 15% OF 1.2   0.07

2. **INDIRECT MANUFACTURING**
   1. DEPREC./LOCAL TAXES/INSURANCE/INTEREST, 21% OF FIXED CAP. 1.91
      (10%)　　　(2%)　　　(1%)　　　(8%)

3. PLANT OVERHEAD, 60% OF (1.2 + 1.4 + 1/2 1.5)   0.58

4. TOTAL MANUFACTURING COST   6.70

5. GENERAL EXPENSES, ADMIN/DIST. & SALES/R & D 15% OF MAN. COST 1.01
   (6%)　　　(6%)　　　(3%)

6. TOTAL COST OF PRODUCT   7.71

SiF$_4$ PURIFICATION PROCESS
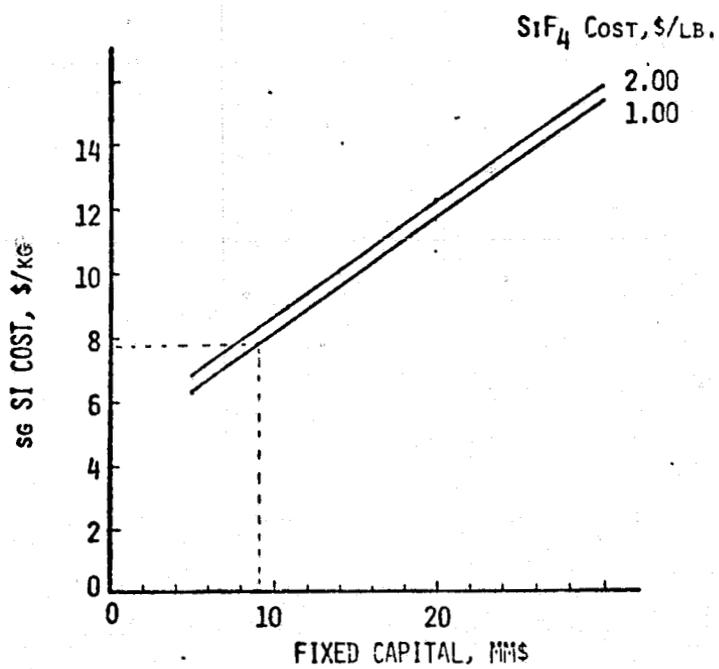

Figure 2.5.4 Sg silicon product cost vs. fixed capital
investment for SiF$_4$ cost of $1 and $2/lb.

3.0 CONCLUSIONS AND RECOMMENDATIONS

During the course of Motorola's investigation on the $(SiF_2)_x$ polymer purification process as a low cost, high volume method of production of semiconductor grade silicon the following conclusions have been made:

(i) The low projected product cost and short energy payback time suggest that the economics of this process will result in a cost less than the J.P.L./D.O.E. goal of $10/Kg.

(ii) During the initial phases of the investigation the silicon analysis procedure relied heavily on S.S.M.S. and E.S. analysis. These analysis demonstrated that major purification had occurred and some analysis were indistinguishable from semiconductor grade silicon (except possibly for phosphorus). However, more recent electrical analysis via crystal growth reveal that the product still contains compensated phosphorus and boron. Work on the removal or control of electrically active donors and acceptors could yield a product suitable for solar application.

(iii) Following a successful demonstration of the pilot facility, the process appears to be readily scalable to a major silicon purification facility as was proposed by Motorola and R. Katzen.

The above conclusions were based on the following observations:

(i) The 4 step purification process can be conducted in a continuous and cyclic manner. The products of each step are consumed in the following step with the SiF_4 product being indistinguishable from the starting material.

(ii) All (95 to 98%) SiF_4 starting material is reclaimed as SiF_4 at the completion of the cycle.

(iii) Each step has a high reaction efficiency with step 1 equaling 70-80%; step 2 $\geq$90%; step 3 $\geq$90% and step 4 $\geq$95%.

(iv) Purification occurs throughout the process and S.S.M.S. and E.S. analysis on the Si being prepared is indistinguishable from semiconductor grade Si (except possibly for dopants such as boron and phosphorus).

147

Furthermore, electrical resistivities on silicon from the process suggest that resistivities in the range of 0.3 to 1.0 ohm cm^{-1} can be expected. These values are reasonable for solar grade silicon.

(v) The operation and application of the low pressure riser and fluidized silicon beds as silicon reactors and harvesters represent a new technology for low cost silicon harvesting.

(vi) The direct scaling of the near-continuous apparatus, 1 inch diameter packed bed reactor (with transport rates of 50 to 75 gm Si/hr), to a 5 inch diameter reactor for the Si pilot facility is straightforward. Furthermore, after pilot plant conformation, the 5 inch diameter reactor could also be scaled to achieve transport rates required for a large scale production plant.

(vii) Using the 1 Kg/hr silicon purification facility as a reference, a 1000 MT/yr facility was also designed. An economic analysis of the proposed 1000 MT/yr facility suggests that a Si product cost of ~$7/Kg (Jan. 1975 $) can be expected from such a plant.

Over the past 3 years, Motorola has consistently recommended that the investigation continue as dictated by the program plan and milestone chart. Furthermore Motorola still recommends that the project be completed through the demonstration of the 1 Kg/hr silicon production facility. This would allow for a more thorough evaluation of the economics and product purity and other factors associated with the process.

IV. NEW TECHNOLOGY

The following new technology items have been uncovered during this program.

I. Description - A Method of Prepurifying mg Silicon Via Reduced
Pressure Atmosphere Control; NASA Case No. NPO-14474

Innovators - William M. Ingle
Stephen W. Thompson
Robert E. Chaney

Progress Reports - Technical Quarterly Report No. 6

Pages - Report No. 6, Page 11-17 and Appendix 1

Date Reported - December 9, 1977

II. Description - A Process for Conversion Amorphous to Crystalline
Silicon with Attendant Purification; NASA Case No. NPO-14223

Innovators - William M. Ingle
Gilbert Vasquez

Progress Reports - Technical Quarterly Report No. 5

Pages - Report No. 5, Pages 11-19

Date Reported - June 1977

III. Description - A Quartz Ball Valve; NASA Case No. NPO-14473

Innovators - William M. Ingle
Carl Goetz

Progress Reports - Technical Progress Report No. 18 - July 1977

Pages - Report No. 18, Pages 8, 9, and 10

Date Reported - December 9, 1977

IV. Description - Apparatus for Uniform $(SiF_2)_x$ Polymer Formation and
Liberation; D.O.E. Case No. S-51334

Innovators - William M. Ingle
Stephen W. Thompson

Progress Reports - Technical Quarterly Report No. 9

Pages - Report No. 9, Pages 16-22

Date Reported - May 1978

149

V.   Description - Low Pressure Pneumatic Lifter; D.O.E. Case No. S-52624
      Innovators - Stephen W. Thompson
                    Douglas W. Bennett
                    William M. Ingle
                    Richard S. Rosler
      Progress Reports - Final Report
      Pages - Final Report, Pages
      Date Reported.

VI.   Description - Low Pressure Fluidized Bed; D.O.E. Case No. S-51694
      Innovators - William M. Ingle
                    Stephen W. Thompson
                    Richard S. Rosler
      Progress Reports - Technical Quarterly Report No. 11 and Final Report
      Pages - Report No. 11, Pages 13-17; Final Report Pages

VII. Description - Silicon Harvesting Via a Duplex $(SiF_2)_x$ Vaporizor,
                    Si_xF_y C.V.D. Fluidized or Lifter Bed Apparatus;
                    D.O.E. Case No. S-51695
      Innovators - William M. Ingle
                    Richard S. Rosler
                    Stephen W. Thompson
      Progress Reports - Technical Quarterly Report No. 11,
      Pages - Report No. 11, Pages 13-17; Final Report, Pages

VIII. Description - Modified Apparatus for Uniform $(SiF_2)_x$ Polymer
                    Formation and Liberation; D.O.E. Case No. S-51334
      Innovators - William M. Ingle
                    Stephen W. Thompson
      Progress Reports - Final Report Pages

IX.   Description - Removable Silicon Harvesting Bed; D.O.E. Case No. S-56665
      Innovators - William M. Ingle
                    Carl A. Goetz
                    Robert D. Darnell
      Progress Reports - Technical Quarterly No. 11,
      Pages - Report No. 11, Pages 24-26; Final Report Pages

X. Description - High Vacuum, High Temperature, Non-contaminating,
                 Low Cost Quartz/Teflon/Viton Seal.

    Innovators - William M. INgle
                  Carl A. Goetz

    Progress Reports - Technical Quarterly Report No. 11,

    Pages - Report No. 11, Pages 22-24; Final Report, Pages

REFERENCES

1. Shafer, <u>Chemical Transport Reactions</u>, Academic Press, 1964.

2. Pease, U.S.A. Patent No. 2,840,588, June 1958.

3. Tims, Kent, Ehlert and Margrave, <u>J. Amer. Chem. Soc.</u>, 87, 282

4. Kapur, et. al., <u>S.R.I. Inst. Quarterly Report #9</u>, JPL/DOE Con
No. 954471, April (1978).

5. Joseph Lindmayer, et. al., <u>Solarex Technical Quarterly Report</u>
JPL/DOE Contract No. 954606, October, (1977).

6. Wm. Ingle, R. Chaney and M. Rodgers, <u>Motorola Technical Quart
Report No. 2</u>, JPL/ERDA Contract No. 954442, July (1976).

7. Matheson Gas Products, Engineering Report G-13, TS, Lyndhurst

8. Perry and Margrave, <u>J. Chem. Ed.</u>, <u>53</u>, (1976) 11.

9. Wm. Ingle, R. Chaney, S. Thompson, R. Rosler and J. Jackson,
<u>Technical Quarterly Report #10</u>, JPL/DOE Contract No. 954442,

10. J. Dowdy, Monsanto, Private communication 10/15/76.

11. Wm. Ingle, R. Chaney, and S. Thompson, <u>Motorola Technical Qua
Report No. 5</u>, JPL/DOE Contract No. 954442, April (1977).

I. INTRODUCTION

The following is a series of thermodynamic calculations for the predicted SiF_4 to SiF_2 conversion efficiencies for reaction step I in the SiF_4 transport purification process. The fol-owing assumptions were made:

1) Ideality of the gases was assumed

2) The silicon bed contains a large excess of Si

3) The vapor pressure of Si at the temperatures in question is negligible

4) Symbols used are the same as the JANAF Tables

II. CALCULATION OF ΔG OF REACTION

In Table I are listed the values of ΔG^O for SiF_2 and SiF_4 at three different temperatures used by Motorola (1623°K), Margrave (1423°K) and Pease (1473°K). These values were inter-polated from the 1967 and the 1976 JANAF Tables.

Based on the table values and standard free energy relationships,

$$\Delta G_{reaction} = \Delta G^O + RT \ln K_p$$

$$\text{for } SiF_4(g) + Si(s) \rightleftarrows 2SiF_2(g)$$
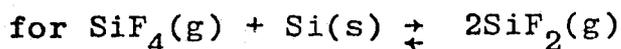
$$\Delta G = 2 \Delta G^O_{f(SiF_2)} - \Delta G^O_{f(SiF_4)} + RT \ln \frac{P^2_{(SiF_2)}}{P_{(SiF_4)}},$$

the $\Delta G_{reaction}$ was calculated from several Motorola experimental runs and for the stated conditions of Pease and Margrave. The

TABLE I

ΔG_f^O Values from JANAF Tables

TEMPERATURE	$\Delta G_{f(SiF_2)}^O$ (Kcal/mole)	% Difference	$\Delta G_{f(SiF_4)}^O$ (Kcal/mole)	% Difference
1423°K				
(1967)	−157.706	4.5	−336.913	.064
(1976)	−150.591		−337.127	
1473°K				
(1967)	−157.940	4.5	−335.188	.065
(1976)	−150.873		−335.408	
1623°K				
(1967)	−158.597	4.4	−329.990	.072
(1976)	−151.677		−330.229	

results are listed in Table II. Use of the 1967 tables yields negative free energies under all conditions, while the 1976 table produces positive free energies of reaction. This indicates that, in all cases, using the new JANAF Tables under the stated conditions, no reaction would have been observed. Figure 1 graphically illustrates these results. The parallelograms for the work of Margrave and of Pease illustrate the reported pressure ranges under which they conducted their experiments.

These results show the effects that a small change in a large value (such as <5% in $\Delta G^O_{f(SiF_2)}$) can have, when small differences in large numbers are used in calculations. If the latest JANAF values for ΔG^O_f are in question then the enthalpy values must also be suspect.

If we were to assume that the system described on line 1 from Table II were at equilibrium, then $\Delta G_{reaction} = 0$. Further using the $\Delta G^O_{f(SiF_4)} = -330.229$ Kcal/mole from the 1976 Table would give a calculated value for $\Delta G^O_{f(SiF_2)}$ of -154.746, which lies between the two (1967 and 1976) JANAF values. The % difference is 2% from the 1976 JANAF value.

III. CALCULATION OF % CONVERSION (α)

In the reaction,

$$SiF_4(g) + Si(s) \rightleftarrows 2SiF_2(g),$$
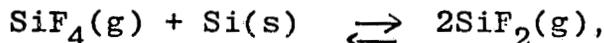
let α be the degree of reaction or percent conversion of SiF_4 to SiF_2. Thus, the concentration of $SiF_2 = 2\alpha$, $SiF_4 = 1-\alpha$ and $Si = 1-\alpha$. Again, assuming Si is in excess and the vapor pressure negligible, the total number of moles in the gas stream is $(1 + \alpha)$ times the original content of SiF_4 and

TABLE II

Summary of $\Delta G_{reaction}$ Calculations

	$\sum P$ (Torr)	T ($^{\circ}$K)	% Eff. (α)	P_{SiF_2} (Torr)	P_{SiF_4} (Torr)	$RT \ln \dfrac{p^2_{SiF_2}}{p_{SiF_4}}$ [1] (Kcal/mole)	Calc. $\Delta G_{reaction}$ Tables Used 1967 (Kcal/mole)	1976 (Kcal/mole)
1) Motorola[2]	0.2	1623	77	.175	.025	−20.737	−7.941	+6.138
2) Motorola[3]	0.7	1623	74.0	.518	.182	−20.14	−7.344	+6.735
3) Motorola	20	1623	34.9	6.98	13.02	−17.136	−4.34	+9.739
4) Motorola	2.2	1623	53.8	1.184	1.016	−20.354	−7.558	+6.521
5) Margrave[4]	0.2	1423	65	0.13	0.07	−22.774	−1.273	+13.171
6) Margrave	0.1	1423	65	.065	.035	−24.734	−3.233	+11.211
7) Pease[5]	3 (inlet)	1473	40	1.2	1.8	−20.088	−0.78	+13.574
8) Pease	0.05 (trap)	1473	40	.02	.03	−32.051	−12.743	+1.611

(1) Pressures in atmospheres
(2) Motorola Quarterly Report No. 6 − batch reactor
(3) Motorola Monthly Report #25, Table II − near continuous reactor
(4) J. Amer. Chem. Soc. 87, 3819 (65); reported pressure from 0.2 to 0.1 torr
(5) U.S. Patent #2,840,588, 1958; reported pressure from 3 to 0.05 torr
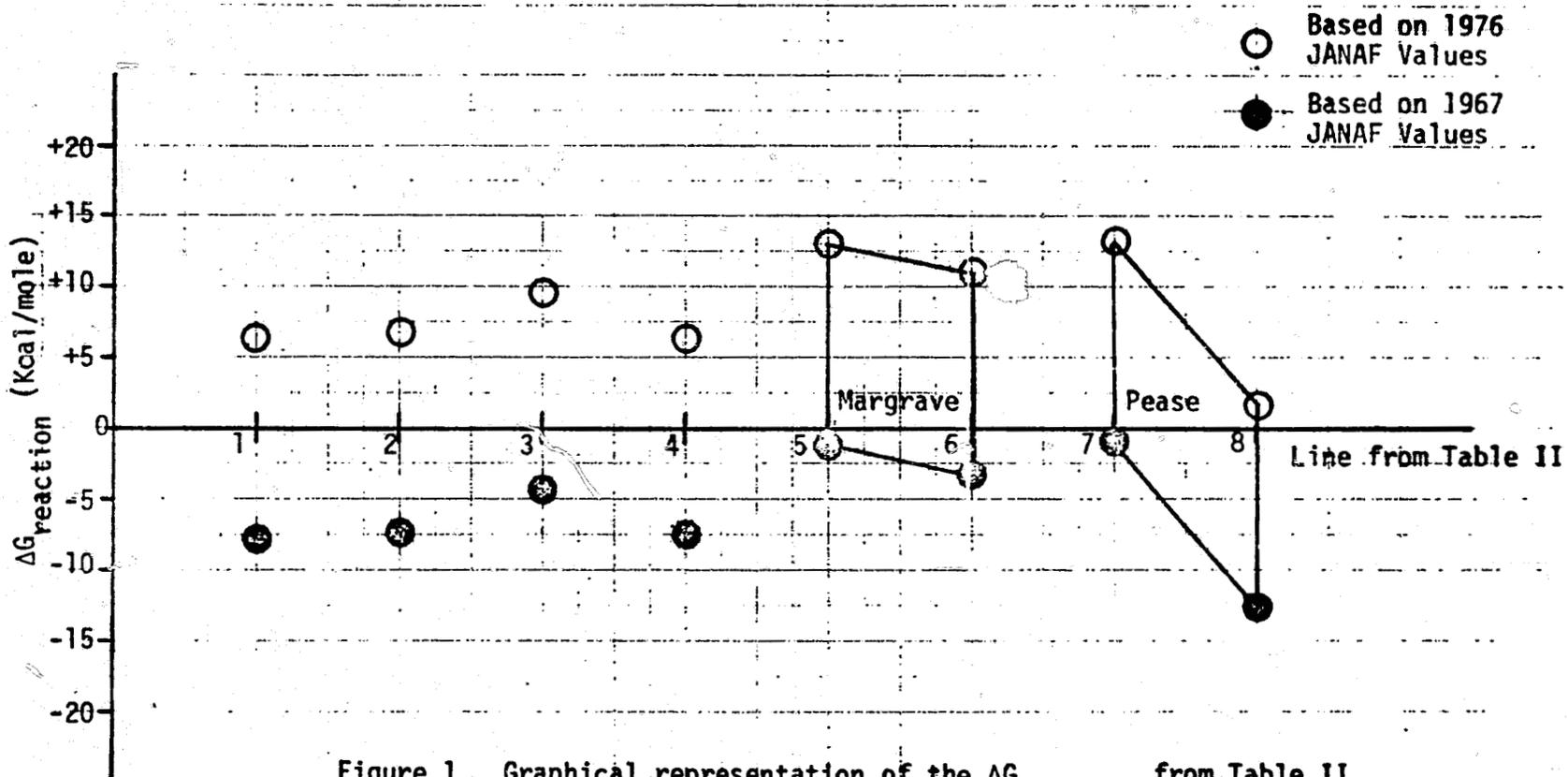
Figure 1. Graphical representation of the $\Delta G_{reaction}$ from Table II based on values from both the 1967 and 1976 JANAF values for ΔG_f^0 of SiF_2 and SiF_4.

$$K_p = \frac{P^2_{(SiF_2)}}{P_{(SiF_4)}}$$

where p is the partial pressure of the gas and P_t is the total pressure.

$$P_{(SiF_2)} = \left(\frac{2\alpha}{1+\alpha}\right) P_t; \quad P_{(SiF_4)} = \left(\frac{1-\alpha}{1+\alpha}\right) P_t$$

$$K_p = \frac{4\alpha^2 P_t}{1-\alpha^2}$$

or

$$\alpha = \left(\frac{K_p}{K_p + 4P_t}\right)^{\frac{1}{2}}$$

At equilibrium, $\Delta G_{reaction} = 0$ and

$$\Delta G^O = -RT \ln K_p$$

$$\ln K_p = \frac{\Delta G^O}{-RT}$$

Using the two JANAF Tables in question, the values for K_p were calculated for the three temperatures discussed above. This allowed the relationship between α and total pressure to be calculated. Figure 2 shows the curves for 1423^OK. The bar illustrates the results of Margrave's work. Similarly in Figure 3, Pease's results are superimposed on the curve for 1473^OK. In Figure 4 are shown the theoretical curves for 1623^OK. The large difference in the curves for each case arise from taking the small differences between large numbers and then raising them to an exponent.

The 1623^OK results are particularly interesting. If we take several examples of our experimental data taken under a variety of conditions and equipment as shown in Figure 4, we see that they fall near a curve between those predicted by

Figure 2. Plot of α vs. log P_t for 1423°K calculated from ΔG_f^o values from JANAF Tables
A) 1967 Tables
B) 1976 Tables
C) Margrave
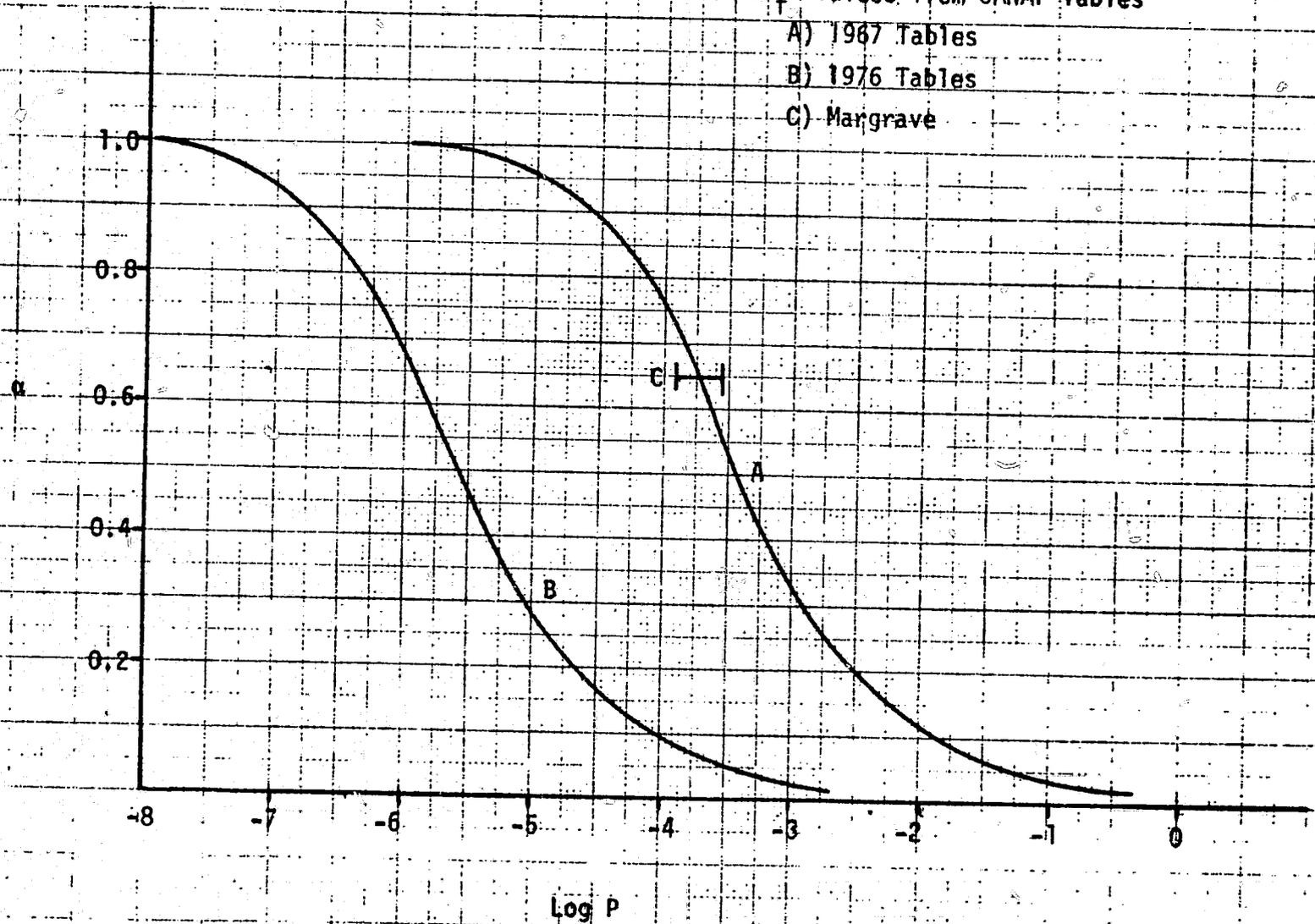
Figure 3. Plot of α vs. log P_t for $1473^\circ K$ calculated
From JANAF Tables
A) 1967 Tables
B) 1976 Tables
C) Pease's data
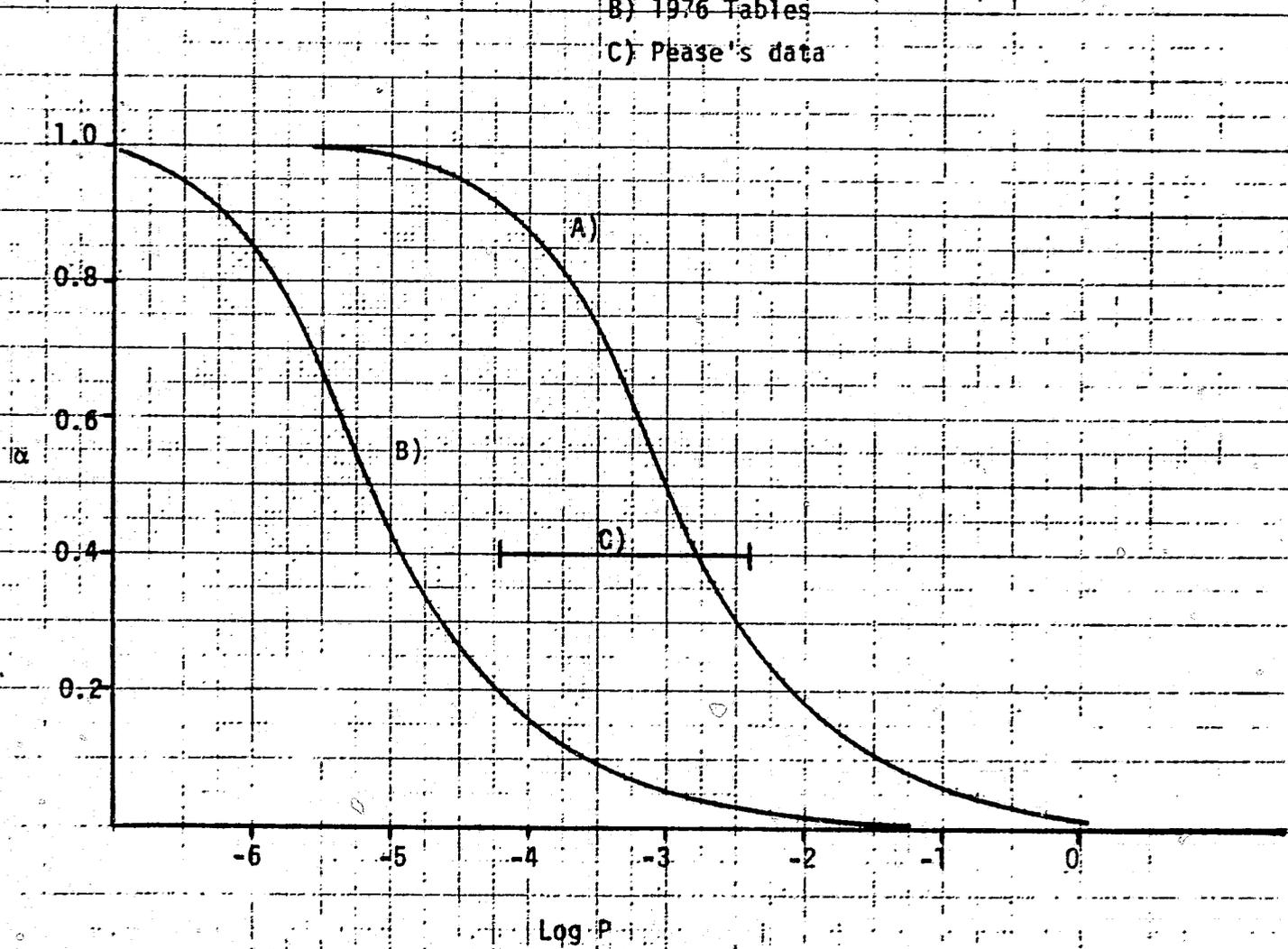
Figure 4. Plot of α vs. log P_t for 1623^0K calculated from ΔG_f^0 values from JANAF Tables

A) 1967 Tables
B) 1976 Tables
C) Based on experimental data
    1) batch reactor, Quarterly Report No. 7 (95% confidence interval for P_t and % conversion; 15 data values)
    2) Batch reactor, Quarterly Report No. 5
    3) near-continuous reactor, Monthly Report No. 25, Table II
    4) batch reactor, Monthly Report No. 25
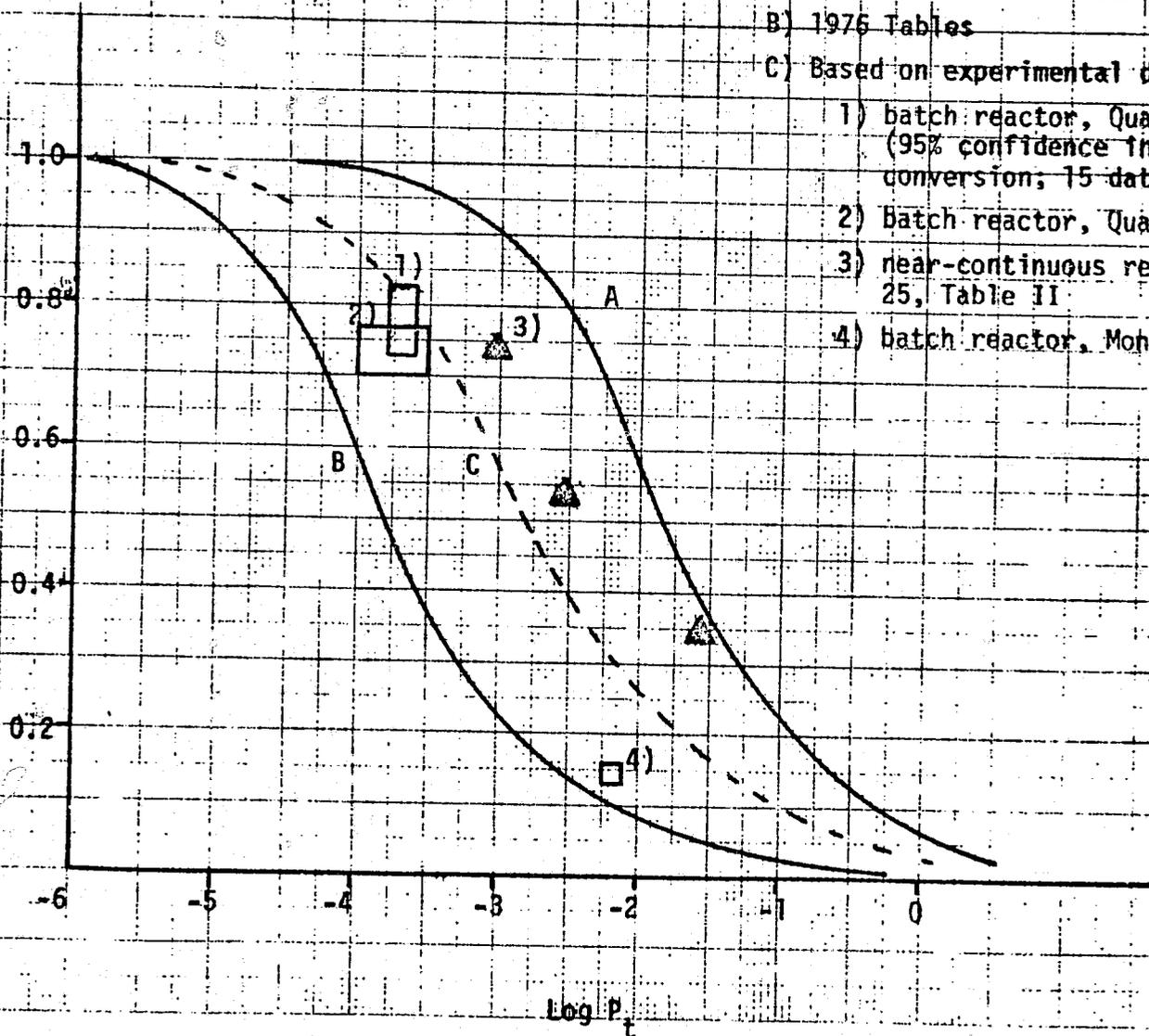
1967 and 1976 JANAF Tables. Again, calculation of $\Delta G^{o}_{f(SiF_2)}$ using the curve C), and using the 1976 value for $\Delta G^{o}_{f(SiF_4)}$ yields -153,621 Kcal/mole, intermediately between the reported values and 1.3 % different than the 1976 value.

IV. CONCLUSIONS

These results lead to the inescapable conclusion that the values listed in the JANAF Table (particularly 1976) are suspect. We submit that Motorola's reported experimental conversion efficiencies are consistent with theoretical calculations and the independent work of Pease and Margrave.